

Design and Development of Bayes' Minimax Linear Classification Systems

Denise M. Reeves

Abstract

This paper considers the design and development of Bayes' minimax, linear classification systems using linear discriminant functions that are Bayes' equalizer rules. Bayes' equalizer rules divide two-class feature spaces into decision regions that have equal classification errors. I will formulate the problem of learning unknown linear discriminant functions from data as a locus problem, thereby formulating geometric locus methods within a statistical framework. Solving locus problems involves finding the equation of a curve or surface defined by a given property, and finding the graph or locus of a given equation. I will devise a system of locus equations that determines Bayes' equalizer rules which is based on a variant of the inequality constrained optimization problem for linear kernel support vector machines. Thereby, I will define a class of learning machines which are fundamental building blocks for Bayes' minimax pattern recognition systems.

Contents

1	Introduction	4
1.1	Long-standing Problems in Machine Learning	5
1.2	The Bias/Variance Dilemma	6
1.2.1	Prewiring of Important Generalizations	6
1.3	The Geometric Locus Dilemma	7
1.3.1	The Geometric Locus Dilemma for SVMs	8
2	Statistical Pattern Recognition Systems	9
2.1	The Binary Classification Problem	10
2.2	Bayes' Criterion	10

2.2.1	The Likelihood Ratio Test	10
2.3	Bayes' Error	12
2.4	Redefined Decision Regions	13
2.5	Bayes' Minimax Criterion	15
2.6	Equalizer Rules	15
2.7	Locus Equations of Bayes' Test	16
2.8	Loci of Likelihoods and Decision Boundaries	18
2.9	Learning Dual Loci of Equalizer Rules	20
2.9.1	Data-Driven Dual Locus of Equalizer Rules	21
3	Locus Methods	21
3.0.2	Locus of a Straight Line	22
3.1	Locus of a Position Vector	23
3.2	Inner Product Statistics	23
3.2.1	Total Energy of Functional Systems	24
3.2.2	Second-order Distance Statistics	24
3.2.3	Scalar Projection Statistics	25
4	Loci of Lines, Planes, and Hyperplanes	26
4.0.4	Vector Equation of a Linear Locus	26
4.0.5	Fundamental Equation of a Linear Locus	27
4.0.6	Principal Eigenaxes of Linear Loci	28
4.0.7	Coordinate Form Equation of a Linear Locus	29
4.0.8	Uniform Property of a Linear Locus	30
4.1	Properties of Principal Eigenaxes	30
4.1.1	Characteristic Eigenenergy	31
4.2	Inherent Property of a Linear Locus	31
4.2.1	Properties Possessed by Points on Linear Loci	31
5	Loci of Bayes' Minimax Linear Classifiers	32
5.1	Key Elements of the Solution	33
5.2	Conditional Risks for Data Distributions	33
5.2.1	Extreme Points	33
5.3	Linear Eigenlocus Transforms	35
5.4	Primal Equation of a Linear Eigenlocus	36
5.5	Why the Wolfe Dual Eigenlocus Matters	36
5.5.1	The Real Unknowns	37
5.5.2	The Fundamental Unknowns	37
5.6	Strong Dual Linear Eigenlocus Transforms	37
5.7	The Lagrangian of the Linear Eigenlocus	38
5.8	Wolfe Dual Equation of a Linear Eigenlocus	38
5.8.1	Loci of Quadratic Forms	39
5.9	The Constrained Primal Linear Eigenlocus	39

5.9.1	Properties of Extreme Vectors	40
5.10	Primal Linear Eigenlocus Components	41
5.11	Regularization Components	42
5.11.1	Parameter Selection	43
6	Equation of an Equalizer Rule	43
6.0.2	KKT Complementary Conditions	43
6.0.3	Equation of a Linear Decision Boundary $D_0(\mathbf{x})$.	45
6.0.4	Equation of the $D_{+1}(\mathbf{x})$ Decision Border	45
6.0.5	Equation of the $D_{-1}(\mathbf{x})$ Decision Border	45
6.1	Eigenaxis of Symmetry	47
6.2	Regulation of Decision Space Z	47
6.3	Regulation of Decision Regions Z_1 and Z_2	48
6.4	Equation of τ_0	49
6.5	The Linear Eigenlocus Test	50
6.5.1	The Decision Locus	50
7	The Wolfe Dual Eigenspace	52
7.1	Eigenenergy Constraint on ψ	53
7.2	Equilibrium Constraint on ψ	54
7.3	Symmetrical Balance Exhibited by Axis of ψ	54
7.4	Eigenspectrum Shaping of Quadratic Surfaces	55
7.5	Statistics for Quadratic Partitions	56
8	The Property of Symmetrical Balance	57
8.0.1	Symmetrical Balance and Bilateral Symmetry . .	58
8.1	First and Second-Order Statistical Moments	65
8.2	Unidirectional Covariance Statistics	66
8.2.1	Omnidirectional Covariance Statistics	67
8.2.2	Pointwise Covariance Statistics	67
8.2.3	Discovery of Extreme Data Points	68
9	Inside the Wolfe Dual Eigenspace	70
9.1	Symmetrically Balanced Covariance Statistics	72
9.2	Similar Properties Exhibited by ψ and τ	80
9.3	Equivalence Between Eigenenergies of ψ and τ	83
9.4	Parameter Vectors θ of Probability Densities	84
9.5	Pointwise Conditional Densities	85
9.6	Class-conditional Probability Densities	87
9.7	Conditional Probability of Decision Error $P(D_2 \omega_1)$. . .	88
9.8	Conditional Probability of Decision Error $P(D_1 \omega_2)$. . .	89
9.9	Finding the Right Mix of Component Lengths	91
9.10	Balanced Eigenlocus Equations	91

9.10.1 Critical Magnitude Constraints	92
10 Risk Minimization	93
10.1 Equations for Total Allowed Eigenenergies	93
10.1.1 The Total Allowed Eigenenergy of τ_1	94
10.1.2 The Total Allowed Eigenenergy of τ_2	95
10.1.3 The Total Allowed Eigenenergy of τ	97
10.2 The Statistical Balancing Feat in Eigenspace	98
10.2.1 Balancing the Eigenenergies of $\tau_1 - \tau_2$	99
10.2.2 Properties of ∇_{eq} in Eigenspace	101
10.3 The Statistical Balancing Feat in Decision Space	103
10.4 Balancing the Bayes' Risk	105
10.5 Linear Eigenlocus of Discrete Probabilities	108
10.6 The Probabilistic Eigenlocus Test	110
11 Design and Development of Bayes' Minimax Pattern Recognition Systems	111
11.1 Systems of Scalable Modules	112
11.2 Decision Banks	114
11.3 Design of Feature Vectors	114
11.3.1 Measures of Feature Vector Effectiveness	115
11.4 A Practical Statistical Multimeter	115
11.5 A Practical Statistical Gauge	117
12 Concluding Remarks	117
Keywords: geometric locus, bias/variance dilemma, geometric locus dilemma, linear kernel support vector machine, Bayes' minimax risk, Bayes' minimax test, Bayes' equalizer rule, linear eigenlocus, linear eigenlocus transform, symmetrical balance, Bayes' minimax pattern recognition system.	

1 Introduction

The discoveries presented in this paper are motivated by deep-seated problems in machine learning. In this paper, I will formulate the problem of learning unknown linear discriminant functions from data as a locus problem, thereby formulating geometric locus methods within a statistical framework. Geometric locus problems involve algebraic equations of curves or surfaces, where the coordinates of any given point on a curve or surface satisfy an algebraic equation, and all of the points on any given curve or surface possess a uniform geometric property (Nichols, 1893; Tanner and Allen, 1898; Whitehead, 1911; Eisenhart, 1939). For

example, a circle is a locus of points, all of which are at the same distance (the radius) from a fixed point (the center).

I will develop locus equations of linear decision boundaries that delineate decision regions which have equal Bayes' risks, i.e., equal classification errors. The locus equations involve solving a variant of the inequality constrained optimization problem for linear kernel support vector machines (SVMs).

The main purpose of the paper is to rigorously define a class of learning machines which are fundamental building blocks for Bayes' minimax, binary and multiclass, linear classification systems. Any given learning machine minimizes Bayes' minimax risk. A decision rule that minimizes Bayes' minimax risk is called a minimax test or an equalizer rule. An equalizer rule divides a two-class feature space into decision regions that have equal classification errors. In some cases, the threshold for a minimax test is identical to the threshold for a minimum probability of error test.

The other purpose of the paper is to introduce new ways of thinking about linear kernel SVMs. By way of motivation, I will begin with an overview of long-standing problems and unresolved questions in machine learning.

1.1 Long-standing Problems in Machine Learning

Fitting learning machine architectures to unknown functions of data involves multiple and interrelated difficulties. Learning machine architectures are sensitive to algebraic and topological structures that include functionals, reproducing kernels, kernel parameters, and constraint sets (see, e.g., Geman et al., 1992; Gershenfeld, 1999; Byun and Lee, 2002; Haykin, 2009; Reeves, 2015), as well as regularization parameters and eigenspectrums of data matrices (see, e.g., Haykin, 2009; Reeves and Jacyna, 2011; Reeves, 2015). Identifying the correct form of an equation for a statistical model is also a large concern (Daniel and Wood, 1979; Breiman, 1991; Geman et al., 1992; Gershenfeld, 1999; Duda et al., 2001).

Machine learning problems are generally considered extrapolation problems for unknown functions, e.g., nontrivial black box estimates. Black boxes are defined in terms of inputs, subsequent outputs, and the mathematical functions that relate them. Because training points will never cover a space of possible inputs, practical learning machines must extrapolate in manners that provide effective generalization performance (Geman et al., 1992; Gershenfeld, 1999; Haykin, 2009).

Fitting all of the training data is generally considered bad statistical practice. Learning machine architectures that correctly interpolate collections of noisy training points tend to fit the idiosyncrasies of the noise,

and are not expected to exhibit good generalization performance. Highly flexible architectures with indefinite parameter sets are said to overfit the training data (Wahba, 1987; Breiman, 1991; Geman et al., 1992; Barron et al., 1998; Boser et al., 1992; Gershenfeld, 1999; Duda et al., 2001; Hastie et al., 2001; Haykin, 2009). Then again, learning machine architectures that interpolate insufficient numbers of data points exhibit underfitting difficulties (Guyon et al., 1992; Ivanciuc, 2007). Architectures with too few parameters ignore both the noise and the meaningful behavior of the data (Gershenfeld, 1999).

All of the above difficulties indicate that learning unknown functions from training data involves trade-offs between underfittings and overfittings of data points. The bias/variance dilemma describes statistical facets of these trade-offs (Geman et al., 1992; Gershenfeld, 1999; Duda et al., 2001; Scholkopf and Smola, 2002; Haykin, 2009).

1.2 The Bias/Variance Dilemma

All learning machine architectures are composed of training data. Moreover, the estimation error between a learning machine and its target function depends on the training data in a twofold manner. Geman, Bienenstock, and Doursat (1992) examined these dual sources of estimation error in their article titled *Neural Networks and the Bias/Variance Dilemma*. The crux of the dilemma is that estimation error is composed of two distinct components termed a bias and a variance. Large numbers of parameter estimates raise the variance, whereas incorrect statistical models increase the bias (Geman et al., 1992; Gershenfeld, 1999; Duda et al., 2001; Hastie et al., 2001; Haykin, 2009).

The bias/variance dilemma can be summarized as follows. Model-free architectures based on insufficient data samples are unreliable and have slow convergence speeds. However, model-based architectures based on incorrect statistical models are also unreliable. Except, model-based architectures based on accurate statistical models are both reliable and have reasonable convergence speeds. Even so, proper statistical models for model-based architectures are difficult to identify.

1.2.1 Prewiring of Important Generalizations

I have considered the arguments presented by Geman et al. (1992), and I have come to the overall conclusion that learning an unknown function from data requires prewiring important generalizations into a learning machine's architecture. For classification systems, generalizations involve effective representations of discriminant functions and decision boundaries. So how do we identify the important generalizations for a given problem? How should these generalizations be prewired? How

do important generalizations represent key aspects of statistical decision systems? What does it really mean to introduce a carefully designed bias into a learning machine’s architecture? How does the introduction of a proper bias involve a model-based architecture? How do we discover model-based architectures? What is a model-based architecture?

In this paper, I will develop a model-based architecture that describes Bayes’ decision rule and boundary for training data drawn from any two distributions that have similar covariance matrices. Any given learning machine achieves Bayes’ error rate which is the lowest error rate that can be achieved by any linear discriminant function (VanTrees, 1968; Fukunaga, 1990; Duda et al., 2001).

All of the above problems indicate that learning unknown functions from data involves indeterminate problems which remain largely unidentified. I have identified a problem which I have named the geometric locus dilemma (Reeves, 2015). The dilemma is summarized below.

1.3 The Geometric Locus Dilemma

A conic section or quadratic surface is a *predetermined* geometric configuration of vectors whose Cartesian coordinate locations satisfy, i.e., are determined by, an algebraic equation. Moreover, curves or surfaces of standard locus equations are determined by properties of geometric loci with respect to coordinate axes of arbitrary Cartesian coordinate systems. Thereby, an algebraic equation of a classical locus of points generates an explicit curve or surface in an arbitrarily specified Cartesian space. It follows that any point on a classical geometric locus naturally exhibits the uniform property of the locus.

Now, consider fitting a collection of training data to standard locus equations. Given the correlated, algebraic and geometric constraints on a traditional locus of points, it follows that any attempt to fit an N -dimensional set of d -dimensional random data points to the standard equation(s) of a geometric locus, involves the unsolvable problem of determining an effective constellation of an $(N - M) \times d$ subset of $N \times d$ random vector coordinates that (1) inherently satisfy prespecified (and therefore fixed) magnitude, i.e., length, constraints on each of the respective d Cartesian coordinate axes, and thereby (2) generate predetermined curves or surfaces in Cartesian space \mathbb{R}^d . Such estimation tasks are not possible. It follows that fitting collections of random data points to standard locus equations is an impossible estimation task.

Given the limitations imposed by the geometric locus dilemma, the design and development of learning machine architectures has primarily been based on curve and surface fitting methods of interpolation or regression, alongside statistical methods of reducing data to minimum

numbers of relevant parameters. For example, multilayer artificial neural networks (ANNs) estimate nonlinear regressions with optimally pruned architectures. Good generalization performance for ANNs is considered an effect of a good nonlinear interpolation of the training data (German et al., 1992; Haykin, 2009). Alternatively, support vector machines (SVMs) fit linear curves or surfaces to minimum numbers of training points. Good generalization performance for SVMs is largely attributed to maximally separated linear decision borders (Boser et al., 1992; Cortes and Vapnik, 1995; Bennett and Campbell, 2000; Cristianini and Shawe-Taylor, 2000; Scholkopf and Smola, 2002).

1.3.1 The Geometric Locus Dilemma for SVMs

SVMs estimate linear and nonlinear decision boundaries by solving a quadratic programming problem. SVM methods specify a pair of linear borders, termed margin hyperplanes, that pass through data points called support vectors. The capacity or complexity of SVM decision boundaries is regulated by means of a geometric margin of separation between a pair of margin hyperplanes. The SVM method minimizes the capacity of a separating hyperplane by maximizing the distance between a pair of margin hyperplanes or linear borders. Large distances between margin hyperplanes (1) allow for considerably fewer hyperplane orientations and (2) enforce a limited capacity to separate training data. Thus, maximizing the distance between margin hyperplanes regulates the complexity of separating hyperplane estimates (Boser et al., 1992; Cortes and Vapnik, 1995; Burges, 1998; Bennett and Campbell, 2000; Cristianini and Shawe-Taylor, 2000; Scholkopf and Smola, 2002).

An Impossible Estimation Task Identifying interpolation methods that provide effective fits of separating lines, planes, or hyperplanes, involves the long-standing problem of fitting linear decision boundaries to overlapping sets of data points; see, for example Cover (1965) and Cortes and Vapnik (1995). Soft margin linear kernel SVMs are said to resolve this problem by means of non-negative, random slack variables $\xi_i \geq 0$, each of which allows a correlated data point \mathbf{x}_i that lies between a pair of linear decision borders to satisfy a linear border. Nonlinear kernel SVMs also employ non-negative, random slack variables, each of which allows a transformed, correlated data point to satisfy a hyperplane decision border in some higher dimensional feature space (Cortes and Vapnik, 1995; Bennett and Campbell, 2000; Cristianini and Shawe-Taylor, 2000; Hastie et al., 2001).

SVM applications of slack variables imply that non-negative, random slack variables encode distances of data points from unknown linear curves or surfaces. Clearly, this is an impossible estimation task. There-

fore, given l overlapping data points, it is concluded that computing effective values for l non-negative, random slack variables $\{\xi_i | \xi_i \geq 0\}_{i=1}^l$ is an impossible estimation task.

SVMs are widely reported to perform well on classification tasks. However, SVMs require computationally expensive hyperparameter tuning (Byun and Lee, 2002; Liang et al., 2011). For nonlinear kernel SVMs, the user must select the polynomial degree or the kernel width. In addition, the user must select regularization parameters for linear and nonlinear kernel SVMs (Reeves, 2009; Reeves and Jacyna, 2011). Generally speaking, the performance of SVMs depends on regularization parameters, the type of kernel, and the kernel parameter for nonlinear kernels. The choice of a nonlinear kernel and its parameter for a given problem is a research issue (Burges, 1998).

In this paper, I will introduce new ways of thinking about linear kernel support vector machines. In the process, I will define a class of learning machines which are fundamental building blocks for statistical pattern recognition systems.

2 Statistical Pattern Recognition Systems

Statistical pattern recognition systems provide an automated means to identify or discover information and objects contained within large collections of digitized (1) images or videos, (2) waveforms, signals, or sequences, and (3) documents. Statistical pattern recognition systems provide automated processes such as optical character recognition, geometric object recognition, speech recognition, handwriting recognition, waveform recognition, system identification, spectrum identification, fingerprint identification, and DNA sequencing.

Design of Statistical Pattern Recognition Systems The design of statistical pattern recognition systems involves two fundamental problems. The first problem concerns identifying measurements or numerical features of the objects being classified and using these measurements to form pattern or feature vectors for each pattern class. For M classes of patterns, a pattern space is composed of M regions, where each region contains the pattern vectors of a class. The second problem involves generating decision boundaries that divide a pattern space into M regions. Functions that determine decision boundaries are called discriminant functions. A statistical pattern recognition system divides a pattern space into decision regions that are separated by decision boundaries (VanTrees, 1968; Srinath et al., 1996; Duda et al., 2001). Pattern spaces are commonly known as feature spaces.

2.1 The Binary Classification Problem

The basic classification problem of deciding between two pattern or feature vectors is essentially one of partitioning a feature space Z into two suitable regions Z_1 and Z_2 , such that whenever a pattern vector \mathbf{x} lies in region Z_1 , the classifier decides that \mathbf{x} belongs to class ω_1 , and whenever \mathbf{x} lies in region Z_2 , the classifier decides that \mathbf{x} belongs to class ω_2 . When the classifier makes a wrong decision, the classifier is said to make an error. A suitable criterion is necessary to determine the best possible partitioning for a given feature space Z (VanTrees, 1968; Srinath et al., 1996; Duda et al., 2001).

2.2 Bayes' Criterion

Bayes' criterion divides a feature space Z in a manner that minimizes the probability of classification error $\mathcal{P}_e(Z)$. Bayes' decision rule is determined by partitioning a feature space Z into two regions Z_1 and Z_2 , where the average risk \mathfrak{R}_B of the total probability of making a decision error $\mathcal{P}_e(Z)$ is minimized. The overall cost C that determines the risk \mathfrak{R}_B is controlled by assigning points to two suitable regions Z_1 and Z_2 , where each region has a conditional risk $\mathfrak{R}(Z_1)$ and $\mathfrak{R}(Z_2)$ that determines the probability of error $\mathcal{P}_e(Z_1)$ and $\mathcal{P}_e(Z_2)$ for the region.

A Bayes' test is based on two assumptions. The first is that prior probabilities $P(\omega_1)$ and $P(\omega_2)$ of the pattern classes ω_1 and ω_2 represent information about the pattern vector sources. The second assumption is that a cost is assigned to each of the four possible outcomes associated with a decision. Denote the costs for the four possible outcomes by C_{11} , C_{21} , C_{22} , and C_{12} , where the first subscript indicates the chosen class and the second subscript indicates the true class. Accordingly, each time that the classifier makes a decision, a certain cost will be incurred (VanTrees, 1968; Srinath et al., 1996; Duda et al., 2001).

2.2.1 The Likelihood Ratio Test

Minimization of the Bayes' risk \mathfrak{R}_B produces decision regions defined by the following expression:

If

$$P(\omega_1)(C_{21} - C_{11})p(\mathbf{x}|\omega_1) \geq P(\omega_2)(C_{12} - C_{22})p(\mathbf{x}|\omega_2),$$

then assign the pattern vector \mathbf{x} to region Z_1 and say that class ω_1 is true. Otherwise, assign the pattern vector \mathbf{x} to region Z_2 and say that class ω_2 is true.

The resulting discriminant function is the likelihood ratio test:

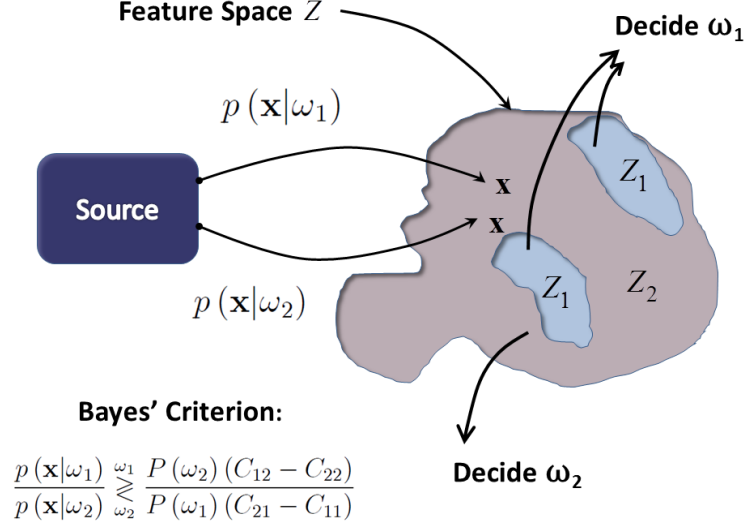


Figure 1: The likelihood ratio test divides a feature space Z into decision regions Z_1 and Z_2 which minimize Bayes' risk \mathfrak{R}_B .

$$\Lambda(\mathbf{x}) \triangleq \frac{p(\mathbf{x}|\omega_1)}{p(\mathbf{x}|\omega_2)} \underset{\omega_2}{\overset{\omega_1}{\gtrless}} \frac{P(\omega_2)(C_{12} - C_{22})}{P(\omega_1)(C_{21} - C_{11})}, \quad (1)$$

where $p(\mathbf{x}|\omega_1)$ and $p(\mathbf{x}|\omega_2)$ are class-conditional density functions. Given the likelihood ratio test, a decision boundary divides a feature space Z into two decision regions Z_1 and Z_2 , where a decision rule $\Lambda(\mathbf{x}) \underset{\omega_2}{\overset{\omega_1}{\gtrless}} \eta$ is based on a threshold η . Figure 1 illustrates how Bayes' decision rule divides a feature space into decision regions (VanTrees, 1968; Srinath et al., 1996).

Bayes' decision rule in Eq. (1) computes the likelihood ratio for a feature vector \mathbf{x}

$$\Lambda(\mathbf{x}) = \frac{p(\mathbf{x}|\omega_1)}{p(\mathbf{x}|\omega_2)},$$

and makes a decision by comparing the ratio $\Lambda(\mathbf{x})$ to the threshold η

$$\eta = \frac{P(\omega_2)(C_{12} - C_{22})}{P(\omega_1)(C_{21} - C_{11})}.$$

Costs and prior probabilities are usually based on educated guesses. Therefore, it is common practice to determine a likelihood ratio $\Lambda(\mathbf{x})$ that is independent of costs and prior probabilities, and let η be a variable threshold that accommodates changes in estimates of cost assignments and prior probabilities (VanTrees, 1968; Srinath et al., 1996).

Because Bayes' likelihood ratio test is based on probability density functions, Bayes' classifiers are difficult to design (VanTrees, 1968; Fukunaga, 1990; Srinath et al., 1996; Duda et al., 2001).

Minimal Probability of Error Criterion

If $C_{11} = C_{22} = 0$ and $C_{21} = C_{12} = 1$, then the average risk \mathfrak{R}_B is given by

$$\mathfrak{R}_B = P(\omega_2) \int_{Z_1} p(\mathbf{x}|\omega_2) d\mathbf{x} + P(\omega_1) \int_{Z_2} p(\mathbf{x}|\omega_1) d\mathbf{x}, \quad (2)$$

which is the total probability of making an error. Given this cost assignment, the Bayes' test

$$\ln \Lambda(\mathbf{x}) \underset{\omega_2}{\overset{\omega_1}{\geq}} \ln \frac{P(\omega_2)}{P(\omega_1)} = \ln P(\omega_2) - \ln P(\omega_1),$$

is minimizing the total probability of error. When two given pattern classes are equally likely, the threshold is zero. The probability of misclassification is called the Bayes' error (VanTrees, 1968; Fukunaga, 1990; Srinath et al., 1996; Duda et al., 2001).

2.3 Bayes' Error

The performance of a discriminant function can be determined by evaluating errors associated with making decisions. For a binary classification problem, there are two types of decision errors. A classifier may decide D_2 class ω_2 when the true class is ω_1 , or a classifier may decide D_1 class ω_1 when the true class is ω_2 . Each type of decision error has a probability associated with it which depends on the class-conditional densities and the decision rule.

Let P_1 denote the probability of error corresponding to deciding D_2 class ω_2 when the true class is ω_1 . The P_1 Bayes' error is given by the integral

$$\begin{aligned} P_1 &= P(D_2|\omega_1) = \int_{\eta}^{\infty} p(\mathbf{x}|\omega_1) d\mathbf{x}, \\ &= \int_{Z_2} p(\mathbf{x}|\omega_1) d\mathbf{x}, \end{aligned} \quad (3)$$

which is a conditional probability given the class-conditional density $p(\mathbf{x}|\omega_1)$ and the decision region Z_2 .

Let P_2 denote the probability of error corresponding to deciding D_1 class ω_1 when the true class is ω_2 . The P_2 Bayes' error is given by the

integral

$$\begin{aligned} P_2 &= P(D_1|\omega_2) = \int_{-\infty}^{\eta} p(\mathbf{x}|\omega_2) d\mathbf{x}, \\ &= \int_{Z_1} p(\mathbf{x}|\omega_2) d\mathbf{x}, \end{aligned} \quad (4)$$

which is a conditional probability given the class-conditional density $p(\mathbf{x}|\omega_2)$ and the decision region Z_1 . Once the decision regions Z_1 and Z_2 are chosen, the values of the error integrals in Eqs (3) and (4) are determined (VanTrees, 1968; Srinath et al., 1996).

In the next section, I will redefine decision regions based solely on regions that are associated with decision errors or lack thereof.

2.4 Redefined Decision Regions

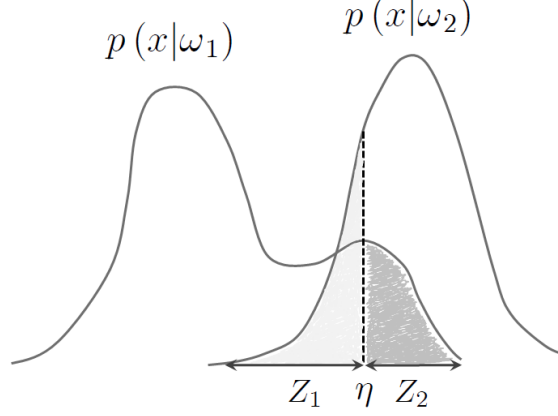
Decision regions Z_1 and Z_2 consist of values of \mathbf{x} for which the likelihood ratio $\Lambda(\mathbf{x})$ is, respectively, less than or greater than the threshold η , where any given pair of decision regions Z_1 and Z_2 spans an entire feature space. Figure 1 depicts how a pair of decision regions Z_1 and Z_2 spans an entire feature space Z , where

$$Z = Z_1 + Z_2 = Z_1 \cup Z_2.$$

I will now redefine decision regions based solely on regions that are associated with decision errors or lack thereof.

For non-overlapping data distributions, the decision region Z_1 which is associated with class ω_1 spans a region between the tail region of $p(\mathbf{x}|\omega_1)$ and the decision threshold η , and the decision region Z_2 which is associated with class ω_2 spans a region between the decision threshold η and the tail region of $p(\mathbf{x}|\omega_2)$ (see, e.g., Fig. 5). Because the risk $\mathfrak{R}(Z_1)$ in the decision region Z_1 only involves pattern vectors \mathbf{x} generated by $p(\mathbf{x}|\omega_1)$, $\mathfrak{R}(Z_1) = 0$. Likewise, because the risk $\mathfrak{R}(Z_2)$ in the decision region Z_2 only involves pattern vectors \mathbf{x} generated by $p(\mathbf{x}|\omega_2)$, $\mathfrak{R}(Z_2) = 0$. Accordingly, the Bayes' risk \mathfrak{R}_B is zero: $\mathfrak{R}_B = \mathfrak{R}(Z_1) + \mathfrak{R}(Z_2) = 0$.

For overlapping data distributions, decision regions are defined to be those regions that span regions of *data distribution overlap*. Accordingly, the decision region Z_1 which is associated with class ω_1 spans a region between the region of distribution overlap between $p(\mathbf{x}|\omega_1)$ and $p(\mathbf{x}|\omega_2)$ and the decision threshold η , and the decision region Z_2 which is associated with class ω_2 spans a region between the decision threshold η and the region of distribution overlap between $p(\mathbf{x}|\omega_2)$ and $p(\mathbf{x}|\omega_1)$ (see, e.g., Figs 4 and 6). It follows that the risk $\mathfrak{R}(Z_1)$ in the decision region Z_1 involves pattern vectors \mathbf{x} generated by $p(\mathbf{x}|\omega_1)$ and $p(\mathbf{x}|\omega_2)$,



$$\mathfrak{R}_{\mathfrak{B}}(Z) = \int_{Z_1} p(x|\omega_2) dx + \int_{Z_2} p(x|\omega_1) dx$$

Figure 2: Bayes' risk \mathfrak{R}_B , i.e., Bayes' classification error $\mathcal{P}_e(Z)$, is determined by a threshold η , i.e., a decision boundary, and decision regions Z_1 and Z_2 , where each decision region has a conditional risk $\mathfrak{R}(Z_1)$ and $\mathfrak{R}(Z_2)$ that determines the probability of error $\mathcal{P}_e(Z_1)$ and $\mathcal{P}_e(Z_2)$ for the region.

where pattern vectors \mathbf{x} generated by $p(\mathbf{x}|\omega_2)$ contribute to decision errors $\mathcal{P}_e(Z_1)$ and the Bayes' risk \mathfrak{R}_B . It also follows that the risk $\mathfrak{R}(Z_2)$ in the decision region Z_2 involves pattern vectors \mathbf{x} generated by $p(\mathbf{x}|\omega_2)$ and $p(\mathbf{x}|\omega_1)$, where pattern vectors \mathbf{x} generated by $p(\mathbf{x}|\omega_1)$ contribute to decision errors $\mathcal{P}_e(Z_2)$ and the Bayes' risk \mathfrak{R}_B . Accordingly, the Bayes' risk \mathfrak{R}_B is $\mathfrak{R}_B = \mathfrak{R}(Z_1) + \mathfrak{R}(Z_2)$.

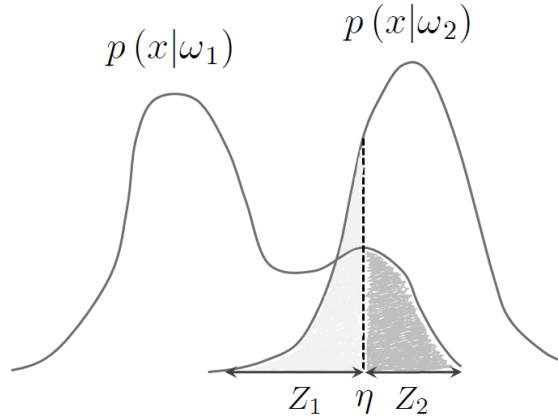
Given the definition for decision regions based solely on regions that are associated with decision errors, Fig. 2 illustrates how values of the error integrals in Eqs (3) and (4) are determined by a threshold η and corresponding decision regions Z_1 and Z_2 .

The decision regions Z_1 and Z_2 consist of values of \mathbf{x} for which the likelihood ratio $\Lambda(\mathbf{x})$ is, respectively, less than or greater than the threshold η . Accordingly, the Bayes' error in Eq. (3) can be written in terms of $\Lambda(\mathbf{x})$ as

$$P_1 = \int_{Z_2} p(\Lambda(\mathbf{x})|\omega_1) d\Lambda, \quad (5)$$

and the Bayes' error in Eq. (4) can be written in terms of $\Lambda(\mathbf{x})$ as

$$P_2 = \int_{Z_1} p(\Lambda(\mathbf{x})|\omega_2) d\Lambda, \quad (6)$$



$$\Re_{\mathfrak{B}}(Z|\Lambda(\mathbf{x})) = \int_{Z_1} p(\Lambda(\mathbf{x})|\omega_2) d\Lambda + \int_{Z_2} p(\Lambda(\mathbf{x})|\omega_1) d\Lambda$$

Figure 3: Bayes' decision rule partitions a feature space Z in a manner that minimizes the conditional probabilities of decision error P_1 and P_2 , given the likelihood ratio $\Lambda(\mathbf{x})$ and the decision regions Z_1 and Z_2 .

where P_1 and P_2 are conditional probabilities given the decision regions Z_1 and Z_2 and the likelihood ratio $\Lambda(\mathbf{x})$ (VanTrees, 1968; Srinath et al., 1996). Figure 3 illustrates how Bayes' error is a function of the likelihood ratio $\Lambda(\mathbf{x})$ and the decision regions Z_1 and Z_2 .

2.5 Bayes' Minimax Criterion

The Bayes' criterion requires that costs be assigned to various decisions, and that values be assigned to prior probabilities for pattern classes. If not enough is known about the sources or mechanisms generating a set of pattern or feature vectors, then prior probabilities cannot be determined and the Bayes' criterion cannot be applied. However, a decision rule can be obtained by using a criterion known as the minimax risk which involves minimization of the maximum risk. A decision rule that minimizes Bayes' minimax risk is called a minimax test. In some cases, the threshold for the minimax test is identical to the threshold for the minimum probability of error test (VanTrees, 1968; Srinath et al., 1996).

2.6 Equalizer Rules

A minimax test is also called an *equalizer rule*, where any given equalizer rule performs well over a range of prior probabilities (Poor, 1994). The

minimax risk \mathfrak{R}_{mm} which is given by the integral equation

$$\begin{aligned}\mathfrak{R}_{mm}(Z) &= C_{22} + (C_{12} - C_{22}) \int_{Z_1} p(\mathbf{x}|\omega_2) d\mathbf{x} \\ &= C_{11} + (C_{21} - C_{11}) \int_{Z_2} p(\mathbf{x}|\omega_1) d\mathbf{x},\end{aligned}\quad (7)$$

determines a Bayes' decision rule with equal conditional risks $\mathfrak{R}(Z_1) = \mathfrak{R}(Z_2)$ (VanTrees, 1968; Srinath et al., 1996).

For the case when $C_{11} = C_{22} = 0$ and $C_{21} = C_{12} = 1$, the minimax equation reduces to $P_2 = P_1$, where the minimax cost is the average probability of error. It follows that the minimax risk \mathfrak{R}_{mm} is given by

$$\begin{aligned}\mathfrak{R}_{mm}(Z) &= \int_{Z_1} p(\mathbf{x}|\omega_2) d\mathbf{x} \\ &= \int_{Z_2} p(\mathbf{x}|\omega_1) d\mathbf{x},\end{aligned}\quad (8)$$

where the conditional probability of making an error for class ω_2 is equal to the conditional probability of making an error for class ω_1 :

$$\int_{Z_1} p(\mathbf{x}|\omega_2) d\mathbf{x} = \int_{Z_2} p(\mathbf{x}|\omega_1) d\mathbf{x}.$$

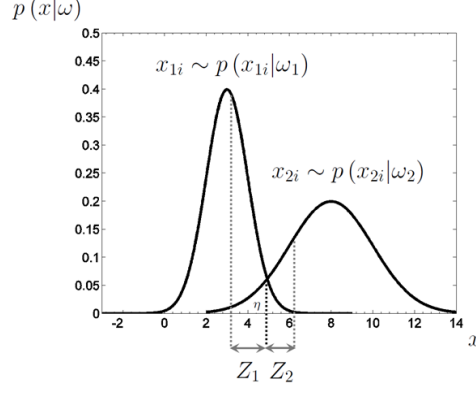
By way of illustration, Fig. 4 shows how an equalizer rule determines decision regions Z_1 and Z_2 for overlapping data, where Bayes' risk for class ω_2 is equal to Bayes' risk for class ω_1 ; Fig. 5 shows how an equalizer rule determines decision regions Z_1 and Z_2 for non-overlapping data, where Bayes' risk for class ω_2 and class ω_1 is zero.

2.7 Locus Equations of Bayes' Test

Bayes' decision rule and boundary are completely defined within the likelihood ratio expression $\Lambda(\mathbf{x})$ for Gaussian data

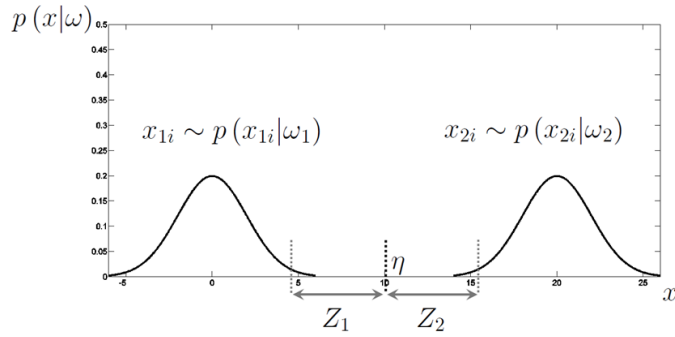
$$\begin{aligned}\Lambda(\mathbf{x}) &= \frac{|\Sigma_2|^{1/2} \exp\left\{-\frac{1}{2}(\mathbf{x} - \mu_1)^T \Sigma_1^{-1}(\mathbf{x} - \mu_1)\right\}}{|\Sigma_1|^{1/2} \exp\left\{-\frac{1}{2}(\mathbf{x} - \mu_2)^T \Sigma_2^{-1}(\mathbf{x} - \mu_2)\right\}} \\ &\stackrel{\omega_1}{\geq} \frac{P(\omega_2)(C_{12} - C_{22})}{P(\omega_1)(C_{21} - C_{11})},\end{aligned}\quad (9)$$

where μ_1 and μ_2 are d -component mean vectors, Σ_1 and Σ_2 are d -by- d covariance matrices, Σ^{-1} and $|\Sigma|$ denote the inverse and determinant of a covariance matrix, and ω_1 or ω_2 is the true data category.



$$\begin{aligned}\mathfrak{R}_{mm}(Z|\hat{\Lambda}(x)) &= \int_{Z_1} p(\hat{\Lambda}(x)|\omega_2) d\hat{\Lambda} \\ &= \int_{Z_2} p(\hat{\Lambda}(x)|\omega_1) d\hat{\Lambda}\end{aligned}$$

Figure 4: For overlapping data, Bayes' minimax tests divide feature spaces Z into decision regions Z_1 and Z_2 that have equal conditional risks: $\mathfrak{R}(Z_1) = \mathfrak{R}(Z_2)$.



$$\begin{aligned}\mathfrak{R}_{mm}(Z|\hat{\Lambda}(x)) &= \int_{Z_1} p(\hat{\Lambda}(x)|\omega_2) d\hat{\Lambda} \\ &= \int_{Z_2} p(\hat{\Lambda}(x)|\omega_1) d\hat{\Lambda} = 0\end{aligned}$$

Figure 5: For non-overlapping data, Bayes' minimax tests divide feature spaces Z into decision regions Z_1 and Z_2 that have zero conditional risks: $\mathfrak{R}(Z_1) = \mathfrak{R}(Z_2) = 0$.

The likelihood ratio $\Lambda(\mathbf{x})$ in Eq. (9) can be reduced to an algebraic equation

$$\begin{aligned} \ln[\Lambda(\mathbf{x})] &= \mathbf{x}^T (\Sigma_1^{-1} \mu_1 - \Sigma_2^{-1} \mu_2) \\ &+ \frac{1}{2} \mathbf{x}^T (\Sigma_2^{-1} \mathbf{x} - \Sigma_1^{-1} \mathbf{x}) \\ &+ \frac{1}{2} \mu_2^T \Sigma_2^{-1} \mu_2 - \frac{1}{2} \mu_1^T \Sigma_1^{-1} \mu_1 \stackrel{\omega_1}{\underset{\omega_2}{\gtrless}} \eta, \\ \eta &\triangleq \ln(P(\omega_2)) - \ln(P(\omega_1)), \end{aligned} \quad (10)$$

that defines the general form of the discriminant function for the general Gaussian binary classification problem, where no costs ($C_{11} = C_{22} = 0$) are associated with correct decisions, and $C_{12} = C_{21} = 1$ are costs associated with incorrect decisions (VanTrees, 1968; Duda et al., 2001).

The algebraic equation in Eq. (10) describes Bayes' decision boundaries for any two classes of data drawn from Gaussian distributions. Bayes' decision boundaries are characterized by the class of hyperquadric decision surfaces which include hyperplanes, pairs of hyperplanes, hyperspheres, hyperellipsoids, hyperparaboloids, and hyperhyperboloids (VanTrees, 1968; Duda et al., 2001).

If $P(\omega_1) = P(\omega_2) = 1/2$, where $\eta = 0$, then Bayes' decision boundaries are defined by regions for which Bayes' error is equal

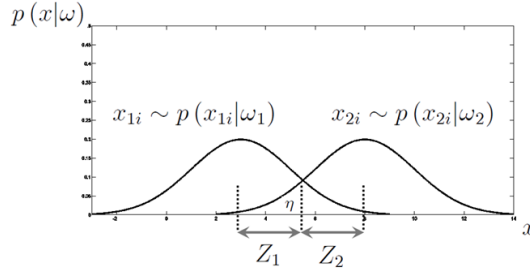
$$\begin{aligned} \mathfrak{R}_{mm}(Z) &= \int_{Z_2} p(\Lambda(\mathbf{x}) | \omega_1) d\Lambda \\ &= \int_{Z_1} p(\Lambda(\mathbf{x}) | \omega_2) d\Lambda, \end{aligned} \quad (11)$$

where any given equalizer rule $\ln[\Lambda(\mathbf{x})]$ performs well over a range of prior probabilities. Therefore, given the assumption that $\eta = 0$, it follows that the discriminant function $\ln[\Lambda(\mathbf{x})]$ for the general Gaussian binary classification problem is an equalizer rule that satisfies the minimax risk \mathfrak{R}_{mm} in Eq. (11).

Figure 4 illustrates an equalizer rule $\hat{\Lambda}(\mathbf{x}) \stackrel{\omega_1}{\underset{\omega_2}{\gtrless}} 0$ for overlapping data drawn from Gaussian distributions that have dissimilar covariance matrices, whereas Fig. 6 illustrates an equalizer rule $\hat{\Lambda}(\mathbf{x}) \stackrel{\omega_1}{\underset{\omega_2}{\gtrless}} 0$ for overlapping data drawn from Gaussian distributions that have similar covariance matrices.

2.8 Loci of Likelihoods and Decision Boundaries

Any given decision boundary described by Eq. (10) is the *locus* (the position) of all of the points \mathbf{x} whose coordinates are solutions of Eq.



$$\begin{aligned}\mathfrak{R}_{\mathfrak{B}}\left(Z|\hat{\Lambda}(\mathbf{x})\right) &= \int_{Z_1} p\left(\hat{\Lambda}(\mathbf{x})|\omega_2\right) d\hat{\Lambda} \\ &= \int_{Z_2} p\left(\hat{\Lambda}(\mathbf{x})|\omega_1\right) d\hat{\Lambda}\end{aligned}$$

Figure 6: For overlapping Gaussian distributions that have similar covariance matrices, Bayes' minimax tests $\hat{\Lambda}(\mathbf{x}) \underset{\omega_2}{\overset{\omega_1}{\geq}} 0$ divide feature spaces Z into decision regions Z_1 and Z_2 that have equal conditional risks $\mathfrak{R}(Z_1) = \mathfrak{R}(Z_2)$.

(10). Given the assumption that $\eta = 0$, any given point \mathbf{x} on a decision boundary satisfies Bayes' minimax risk \mathfrak{R}_{mm} in Eq. (11). Therefore, any given likelihood ratio $\ln[\Lambda(\mathbf{x})]$ is also determined by points \mathbf{x} whose coordinates are solutions of Eq. (10), where any given point \mathbf{x} of the likelihood ratio $\ln[\Lambda(\mathbf{x})]$ satisfies the minimax risk \mathfrak{R}_{mm} in Eq. (11). It follows that any given likelihood ratio $\ln[\Lambda(\mathbf{x})]$ and decision boundary described by Eq. (10) are jointly determined by points \mathbf{x} whose coordinates satisfy the minimax risk \mathfrak{R}_{mm} in Eq. (8).

Geometric Locus The general idea of a curve or surface which at any point of it exhibits some uniform property is expressed in geometry by the term *locus* (Whitehead, 1911). Generally speaking, a geometric locus is a curve or surface formed by points, all of which possess some uniform property. Any given point on a geometric locus possesses a property which is common to all points on the locus, and *no other points*. Any given geometric locus is described by an algebraic equation, where the locus of the algebraic equation is the location of all those points whose coordinates are solutions of the equation (Nichols, 1893; Tanner and Allen, 1898; Whitehead, 1911; Eisenhart, 1939).

Dual Locus of Equalizer Rules

Using the general idea of a geometric locus, it follows that the algebraic equation for Bayes' likelihood ratio $\ln[\Lambda(\mathbf{x})]$ in Eq. (10) describes the *dual locus* of a decision boundary *and* a likelihood ratio. Therefore, take any given likelihood ratio $\ln[\Lambda(\mathbf{x})]$ and decision boundary described by Eq. (10). It follows that all of the points \mathbf{x} that satisfy Eq. (10) possess a property which is common to points \mathbf{x} of the likelihood ratio $\ln[\Lambda(\mathbf{x})]$ *and* the decision boundary. Moreover, if $\eta = 0$, all of the points \mathbf{x} of the likelihood ratio $\ln[\Lambda(\mathbf{x})]$ and the decision boundary determine an equalizer rule that satisfies Bayes' minimax risk \mathfrak{R}_{mm} in Eq. (11). Accordingly, Eq. (10) describes the *dual locus of equalizer rules* for Gaussian data.

2.9 Learning Dual Loci of Equalizer Rules

I have conducted simulation studies which demonstrate that properly regularized, linear kernel SVMs learn Bayes' linear decision boundaries for *any* two classes of Gaussian data, where $\Sigma = \Sigma_1 = \Sigma_2$ (see Reeves, 2009; Reeves and Jacyna, 2011), including completely overlapping data distributions (Reeves, 2015). I have also conducted simulation studies which demonstrate that properly regularized, second-order polynomial kernel SVMs learn Bayes' decision boundaries for data drawn from *any* two Gaussian distributions, including completely overlapping data distributions (Reeves, 2015).

Given Eq. (10), my findings are very surprising. Using Eq. (10), for any given pair of homogeneous distributions, where $\Sigma_1 = \Sigma_2$ and $\mu_1 = \mu_2$, the Bayes' test

$$\begin{aligned} \ln[\Lambda(\mathbf{x})] &= \mathbf{x}^T \Sigma^{-1} (\mu_1 - \mu_2) + \frac{1}{2} \mu_2^T \Sigma^{-1} \mu_2 - \frac{1}{2} \mu_1^T \Sigma^{-1} \mu_1 \underset{\omega_2}{\overset{\omega_1}{\geq}} 0, \\ &= 0 \underset{\omega_2}{\overset{\omega_1}{\geq}} 0, \end{aligned}$$

reduces to the constant 0, and *is undefined*. It follows that Bayes' decision rule and boundary *are also undefined*. However, I have conducted simulation studies which show that Bayes' decision rule and boundary *are both described* by a system of *locus equations*, where *data points* satisfy a *data-driven dual locus* of Bayes' decision boundary *and* likelihood ratio.

The system of locus equations is based on the support-vector network algorithm developed by Boser, Guyon, and Vapnik (1992) and Cortes and Vapnik (1995).

2.9.1 Data-Driven Dual Locus of Equalizer Rules

In this paper, I will develop locus equations of linear decision boundaries that satisfy Bayes' minimax risk \mathfrak{R}_{mm} in Eq. (11). The locus equations are based on the inequality constrained optimization problem for linear kernel SVMs. I will develop locus equations of Bayes' likelihood ratio and linear decision boundary, where $\eta = 0$, for any two classes of Gaussian data, where $\Sigma = \Sigma_1 = \Sigma_2$, such that a *data-driven dual locus* describes the *locus* of Bayes' decision boundary *and* likelihood ratio of Eq. (10) in terms of an equalizer rule that satisfies Bayes' minimax risk \mathfrak{R}_{mm} in Eq. (11). Moreover, the equalizer rule describes the locus of a linear decision boundary for *any* two classes of pattern vectors.

By way of motivation, an overview of locus methods will be followed by an analysis of linear loci. The material from the overview can be found in Nichols (1893), Tanner and Allen (1898), and Eisenhart (1939).

3 Locus Methods

The graph of an equation is the locus (the *place*) of all points whose coordinates are solutions of the equation. Any given point on a locus possesses a geometric property which is common to all points of the locus, and no other points. For example, a circle is a locus of points (x, y) , all of which are at the same distance, the radius r , from a fixed point (x_0, y_0) , the center. The algebraic equation of the locus of a circle in Cartesian coordinates is

$$(x - x_0)^2 + (y - y_0)^2 = r^2. \quad (12)$$

Only those coordinates (x, y) that satisfy Eq. (12) contribute to the geometric locus of a specified circle. Classic examples of geometric loci include circles, ellipses, hyperbolae, parabolas, lines, and points. Locus problems for all of the second-order curves have been widely studied in analytic (coordinate) geometry Nichols (1893); Tanner and Allen (1898); Eisenhart (1939).

Solving a locus problem requires finding the equation of a curve defined by a given property and drawing the graph or locus of a given equation. Methods for solving locus problems are based on two fundamental problems in analytic geometry, both of which involve the graph or locus of an equation.

The identification of the geometric property of a locus of points is a central problem in coordinate geometry. The inverse problem finds the algebraic form of an equation whose solutions give the coordinates of all of the points on a locus which has been defined geometrically. A geometric figure is any set of points which exhibit a uniform property.

Accordingly, any point, line, line segment, angle, polygon, curve, region, plane, surface, solid, etc. is a geometric figure. Geometric figures are defined in two ways: (1) as a figure with certain known properties, and (2) as the path of a point which moves under known conditions Nichols (1893); Tanner and Allen (1898); Eisenhart (1939).

Finding the algebraic form of an equation for a given geometric figure or locus is often a difficult problem. Solving locus problems involves identifying algebraic and geometric constraints for a given locus of points. The algebraic form of an equation of a locus hinges on both the geometric property and the frame of reference (the coordinate system) of the locus. Changing the position of the coordinate axes changes the algebraic form of the locus that references the axes and the coordinates of any point on the locus. The equation of a locus and the identification of the geometric property of the locus can be greatly simplified by changing the position of the axes to which the locus of points is referenced Nichols (1893); Tanner and Allen (1898); Eisenhart (1939).

3.0.2 Locus of a Straight Line

The equations of a straight line in the coordinate plane have been widely studied in analytical and coordinate geometry. Standard forms of the equation of a linear locus are outlined below.

Standard Equations of the First Degree The geometric locus of every equation of the first degree is a straight line. The general equation of the first degree in two coordinate variables x and y has the form

$$Ax + By + C = 0,$$

where A , B , C are constants which may have any real values, subject to the restriction that A and B cannot both be zero. Only two geometric conditions are deemed necessary to determine the equation of a particular line. Either a line should pass through two given points or should pass through a given point and have a given slope. Standard equations of a straight line include the point-slope, slope-intercept, two-point, intercept, and normal forms Nichols (1893); Tanner and Allen (1898); Eisenhart (1939).

Excluding the point, a straight line appears to be the simplest type of geometric locus. Yet, the locus of a point is ill-defined (a locus has more than one point) and the uniform geometric property of a straight line remains unidentified. I will identify several correlated uniform properties exhibited by all of the points on a linear locus shortly. I will now define the locus of a point in terms of the locus of a position vector.

3.1 Locus of a Position Vector

The locus of a position vector will play a significant role in the analyses that follow. A position vector $\mathbf{x} = (x_1, x_2, \dots, x_d)^T$ is defined to be the locus of a directed straight line segment formed by two points $P_0(0, 0, \dots, 0)$ and $P_x(x_1, x_2, \dots, x_d)$ which are at a distance of $\|\mathbf{x}\| = (x_1^2 + x_2^2 + \dots + x_d^2)^{1/2}$ from each other, such that each point coordinate x_i or vector component x_i is at a signed distance of $\|\mathbf{x}\| \cos \alpha_{ij}$ from the origin P_0 , along the direction of an orthonormal coordinate axis \mathbf{e}_j , where $\cos \alpha_{ij}$ is the direction cosine between the vector component x_i and the orthonormal coordinate axis \mathbf{e}_j . It follows that the locus of a position vector \mathbf{x} is determined by an ordered set of signed magnitudes

$$\mathbf{x} \triangleq (\|\mathbf{x}\| \cos \alpha_{x_1 1}, \|\mathbf{x}\| \cos \alpha_{x_2 2}, \dots, \|\mathbf{x}\| \cos \alpha_{x_d d})^T, \quad (13)$$

along the axes of the standard set of basis vectors

$$\{\mathbf{e}_1 = (1, 0, \dots, 0), \dots, \mathbf{e}_d = (0, 0, \dots, 1)\},$$

all of which describe a unique, ordered d -tuple of geometric locations on d axes \mathbf{e}_j , where $\|\mathbf{x}\|$ is the length of the vector \mathbf{x} , $(\cos \alpha_{x_1 1}, \dots, \cos \alpha_{x_d d})$ are the direction cosines of the components (x_1, \dots, x_d) of the vector \mathbf{x} relative to the standard set of orthonormal coordinate axes $\{\mathbf{e}_j\}_{j=1}^d$, and each vector component x_i determines a point coordinate x_i of the endpoint P_x of the vector \mathbf{x} .

Using Eq. (13), a point is the endpoint on the locus of a position vector, such that a correlated point P_x and position vector \mathbf{x} both describe an ordered pair of real numbers in the real Euclidean plane or an ordered d -tuple of real numbers in real Euclidean space, all of which jointly determine a geometric location in \mathbb{R}^2 or \mathbb{R}^d . In the analyses that follow, the term vector refers to a position vector.

I will now demonstrate that the multiplication of any two vectors encodes a rich system of algebraic and topological relationships between the loci of the two vectors. The inner product statistics defined next determine a Hilbert space.

3.2 Inner Product Statistics

The inner product expression $\mathbf{x}^T \mathbf{x}$ defined by

$$\mathbf{x}^T \mathbf{x} = x_1 x_1 + x_2 x_2 + \dots + x_d x_d,$$

generates the norm $\|\mathbf{x}\|$ of the vector \mathbf{x}

$$\|\mathbf{x}\| = (x_1^2 + x_2^2 + \dots + x_d^2)^{1/2},$$

which determines the Euclidean distance between the endpoint $P_{\mathbf{x}}$ of \mathbf{x} and the origin $P_{\mathbf{o}}$, so that the norm $\|\mathbf{x}\|$ measures the length of the vector \mathbf{x} which is also the magnitude of \mathbf{x} . For any given scalar $\zeta \in \mathbb{R}^1$, $\|\zeta\mathbf{x}\| = |\zeta| \|\mathbf{x}\|$ (Naylor and Sell, 1971).

The inner product function $\mathbf{x}^T \mathbf{y}$ also determines the angle between two vectors \mathbf{x} and \mathbf{y} in \mathbb{R}^d . Given any two vectors \mathbf{x} and \mathbf{y} , the inner product expression

$$\mathbf{x}^T \mathbf{y} = x_1 y_1 + x_2 y_2 + \cdots + x_d y_d, \quad (14)$$

is equivalent to the algebraic relationship

$$\mathbf{x}^T \mathbf{y} = \|\mathbf{x}\| \|\mathbf{y}\| \cos \theta, \quad (15)$$

where θ is the angle between the vectors \mathbf{x} and \mathbf{y} .

If $\theta = 90^\circ$, then $\mathbf{x}^T \mathbf{y} = 0$ and the vectors \mathbf{x} and \mathbf{y} are said to be orthogonal to each other. Accordingly, the inner product function $\mathbf{x}^T \mathbf{y}$ allows us to describe vectors which are orthogonal or perpendicular to each other (Naylor and Sell, 1971). Orthogonal vectors are denoted by $\mathbf{x} \perp \mathbf{y}$.

3.2.1 Total Energy of Functional Systems

The functional $\|\mathbf{x}\|^2$ determines the energy of the vector \mathbf{x} . A vector \mathbf{x} exhibits an energy $\|\mathbf{x}\|^2$ according to its locus, so that a scaled vector $\zeta\mathbf{x}$ exhibits an energy $\zeta^2 \|\mathbf{x}\|^2$ with respect to the configuration of the scaled vectors $\{\zeta_i \mathbf{x}_i\}_{i=1}^l$ and total energy $\sum_{i=1}^l \zeta_i^2 \|\mathbf{x}_i\|^2$ of a functional system.

The algebraic relationships in Eqs (14) and (15) are derived from second-order distance statistics. I will now demonstrate that second-order distance statistics describe a rich system of algebraic and topological relationships between the loci of two vectors.

3.2.2 Second-order Distance Statistics

The algebraic relationship $v^T \nu = \|v\| \|\nu\| \cos \varphi$ between two vectors v and ν can be derived by using the law of cosines (see, e.g., Lay, 2006):

$$\|v - \nu\|^2 = \|v\|^2 + \|\nu\|^2 - 2 \|v\| \|\nu\| \cos \varphi, \quad (16)$$

which reduces to

$$\begin{aligned} \|v\| \|\nu\| \cos \varphi &= v_1 \nu_1 + v_2 \nu_2 + \cdots + v_d \nu_d, \\ &= v^T \nu = \nu^T v. \end{aligned}$$

The algebraic relationships in Eq. (16) indicate that the inner product statistic $v^T \nu$ determines the length $\|v - \nu\|$ of the vector from ν to v ,

i.e., the vector $v - \nu$, which is the distance between the endpoints of v and ν . Because second-order distance statistics are symmetric, the law of cosines

$$\|v - \nu\|^2 = \|\nu\|^2 + \|v\|^2 - 2 \|\nu\| \|v\| \cos \varphi,$$

determines the length $\|v - \nu\|$ of the vector from v to ν (the vector $\nu - v$) which is also the distance between the endpoints of v and ν .

It follows that the inner product statistic $v^T \nu$ between two vectors v and ν in Hilbert space

$$\begin{aligned} v^T \nu &= v_1 \nu_1 + v_2 \nu_2 + \cdots + v_d \nu_d, \\ &= \|v\| \|\nu\| \cos \varphi, \end{aligned}$$

determines the distance between the loci

$$(\|v\| \cos \alpha_{v_1 1}, \|v\| \cos \alpha_{v_2 2}, \cdots, \|v\| \cos \alpha_{v_d d}),$$

and

$$(\|\nu\| \cos \alpha_{\nu_1 1}, \|\nu\| \cos \alpha_{\nu_2 2}, \cdots, \|\nu\| \cos \alpha_{\nu_d d}),$$

of the given vectors. It is concluded that the algebraic relationships contained within Eq. (16) describe a rich system of topological relationships between the loci of two vectors. Figure 7 depicts correlated algebraic and topological structures encoded within an inner product statistic (see Fig. 7a).

Inner product statistics include the component of a vector along another vector, which is also known as a scalar projection. Figure 7 illustrates the geometric nature of scalar projections for obtuse angles (see Fig. 7b) and acute angles (see Fig. 7c) between vectors.

3.2.3 Scalar Projection Statistics

Scalar projection statistics determine signed magnitudes along the axes of given vectors. The inner product statistic $\mathbf{x}^T \mathbf{y} = \|\mathbf{x}\| \|\mathbf{y}\| \cos \theta$ can be interpreted as the length $\|\mathbf{x}\|$ of \mathbf{x} times the scalar projection of \mathbf{y} onto \mathbf{x}

$$\mathbf{x}^T \mathbf{y} = \|\mathbf{x}\| \times [\|\mathbf{y}\| \cos \theta], \quad (17)$$

where the scalar projection of \mathbf{y} onto \mathbf{x} , also known as the component of \mathbf{y} along \mathbf{x} , is defined to be the signed magnitude $\|\mathbf{y}\| \cos \theta$ of the vector projection, where θ is the angle between \mathbf{x} and \mathbf{y} (Stewart, 2009). Scalar projections are denoted by $\text{comp}_{\vec{\mathbf{x}}}(\vec{\mathbf{y}})$, where $\text{comp}_{\vec{\mathbf{x}}}(\vec{\mathbf{y}}) < 0$ if $\pi/2 < \theta \leq \pi$. The scalar projection statistic $\|\mathbf{y}\| \cos \theta$ satisfies the inner product relationship $\|\mathbf{y}\| \cos \theta = \frac{\mathbf{x}^T \mathbf{y}}{\|\mathbf{x}\|}$ between the unit vector $\frac{\mathbf{x}}{\|\mathbf{x}\|}$ and the vector \mathbf{y} .

In the next section, I will develop equations and identify geometric properties of linear loci.

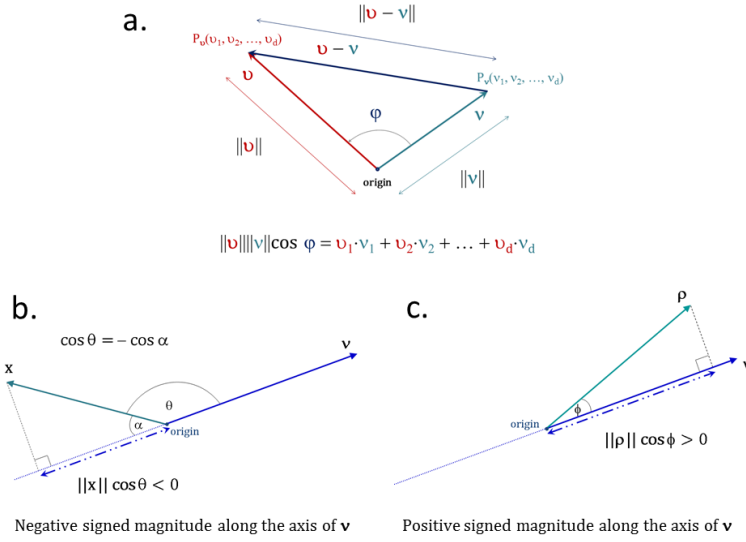


Figure 7: (a) Inner product statistics encode angles and corresponding distances between the geometric loci of vectors. Scalar projection statistics encode (b) negative signed magnitudes or (c) positive signed magnitudes along the axes of given vectors.

4 Loci of Lines, Planes, and Hyperplanes

I will now derive the fundamental locus equation that describes loci of lines, planes, and hyperplanes. I will use this equation to identify correlated uniform properties exhibited by all of the points on a linear locus. I will also develop an eigen-coordinate system that describes all forms of linear loci. The analysis that follows will denote both points and vectors by \mathbf{x} .

4.0.4 Vector Equation of a Linear Locus

Let $\mathbf{v} \triangleq (v_1, v_2)^T$ be a fixed vector in the real Euclidean plane and consider the line l at the endpoint of \mathbf{v} that is perpendicular to \mathbf{v} . It follows that the endpoint of the vector \mathbf{v} is a point on the line l . Thereby, the coordinates (v_1, v_2) of \mathbf{v} delineate and satisfy l . In addition, consider an arbitrary vector $\mathbf{x} \triangleq (x_1, x_2)^T$ whose endpoint is also on the line l . Thereby, the coordinates (x_1, x_2) of the point \mathbf{x} also delineate and satisfy l . Finally, let ϕ be the acute angle between the vectors \mathbf{v} and \mathbf{x} , satisfying $0 \leq \phi \leq \pi/2$ and the algebraic relationship $\cos \phi = \frac{\|\mathbf{v}\|}{\|\mathbf{x}\|}$.

Using all of the above assumptions, it follows that the locus of points (x_1, x_2) on a line l is described by the equation:

$$\mathbf{x}^T \mathbf{v} = \|\mathbf{x}\| \|\mathbf{v}\| \cos \phi, \quad (18)$$

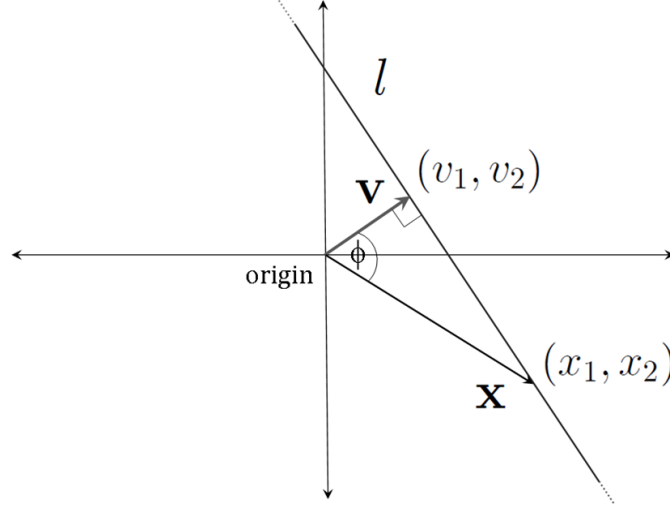


Figure 8: An elegant principal eigen-coordinate system for lines that is readily generalized to planes and hyperplanes. Any vector $\mathbf{x} = (x_1, x_2)^T$ whose endpoint (x_1, x_2) is on the line l explicitly and exclusively references the vector $\mathbf{v} = (v_1, v_2)^T$ which is shown to be the principal eigenaxis of the line l .

which is the vector equation of a line (Davis, 1973). By way of illustration, Fig. 8 depicts the geometric locus of a line in the real Euclidean plane \mathbb{R}^2 .

4.0.5 Fundamental Equation of a Linear Locus

Take any fixed vector \mathbf{v} and consider the line l that is described by Eq. (18), where the axis of \mathbf{v} is perpendicular to the specified line l and the endpoint of \mathbf{v} is on l . Given that any vector \mathbf{x} with its endpoint on the given line l satisfies the algebraic relationship $\|\mathbf{x}\| \cos \phi = \|\mathbf{v}\|$ with the fixed vector \mathbf{v} , it follows that the locus of a line l is also described by the equation:

$$\mathbf{x}^T \mathbf{v} = \|\mathbf{v}\|^2. \quad (19)$$

Equations (18) and (19) are readily generalized to planes p and hyperplanes h in \mathbb{R}^d by letting $\mathbf{v} \triangleq (v_1, v_2, \dots, v_d)^T$ and $\mathbf{x} \triangleq (x_1, x_2, \dots, x_d)^T$. Because Eq. (19) contains no constants or parameters, Eq. (19) is the fundamental equation of a linear locus. Therefore, take any line, plane, or hyperplane in \mathbb{R}^d . It follows that a linear locus is delineated by a fixed vector \mathbf{v} , where the axis of \mathbf{v} is perpendicular to the linear locus and the endpoint of \mathbf{v} is on the linear locus.

Assuming that $\|\mathbf{v}\| \neq 0$, Eq. (19) can also be written as:

$$\frac{\mathbf{x}^T \mathbf{v}}{\|\mathbf{v}\|} = \|\mathbf{v}\|. \quad (20)$$

The axis $\mathbf{v}/\|\mathbf{v}\|$ has length 1 and points in the direction of the vector \mathbf{v} , such that $\|\mathbf{v}\|$ is the distance of a specified line l , plane p , or hyperplane h to the origin. Using Eq. (20), it follows that the distance Δ of a line, plane, or hyperplane from the origin is specified by the magnitude $\|\mathbf{v}\|$ of the axis \mathbf{v} . I will now argue that the vector \mathbf{v} is the principal eigenaxis of linear loci.

4.0.6 Principal Eigenaxes of Linear Loci

Figure 8 shows how the locus of a fixed vector \mathbf{v} determines the locus of a line l . I propose that such fixed vectors provide exclusive, intrinsic reference axes for loci of lines, planes, and hyperplanes. Such intrinsic reference axes are principal eigenaxes of conic sections and quadratic surfaces (Hewson, 2009). I will now demonstrate that the axis denoted by \mathbf{v} in Eqs (18), (19), and (20) is the principal eigenaxis of linear loci.

All of the major axes of conic sections and quadratic surfaces are major intrinsic axes which may also coincide as exclusive, fixed reference axes. Major axes have been referred to as "the axis of the curve" (Nichols, 1893), "the principal axis" and "the principal axis of the curve" (Tanner and Allen, 1898). In order to demonstrate that the vector \mathbf{v} is the principal eigenaxis of linear loci, it must be shown that \mathbf{v} is a major intrinsic axis which is also an exclusive, fixed reference axis. It will first be argued that \mathbf{v} is a major intrinsic axis for a linear locus of points.

Using the definitions of Eqs (18), (19), or (20), the axis \mathbf{v} is a major intrinsic axis because all of the points \mathbf{x} on a linear locus satisfy similar algebraic and geometric constraints related to the locus of \mathbf{v} that are inherently specified by Eqs (18), (19), and (20). Therefore, \mathbf{v} is a major intrinsic axis of a linear locus. The uniform algebraic and geometric constraints satisfied by all of the points on a linear locus determine the properties exhibited by each point on the linear locus.

Again using the definitions of Eqs (18), (19), or (20), the axis \mathbf{v} is an exclusive, fixed reference axis because the uniform properties possessed by all of the points \mathbf{x} on a linear locus are defined solely by their relation to the axis of \mathbf{v} . Therefore, all of the points \mathbf{x} on a given line, plane, or hyperplane, explicitly and exclusively reference the major intrinsic axis \mathbf{v} of the linear locus. It follows that the vector \mathbf{v} provides an exclusive, fixed reference axis for a linear locus.

It is concluded that the vector \mathbf{v} is a major intrinsic axis that coincides as an exclusive, fixed reference axis for a linear locus. It follows

that the vector \mathbf{v} is the major axis of linear loci. Therefore, the vector denoted by \mathbf{v} in Eqs (18), (19), and (20) is the principal eigenaxis of linear curves and plane or hyperplane surfaces in \mathbb{R}^d .

I will now use Eq. (20) to develop a coordinate form locus equation which I will use to identify a uniform property exhibited by any point on a linear curve or surface.

4.0.7 Coordinate Form Equation of a Linear Locus

Using Eq. (20), it follows that any line l in the Euclidean plane \mathbb{R}^2 and any plane p or hyperplane h in Euclidean space \mathbb{R}^d is described by the locus equation

$$\mathbf{x}^T \mathbf{u}_{P_e} = \Delta, \quad (21)$$

where \mathbf{u}_{P_e} is a unit length principal eigenaxis that is perpendicular to l , p , or h , and Δ denotes the distance of l , p , or h to the origin. The unit eigenvector \mathbf{u}_{P_e} specifies the direction of a principal eigenaxis of a linear curve or surface, while the distance Δ of a line, plane, or hyperplane from the origin is specified by the magnitude $\|\mathbf{v}\|$ of its principal eigenaxis \mathbf{v} .

Express \mathbf{u}_{P_e} in terms of standard orthonormal basis vectors

$$\{\mathbf{e}_1 = (1, 0, \dots, 0), \dots, \mathbf{e}_d = (0, 0, \dots, 1)\},$$

so that

$$\mathbf{u}_{P_e} = \cos \alpha_1 \mathbf{e}_1 + \cos \alpha_2 \mathbf{e}_2 + \dots + \cos \alpha_d \mathbf{e}_d,$$

where $\cos \alpha_i$ are the direction cosines between \mathbf{u}_{P_e} and \mathbf{e}_i . The term $\cos \alpha_i$ is the i^{th} component of the unit principal eigenaxis \mathbf{u}_{P_e} along the coordinate axis \mathbf{e}_i , where each eigen-scale $\cos \alpha_i$ is said to be normalized.

Substitution of the expression for \mathbf{u}_{P_e} into Eq. (21) produces a coordinate form locus equation

$$x_1 \cos \alpha_1 + x_2 \cos \alpha_2 + \dots + x_d \cos \alpha_d = \Delta, \quad (22)$$

which is satisfied by the eigen-transformed coordinates $\cos \alpha_i x_i$ of all of the points \mathbf{x} on the locus of a line, plane, or hyperplane. Equation (22) is similar to the well-known coordinate equation version of a linear locus

$$\alpha_1 x_1 + \alpha_2 x_2 + \dots + \alpha_n x_n = p,$$

which is a unique equation for a given linear locus if and only if it contains the components $\cos \alpha_i$ of the unit principal eigenaxis \mathbf{u}_{P_e} of the linear locus. I will now use Eq. (22) to define a uniform property which is exhibited by any point on a linear locus.

4.0.8 Uniform Property of a Linear Locus

Using Eq. (22), it follows that a line, plane, or hyperplane is a locus of points \mathbf{x} , all of which possess a set of normalized, eigen-scaled coordinates:

$$\mathbf{x} = (\cos \alpha_1 x_1, \cos \alpha_2 x_2, \dots, \cos \alpha_d x_d)^T,$$

such that the sum of those coordinates equals the distance Δ that the line, plane, or hyperplane is from the origin $(0, 0, \dots, 0)$:

$$\sum_{i=1}^d \cos \alpha_i x_i = \Delta, \quad (23)$$

where x_i are point coordinates or vector components, and $\cos \alpha_i$ are the direction cosines between a unit length principal eigenaxis \mathbf{u}_{P_e} and the coordinate axes $\mathbf{e}_i : \{\mathbf{e}_1 = (1, 0, \dots, 0), \dots, \mathbf{e}_d = (0, 0, \dots, 1)\}$.

It follows that a point \mathbf{x} is on the locus of a line l , plane p , or hyperplane h , if and only if the normalized, eigen-scaled coordinates of \mathbf{x} satisfy Eq. (23); otherwise, the point \mathbf{x} is not on the locus of points described by Eqs (18), (19), and (21). It is concluded that all of the points \mathbf{x} on a linear locus possess a characteristic set of eigen-scaled coordinates, such that the inner product of each vector \mathbf{x} with a unit length principal eigenaxis \mathbf{u}_{P_e} satisfies the distance Δ of the linear locus from the origin. It is also concluded that the sum of normalized, eigen-scaled coordinates of any point on a linear locus satisfies the magnitude of the principal eigenaxis of the linear locus. Properties of principal eigenaxes are examined next.

4.1 Properties of Principal Eigenaxes

Take any line, plane, or hyperplane in \mathbb{R}^d . Given the line, plane, or hyperplane and Eqs (18) or (19), it follows that a principal eigenaxis \mathbf{v} exists, such that the endpoint of \mathbf{v} is on the line, plane, or hyperplane, and the axis of \mathbf{v} is perpendicular to the line, plane, or hyperplane. Using Eq. (20), it follows that the length $\|\mathbf{v}\|$ of \mathbf{v} is determined by the line, plane, or hyperplane. Using Eq. (22), it follows that the unit principal eigenaxis \mathbf{u}_{P_e} of the linear curve or surface is characterized by a unique set of direction cosines $\{\cos \alpha_i\}_{i=1}^d$ between \mathbf{u}_{P_e} and the standard set of basis vectors $\{\mathbf{e}_i\}_{i=1}^d$.

Next, take any principal eigenaxis \mathbf{v} in \mathbb{R}^d . Given the principal eigenaxis \mathbf{v} and Eqs (18) or (19), it follows that a line, plane, or hyperplane exists that is perpendicular to \mathbf{v} , such that the endpoint of the principal eigenaxis \mathbf{v} is on the line, plane, or hyperplane. Using Eq. (20), it follows that the distance of the line, plane, or hyperplane from the origin is specified by the magnitude $\|\mathbf{v}\|$ of the principal eigenaxis \mathbf{v} . I will now

show that the principal eigenaxis of any linear locus satisfies the linear locus in terms of its eigenenergy.

4.1.1 Characteristic Eigenenergy

Take the principal eigenaxis \mathbf{v} of any line, plane, or hyperplane in \mathbb{R}^d . It follows that the principal eigenaxis \mathbf{v} satisfies Eqs (18), (19), and (20). Using Eqs (18) or (19), it follows that the principal eigenaxis \mathbf{v} satisfies a linear locus in terms of its squared length $\|\mathbf{v}\|^2$:

$$\mathbf{v}^T \mathbf{v} = \|\mathbf{v}\|^2 = \sum_{i=1}^d v_{i*}^2, \quad (24)$$

where v_{i*} are the eigen-coordinates of \mathbf{v} and $\|\mathbf{v}\|^2$ is the eigenenergy of \mathbf{v} . Therefore, the principal eigenaxis \mathbf{v} of any line, plane, or hyperplane exhibits a characteristic eigenenergy $\|\mathbf{v}\|^2$ that is unique for the linear locus. It follows that the locus of any line, plane, or hyperplane is determined by the eigenenergy $\|\mathbf{v}\|^2$ of its principal eigenaxis \mathbf{v} .

4.2 Inherent Property of a Linear Locus

It is concluded that the principal eigenaxis of any linear locus satisfies the linear locus in terms of its eigenenergy. It is also concluded that the locus of any line, plane, or hyperplane is determined by the eigenenergy of its principal eigenaxis. Thereby, the inherent property of a linear locus and its principal eigenaxis \mathbf{v} is the eigenenergy $\|\mathbf{v}\|^2$ exhibited by the principal eigenaxis \mathbf{v} .

4.2.1 Properties Possessed by Points on Linear Loci

Take any point \mathbf{x} on any linear locus. Given Eq. (18) and the point \mathbf{x} on the linear locus, it follows that the length of the component $\|\mathbf{x}\| \cos \phi$ of the vector \mathbf{x} along the principal eigenaxis \mathbf{v} of the linear locus satisfies the length $\|\mathbf{v}\|$ of \mathbf{v} , i.e., $\|\mathbf{x}\| \cos \phi = \|\mathbf{v}\|$, where the length $\|\mathbf{v}\|$ of \mathbf{v} determines the distance Δ of the linear locus from the origin.

Given Eq. (21) and the point \mathbf{x} on the linear locus, it follows that the inner product $\mathbf{x}^T \mathbf{u}_{P_e}$ of the vector \mathbf{x} with the unit principal eigenaxis \mathbf{u}_{P_e} of the linear locus satisfies the distance Δ of the linear locus from the origin, i.e., $\mathbf{x}^T \mathbf{u}_{P_e} = \Delta$. Likewise, using Eq. (23), it follows that the sum of the normalized, eigen-scaled coordinates of the point \mathbf{x} also satisfies the distance Δ of the linear locus from the origin, i.e., $\sum_{i=1}^d \cos \alpha_i x_i = \Delta$.

Finally, using Eq. (19), it follows that the inner product $\mathbf{x}^T \mathbf{v}$ of the vector \mathbf{x} with the principal eigenaxis \mathbf{v} of the linear locus

$$\mathbf{x}^T \mathbf{v} = \|\mathbf{v}\|^2,$$

satisfies the eigenenergy $\|\mathbf{v}\|^2$ of the principal eigenaxis \mathbf{v} of the linear locus.

In conclusion, it has been shown that the uniform properties exhibited by the points \mathbf{x} on a linear locus are determined by the locus of its principal eigenaxis \mathbf{v} which satisfies the linear locus in terms of its eigenenergy $\|\mathbf{v}\|^2$. Thereby, the vector components of a principal eigenaxis determine all forms of linear curves and surfaces, such that all of the points \mathbf{x} on a line, plane, or hyperplane explicitly and exclusively reference the principal eigenaxis \mathbf{v} in Eqs (18), (19), and (20).

It is concluded that the important generalizations for a linear locus are encoded within the eigenenergy of the locus of its principal eigenaxis. Likewise, it is concluded that a principal eigenaxis \mathbf{v} is an exclusive and distinctive coordinate axis that determines all of the points on a linear locus. Thereby, it is concluded that a principal eigenaxis provides an elegant, principal eigen-coordinate system for a linear locus of points.

In the next part of the paper, I will develop locus equations that determine Bayes' minimax, linear classification systems.

5 Loci of Bayes' Minimax Linear Classifiers

The development of locus equations for Bayes' minimax, linear classification systems requires solving three fundamental problems:

Problem 1 *Define the geometric figures in a linear classification system, where geometric figures involve points, vectors, lines, line segments, angles, regions, planes, and hyperplanes.*

Problem 2 *Define the geometric and statistical properties exhibited by all of the geometric figures.*

Problem 3 *Define the algebraic form of the equations that determine the geometric figures.*

I have formulated a solution that answers all three problems. My solution is based on three ideas:

Idea 1 Define a *dual locus of points* that describes Bayes' linear decision boundaries *and* encodes Bayes' likelihood ratio.

Idea 2 The dual locus of points must *encode* the *coordinate system* of the linear decision boundary.

Idea 3 The dual locus of points *must be an equalizer rule* that satisfies Bayes' minimax criterion in Eq. (11).

5.1 Key Elements of the Solution

Given Eq. (24), it follows that the important generalizations for a linear decision boundary are encoded within the eigenenergy of its principal eigenaxis. Given Eqs (19) and (20), it also follows that the principal eigenaxis of a linear decision boundary provides an elegant, statistical eigen-coordinate system for a linear classification system. Accordingly, the dual locus of points *must* be a *locus of principal eigenaxis components*.

In order for the locus of principal eigenaxis components to implement an equalizer rule, the locus of principal eigenaxis components must be formed by data points that are the *source of Bayes' decision error*, thereby determining decision regions that have conditional risks.

Given that the locus of principal eigenaxis components must encode Bayes' likelihood ratio, it follows that the locus of principal eigenaxis components must also be a *parameter vector* that *provides an estimate of class-conditional densities*.

I will now define data points which determine decision regions that have conditional risks.

5.2 Conditional Risks for Data Distributions

Generally speaking, Bayes' decision rule divides a feature space into two parts or regions in a manner that minimizes the probability of misclassification or decision error. Therefore, take a collection of feature vectors for any two pattern classes, where the data distributions are either overlapping or non-overlapping with each other. Data points in overlapping regions or tail regions determine decision regions that have conditional risks. See, e.g., Figs 4, 5), and 6).

5.2.1 Extreme Points

Data points located in overlapping regions or tails regions between two data distributions determine directions for which a given collection of data is most variable or spread out. Call these data points "extreme points," where any given extreme point is the endpoint of an extreme vector. Any given extreme point is characterized by an expected value (a central location) and a covariance (a spread). Figure 9a depicts locations of extreme points for two overlapping regions and Fig. 9b depicts locations of extreme points in two tail regions.

Extreme points are the source of Bayes' decision error. In particular, for any given collection of overlapping feature vectors, the Bayes' error in Eqs (3) and (4) is determined by expected values and covariances of extreme points in overlapping regions between the data distributions. Moreover, for any given collection of overlapping feature vectors and

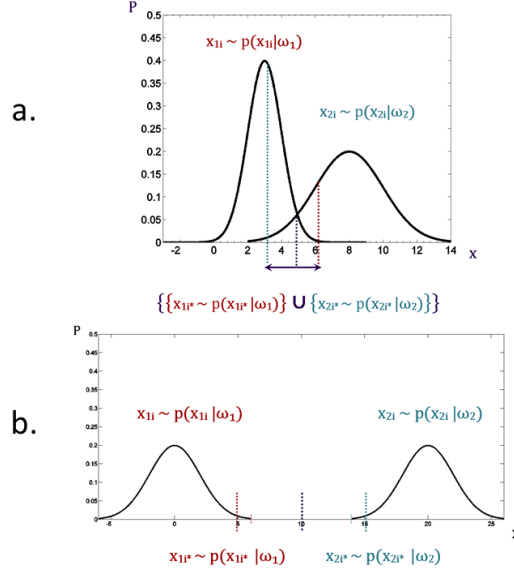


Figure 9: Location properties of extreme data points are determined by overlapping or non-overlapping intervals of probabilities. (a) For overlapping data distributions, overlapping intervals of probabilities determine numbers and locations of extreme data points. (b) Relatively few extreme data points are located within the tail regions of non-overlapping data distributions.

decision rule, the conditional risks (the decision errors) in Eqs (5) and (6) are determined by the locations of extreme points in the overlapping regions between the data distributions *and* the manner in which the feature space is partitioned (the decision regions).

Extreme points also describe tails regions between non-overlapping data distributions. Thus, for any given collection of non-overlapping feature vectors, the Bayes' error in Eqs (3) and (4) is determined by the locations of extreme points in the region between the non-overlapping data distributions. Accordingly, regions that have negligible conditional risk are functions of distances between extreme points. Likewise, the Bayes' error in Eqs (5) and (6) is determined by the locations of extreme points and the decision rule that partitions the feature space.

I will call a dual locus of principal eigenaxis components that encodes an estimate of class-conditional densities for extreme points a "linear eigenlocus." I will refer to the parameter vector that provides an estimate of class-conditional densities for extreme points as a "locus of likelihoods."

A linear eigenlocus is an equalizer rule formed by a dual locus of principal eigenaxis components and likelihoods that describes linear decision boundaries. I will call the process that generates a linear eigenlocus a

”linear eigenlocus transform.” I will introduce the primal equation of a linear eigenlocus in the next section. I will begin the next section by defining important geometric and statistical properties exhibited by weighted extreme points on a linear eigenlocus. I will define these properties in terms of geometric and statistical criterion.

5.3 Linear Eigenlocus Transforms

A high level description of linear eigenlocus transforms is outlined below. The description outlines essential geometric and statistical properties exhibited by weighted extreme points on a linear eigenlocus.

Form a locus of weighted extreme points which is a dual locus of likelihoods and principal eigenaxis components, where each weight encodes a class membership statistic and conditional density for an extreme point, and each weight determines the magnitude and eigenenergy of an extreme vector.

Choose each weight in a manner which ensures that:

Criterion 1 Each conditional density of an extreme point describes the central location (expected value) and the spread (covariance) of the extreme point.

Criterion 2 Distributions of the extreme points are distributed over the locus of likelihoods in a symmetrically balanced and well-proportioned manner.

Criterion 3 The total allowed eigenenergy possessed by each weighted extreme vector describes the probability of observing the extreme point within a localized region.

Criterion 4 The total allowed eigenenergies of weighted extreme vectors are symmetrically balanced with each other about a center of total allowed eigenenergy.

Criterion 5 The locus of principal eigenaxis components formed by weighted extreme vectors partitions any given feature space into congruent decision regions which are symmetrically partitioned by a linear decision boundary.

Criterion 6 The locus of principal eigenaxis components formed by weighted extreme vectors satisfies the linear decision boundary in terms of a critical minimum eigenenergy.

Criterion 7 The locus of likelihoods formed by weighted extreme points satisfies the linear decision boundary in terms of a minimum total probability of error.

Criterion 8 The Bayes' error, i.e., the conditional risk, in the congruent decision regions is equal.

I will develop locus equations that describe an equalizer rule which satisfies all of the above criteria. Linear eigenlocus transforms are produced by the inequality constrained optimization problem introduced next.

5.4 Primal Equation of a Linear Eigenlocus

A linear eigenlocus τ is estimated by solving an inequality constrained optimization problem:

$$\begin{aligned} \min \Psi(\tau) &= \|\tau\|^2/2 + C/2 \sum_{i=1}^N \xi_i^2 \\ \text{s.t. } y_i (\mathbf{x}_i^T \tau + \tau_0) &\geq 1 - \xi_i, \quad \xi_i \geq 0, \quad i = 1, \dots, N, \end{aligned} \quad (25)$$

where τ is a $d \times 1$ constrained, primal linear eigenlocus which is a dual locus of likelihoods and principal eigenaxis components, $\|\tau\|^2$ is the critical minimum eigenenergy exhibited by τ , τ_0 is a functional of τ , C and ξ_i are regularization parameters, and y_i are class membership statistics or weights: if $\mathbf{x}_i \in \omega_1$, assign $y_i = 1$; if $\mathbf{x}_i \in \omega_2$, assign $y_i = -1$.

Equation (25) is the primal equation of a linear eigenlocus in which N primal linear eigenlocus equations must be satisfied:

$$y_i (\mathbf{x}_i^T \tau + \tau_0) \geq 1 - \xi_i, \quad \xi_i \geq 0, \quad i = 1, \dots, N,$$

such that a constrained, primal linear eigenlocus τ satisfies a critical minimum eigenenergy constraint:

$$\gamma(\tau) = \|\tau\|_{\min_c}^2. \quad (26)$$

Solving Eq. (25) involves solving a dual optimization problem that determines the fundamental unknowns of Eq. (25). Denote a Wolfe dual linear eigenlocus by ψ and the locus equation of ψ by $\max \Xi(\psi)$. Let ψ be a Wolfe dual of τ , such that proper and effective strong duality relationships exist between the algebraic systems of $\min \Psi(\tau)$ and $\max \Xi(\psi)$. Thereby, let ψ be related with τ in a symmetrical manner that specifies the locations of the principal eigenaxis components on τ . The Wolfe dual linear eigenlocus ψ is important for the following reasons.

5.5 Why the Wolfe Dual Eigenlocus Matters

Duality relationships for Lagrange multiplier problems are based on the premise that it is the Lagrange multipliers which are the fundamental unknowns associated with a constrained problem. Dual methods solve an alternate problem, termed the dual problem, whose unknowns are

the Lagrange multipliers of the first problem, termed the primal problem. Once the Lagrange multipliers are known, the solution to a primal problem can be determined (Luenberger, 2003).

5.5.1 The Real Unknowns

A constrained, primal linear eigenlocus is a dual locus of an equalizer rule formed by weighted extreme points, where each weight is determined by a class membership statistic and an eigen-scale. Each eigen-scale encodes a conditional density for a weighted extreme point on a locus of likelihoods, and each eigen-scale determines the magnitude of a weighted extreme vector on a locus of principal eigenaxis components. The main issue concerns how the eigen-scales are determined.

5.5.2 The Fundamental Unknowns

The fundamental unknowns are the eigen-scales of the principal eigenaxis components on a Wolfe dual linear eigenlocus ψ .

5.6 Strong Dual Linear Eigenlocus Transforms

For the problem of linear eigenlocus transforms, the Lagrange multipliers method introduces a Wolfe dual linear eigenlocus ψ of principal eigenaxis components, for which the Lagrange multipliers $\{\psi_i\}_{i=1}^N$ are the magnitudes or lengths of a set of Wolfe dual principal eigenaxis components $\{\psi_i \vec{e}_i\}_{i=1}^N$, where $\{\vec{e}_i\}_{i=1}^N$ are non-orthogonal unit vectors, and finds extrema for the restriction of a primal linear eigenlocus τ to a Wolfe dual eigenspace. Accordingly, the fundamental unknowns associated with Eq. (25) are the magnitudes or lengths of the Wolfe dual principal eigenaxis components on ψ .

Strong Duality Because Eq. (25) is a convex programming problem, the theorem for convex duality guarantees an equivalence and corresponding symmetry between a constrained primal linear eigenlocus τ and its Wolfe dual ψ (Nash and Sofer, 1996; Luenberger, 2003). Strong duality holds between the algebraic systems of $\min \Psi(\tau)$ and $\max \Xi(\psi)$, so that the duality gap between the constrained primal and the Wolfe dual linear eigenlocus solution is zero (Luenberger, 1969; Nash and Sofer, 1996; Fletcher, 2000; Luenberger, 2003).

The locus equation of a Wolfe dual linear eigenlocus will be derived by means of the Lagrangian equation that is introduced next.

5.7 The Lagrangian of the Linear Eigenlocus

The inequality constrained optimization problem in Eq. (25) is solved by using Lagrange multipliers $\psi_i \geq 0$ and the Lagrangian:

$$\begin{aligned} L_{\Psi(\tau)}(\tau, \tau_0, \xi, \psi) = & \|\tau\|^2 / 2 \\ & + C/2 \sum_{i=1}^N \xi_i^2 \\ & - \sum_{i=1}^N \psi_i \\ & \times \{y_i (\mathbf{x}_i^T \tau + \tau_0) - 1 + \xi_i\}. \end{aligned} \quad (27)$$

The Karush-Kuhn-Tucker (KKT) constraints on the Lagrangian $L_{\Psi(\tau)}$ produce an algebraic system of locus equations:

$$\tau - \sum_{i=1}^N \psi_i y_i \mathbf{x}_i = 0, \quad i = 1, \dots, N, \quad (28)$$

$$\sum_{i=1}^N \psi_i y_i = 0, \quad i = 1, \dots, N, \quad (29)$$

$$C \sum_{i=1}^N \xi_i - \sum_{i=1}^N \psi_i = 0, \quad (30)$$

$$\psi_i \geq 0, \quad i = 1, \dots, N, \quad (31)$$

$$\psi_i [y_i (\mathbf{x}_i^T \tau + \tau_0) - 1 + \xi_i] \geq 0, \quad i = 1, \dots, N, \quad (32)$$

that are jointly satisfied by a constrained primal and a Wolfe dual linear eigenlocus (Cortes and Vapnik, 1995; Burges, 1998; Cristianini and Shawe-Taylor, 2000; Scholkopf and Smola, 2002). I will define the manner in which the KKT constraints determine geometric and statistical properties exhibited by weighted extreme points on a Wolfe dual ψ and a constrained primal τ linear eigenlocus. I will demonstrate that the KKT constraints on ψ and τ ensure that τ is an equalizer rule which encodes a likelihood ratio that describes linear decision boundaries.

The equation of a Wolfe dual linear eigenlocus is introduced next.

5.8 Wolfe Dual Equation of a Linear Eigenlocus

The resulting expressions for a primal linear eigenlocus τ and regularization parameters ξ_i and C , in terms of a Wolfe dual linear eigenlocus ψ , are substituted into the Lagrangian functional $L_{\Psi(\tau)}$ of Eq. (27) and simplified. This produces the equation of a Wolfe dual linear eigenlocus:

$$\max \Xi(\psi) = \sum_{i=1}^N \psi_i - \sum_{i,j=1}^N \psi_i \psi_j y_i y_j \frac{[\mathbf{x}_i^T \mathbf{x}_j + \delta_{ij}/C]}{2}, \quad (33)$$

which is subject to the algebraic constraints that $\sum_{i=1}^N y_i \psi_i = 0$ and $\psi_i \geq 0$, where δ_{ij} is the Kronecker δ defined as unity for $i = j$ and 0 otherwise.

Equation (33) can be written in vector notation by letting $\mathbf{Q} \triangleq \epsilon \mathbf{I} + \tilde{\mathbf{X}}\tilde{\mathbf{X}}^T$ and $\tilde{\mathbf{X}} \triangleq \mathbf{D}_y \mathbf{X}$, where \mathbf{D}_y is an $N \times N$ diagonal matrix of training weights (labels) y_i and the $N \times d$ data matrix is $\mathbf{X} = (\mathbf{x}_1, \mathbf{x}_2, \dots, \mathbf{x}_N)^T$. This produces the matrix version of the equation of a primal linear eigenlocus within its Wolfe dual eigenspace:

$$\max \Xi(\psi) = \mathbf{1}^T \psi - \frac{\psi^T \mathbf{Q} \psi}{2}, \quad (34)$$

which is subject to the algebraic constraints $\psi^T \mathbf{y} = 0$ and $\psi_i \geq 0$ (Reeves, 2009).

5.8.1 Loci of Quadratic Forms

The representation of a constrained primal linear eigenlocus τ within its Wolfe dual eigenspace involves the eigensystem of the constrained quadratic form $\psi^T \mathbf{Q} \psi$ in Eq. (34), where ψ is the principal eigenvector of \mathbf{Q} , such that $\psi^T \mathbf{y} = 0$ and $\psi_i \geq 0$.

The standard quadratic form

$$\mathbf{x}^T \mathbf{A} \mathbf{x} = 1,$$

is a locus equation that describes d -dimensional circles, ellipses, hyperbolae, parabolas, lines, or points, where a symmetric matrix \mathbf{A} encodes algebraic constraints that are satisfied by the points \mathbf{x} on a given locus. The eigenvalues of \mathbf{A} determine the shape of a given locus and the principal eigenvector of \mathbf{A} determines the major (principal) axis of a given locus (Hewson, 2009).

Alternatively, principal eigenvectors of sample correlation and covariance matrices determine principal axes that describe the direction in which the data is the most variable or spread out (Duda et al., 2001; Hastie et al., 2001; Jolliffe, 2002).

I will demonstrate that the locus equation of ψ produces a dual locus ψ that satisfies a state of statistical equilibrium such that the total allowed eigenenergies $\|\tau\|_{\min_c}^2$ exhibited by τ are symmetrically balanced with each other about a center of total allowed eigenenergy. I will now use the KKT constraints in Eqs (28) and (31) to define the locus equation of a constrained, primal linear eigenlocus τ .

5.9 The Constrained Primal Linear Eigenlocus

The KKT constraint in Eq. (31) requires that the length ψ_i of each principal eigenaxis component $\psi_i \vec{\mathbf{e}}_i$ on ψ either satisfy or exceed zero: $\psi_i \geq 0$. Any principal eigenaxis component $\psi_i \vec{\mathbf{e}}_i$ which has zero length ($\psi_i = 0$) satisfies the origin $P_0(0, 0, \dots, 0)$ and is not on the Wolfe dual linear eigenlocus ψ . It follows that the constrained, primal principal

eigenaxis component $\psi_i \mathbf{x}_i$ also has zero length ($\|\psi_i \mathbf{x}_i\| = 0$) and is not on the constrained, primal linear eigenlocus τ .

Using the KKT constraints in Eqs (28) and (31), it follows that an estimate for τ satisfies the following locus equation:

$$\tau = \sum_{i=1}^N y_i \psi_i \mathbf{x}_i, \quad (35)$$

where the y_i terms are training set labels (weights) (if \mathbf{x}_i is a member of class ω_1 , assign $y_i = 1$; otherwise, assign $y_i = -1$) and the magnitude ψ_i of each principal eigenaxis component $\psi_i \vec{\mathbf{e}}_i$ on ψ is greater than or equal to zero: $\psi_i \geq 0$.

Data points \mathbf{x}_i correlated with Wolfe dual principal eigenaxis components $\psi_i \vec{\mathbf{e}}_i$ that have non-zero magnitudes $\psi_i > 0$ are termed extreme vectors. Accordingly, extreme vectors are unscaled, primal principal eigenaxis components on τ . Geometric and statistical properties of extreme vectors are outlined below.

5.9.1 Properties of Extreme Vectors

Take a collection of training data drawn from any two statistical distributions. An extreme point is defined to be a data point which exhibits a high variability of geometric location, that is, possesses a large covariance, such that it is located (1) relatively far from its distribution mean, (2) relatively close to the mean of the other distribution, and (3) relatively close to other extreme points. Therefore, an extreme point is located somewhere within either an overlapping region or a tail region between the two data distributions.

Given the geometric and statistical properties exhibited by the locus of an extreme point, it follows that a set of extreme vectors determine principal directions of large covariance for a given collection of training data. Thus, extreme vectors are discrete principal components that determine directions for which a given collection of training data is most variable or spread out. Accordingly, the loci of a set of extreme vectors span a region of large covariance between two distributions of training data. Decision regions and conditional risks for overlapping and non-overlapping data distributions are defined next.

Overlapping Data Distributions For overlapping data distributions, the loci of the extreme vectors from each pattern class are distributed within bipartite, joint geometric regions of large covariance, both of which span the region of data distribution overlap. Therefore, decision regions that have significant conditional risks are functions of overlapping intervals of probabilities that determine numbers and locations of extreme points. Figure 9a depicts how extreme points from two pat-

tern classes are located within bipartite, joint geometric regions of large variance that are located between two overlapping data distributions.

Non-overlapping Data Distributions For non-overlapping data distributions, the loci of the extreme vectors are distributed within bipartite, disjoint geometric regions of large covariance, i.e., separate tail regions, that are located between the data distributions. Because tail regions of distributions are determined by intervals of low probability, relatively few extreme points are located within tail regions. Thereby, relatively few extreme points are located between non-overlapping data distributions. Moreover, decision regions that have *negligible* conditional risks are functions of intervals of low probability that determine tail regions. Figure 9b illustrates how small numbers of extreme points are located within the tail regions of non-overlapping Gaussian data distributions.

5.10 Primal Linear Eigenlocus Components

All of the principal eigenaxis components on a constrained, primal linear eigenlocus τ are weighted (labeled), eigen-scaled extreme points in \mathbb{R}^d . Denote the weighted, eigen-scaled extreme vectors that belong to class ω_1 and ω_2 by $\psi_{1_{i*}} \mathbf{x}_{1_{i*}}$ and $-\psi_{2_{i*}} \mathbf{x}_{2_{i*}}$, with eigen-scales $\psi_{1_{i*}}$ and $\psi_{2_{i*}}$, extreme vectors $\mathbf{x}_{1_{i*}}$ and $\mathbf{x}_{2_{i*}}$, and weights (labels) $y_i = 1$ and $y_i = -1$ respectively. Let there be l_1 weighted, eigen-scaled extreme points $\{\psi_{1_{i*}} \mathbf{x}_{1_{i*}}\}_{i=1}^{l_1}$ and l_2 weighted, eigen-scaled extreme points $\{-\psi_{2_{i*}} \mathbf{x}_{2_{i*}}\}_{i=1}^{l_2}$.

Given Eq. (35) and the assumptions outlined above, it follows that an estimate for a constrained, primal linear eigenlocus τ is based on the vector difference between a pair of constrained, primal linear eigenlocus components:

$$\begin{aligned} \tau &= \sum_{i=1}^{l_1} \psi_{1_{i*}} \mathbf{x}_{1_{i*}} - \sum_{i=1}^{l_2} \psi_{2_{i*}} \mathbf{x}_{2_{i*}}, \\ &= \tau_1 - \tau_2, \end{aligned} \tag{36}$$

where the constrained, primal linear eigenlocus components $\sum_{i=1}^{l_1} \psi_{1_{i*}} \mathbf{x}_{1_{i*}}$ and $\sum_{i=1}^{l_2} \psi_{2_{i*}} \mathbf{x}_{2_{i*}}$ are denoted by τ_1 and τ_2 respectively. The eigen-scaled extreme points $\{\psi_{1_{i*}} \mathbf{x}_{1_{i*}}\}_{i=1}^{l_1}$ and $\{\psi_{2_{i*}} \mathbf{x}_{2_{i*}}\}_{i=1}^{l_2}$ on τ_1 and τ_2 determine the loci of τ_1 and τ_2 and therefore determine the dual locus of $\tau = \tau_1 - \tau_2$. Figure 10 depicts how the loci of τ_1 and τ_2 determine the dual locus of τ .

I will now define how the regularization parameters C and ξ_i in Eqs (25) and (34) affect the dual locus of τ .

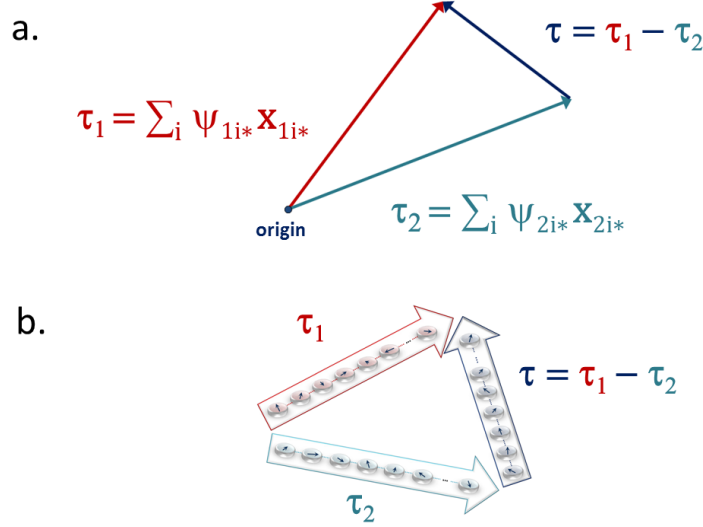


Figure 10: (a) A primal linear eigenlocus τ within its Wolfe dual eigenspace is represented by the vector difference $\tau_1 - \tau_2$ between a pair of constrained, primal linear eigenlocus components τ_1 and τ_2 . (b) The eigen-scaled extreme points on τ_1 and τ_2 are depicted by variable length arrows pointing in various directions, which illustrate eigen-scaled extreme vectors that possess unchanged directions and eigen-balanced lengths.

5.11 Regularization Components

Regularization components are essential numerical ingredients in algorithms that involve inversions of data matrices (Linz, 1979; Groetsch, 1984; Wahba, 1987; Groetsch, 1993; Hansen, 1998; Engl et al., 2000; Zhdanov, 2002; Linz and Wang, 2003). Because linear eigenlocus transforms involve an inversion of the Gram matrix \mathbf{Q} in Eq. (34), some type of regularization is required for low rank Gram matrices (Reeves, 2009; Reeves and Jacyna, 2011).

Weak Dual Linear Eigenlocus Transforms

It has been shown that the number and the locations of the principal eigenaxis components on ψ and τ are considerably affected by the rank and eigenspectrum of \mathbf{Q} . In particular, low rank Gram matrices \mathbf{Q} generate "weak dual" linear eigenlocus transforms that produce irregular linear partitions of decision spaces (Reeves, 2015).

For example, given non-overlapping data distributions and low rank Gram matrices, weak dual linear eigenlocus transforms produce asymmetric linear partitions that exhibit optimal generalization performance at the expense of unnecessary principal eigenaxis components, where *all* of the training data is transformed into constrained, primal principal

eigenaxis components. For overlapping data distributions, incomplete eigenspectrums of low rank Gram matrices \mathbf{Q} result in weak dual linear eigenlocus transforms which determine ill-formed linear decision boundaries that exhibit substandard generalization performance (Reeves, 2009; Reeves and Jacyna, 2011; Reeves, 2015). All of these problems are solved by the regularization method that is described next.

5.11.1 Parameter Selection

For any collection of N training vectors of dimension d , where $d < N$, the Gram matrix \mathbf{Q} has low rank. It has been shown that the regularized form of \mathbf{Q} , for which $\epsilon \ll 1$ and $\mathbf{Q} \triangleq \epsilon \mathbf{I} + \tilde{\mathbf{X}}\tilde{\mathbf{X}}^T$, ensures that \mathbf{Q} has full rank and a complete eigenvector set, and therefore ensures that \mathbf{Q} has a complete eigenspectrum. The regularization constant C is related to the regularization parameter ϵ by $\frac{1}{C}$ (Reeves and Jacyna, 2011).

For N training vectors of dimension d , where $d < N$, all of the regularization parameters $\{\xi_i\}_{i=1}^N$ in the primal linear eigenlocus of Eq. (25) and all of its derivatives are set equal to a very small value: $\xi_i = \xi \ll 1$. The regularization constant C is set equal to $\frac{1}{\xi}$: $C = \frac{1}{\xi}$.

For N training vectors of dimension d , where $N < d$, all of the regularization parameters $\{\xi_i\}_{i=1}^N$ in the primal linear eigenlocus of Eq. (25) and all of its derivatives are set equal to zero: $\xi_i = \xi = 0$. The regularization constant C is set equal to infinity: $C = \infty$.

I will now define locus equations that determine the manner in which a constrained, primal linear eigenlocus partitions any given feature space into congruent decision regions.

6 Equation of an Equalizer Rule

A constrained, primal linear eigenlocus is a linear discriminant function. The KKT complementary conditions of optimization theory and the KKT constraint in Eq. (32) determine the manner in which the dual locus of τ partitions a feature space.

6.0.2 KKT Complementary Conditions

The KKT complementary conditions of optimization theory require that for all constraints that are not active, where locus equations are not satisfied as equalities:

$$y_i (\mathbf{x}_i^T \boldsymbol{\tau} + \tau_0) - 1 + \xi_i > 0,$$

and therefore are ill-defined, the corresponding magnitudes ψ_i of the Wolfe dual principal eigenaxis components $\psi_i \vec{\mathbf{e}}_i$ must be zero: $\psi_i = 0$ (Sundaram, 1996).

Let there be l active constraints. The theorem of Karush, Kuhn and Tucker provides the guarantee that a Wolf dual linear eigenlocus ψ exists

such that the following constraints are satisfied:

$$\{\psi_{i*} > 0\}_{i=1}^l,$$

and the following locus equations are satisfied:

$$\psi_{i*} [y_i (\mathbf{x}_{i*}^T \tau + \tau_0) - 1 + \xi_i] = 0, \quad i = 1, \dots, l,$$

where l Wolfe dual principal eigenaxis components $\psi_{i*} \vec{\mathbf{e}}_i$ have non-zero magnitudes $\{\psi_{i*} \vec{\mathbf{e}}_i | \psi_{i*} > 0\}_{i=1}^l$ (Sundaram, 1996).

The above condition is known as the condition of complementary slackness. Therefore, in order for the constraint $\psi_{i*} > 0$ to hold, the following locus equation must be satisfied:

$$y_i (\mathbf{x}_{i*}^T \tau + \tau_0) - 1 + \xi_i = 0.$$

Let there be l_1 locus equations that are precisely met as equalities:

$$\mathbf{x}_{1i*}^T \tau + \tau_0 + \xi_i = 1, \quad i = 1, \dots, l_1,$$

where $y_i = +1$, and let there be l_2 locus equations that are precisely met as equalities:

$$\mathbf{x}_{2i*}^T \tau + \tau_0 - \xi_i = -1, \quad i = 1, \dots, l_2,$$

where $y_i = -1$, and either $\xi_i = 0$ or $\xi_i \ll 1$.

It follows that the linear discriminant function

$$D(\mathbf{x}) = \tau^T \mathbf{x} + \tau_0, \tag{37}$$

satisfies the set of constraints:

$$D_0(\mathbf{x}) = 0, \quad D_{+1}(\mathbf{x}) = +1, \quad \text{and} \quad D_{-1}(\mathbf{x}) = -1.$$

I will now show that the constraints on the linear discriminant function $D(\mathbf{x})$ determine three equations of symmetrical, linear partitioning curves or surfaces, where the points on all three linear loci reference the constrained, primal linear eigenlocus τ . Returning to Eq. (20), recall that the equation of a linear locus can be written as

$$\frac{\mathbf{x}^T \mathbf{v}}{\|\mathbf{v}\|} = \|\mathbf{v}\|,$$

where the principal eigenaxis $\mathbf{v}/\|\mathbf{v}\|$ has length 1 and points in the direction of a principal eigenvector \mathbf{v} , and $\|\mathbf{v}\|$ is the distance of a line, plane, or hyperplane to the origin. Any point \mathbf{x} that satisfies the above equation is on the linear locus of points specified by \mathbf{v} , where all of the points \mathbf{x} on the linear locus reference the principal eigenaxis \mathbf{v} .

I will now define the locus equation of a linear decision boundary $D_0(\mathbf{x})$.

6.0.3 Equation of a Linear Decision Boundary $D_0(\mathbf{x})$

Using Eq. (20) and assuming that $D(\mathbf{x}) = 0$, the linear discriminant function

$$D(\mathbf{x}) = \tau^T \mathbf{x} + \tau_0,$$

can be rewritten as:

$$\frac{\mathbf{x}^T \tau}{\|\tau\|} = -\frac{\tau_0}{\|\tau\|}, \quad (38)$$

where $\frac{|\tau_0|}{\|\tau\|}$ is the distance of a linear decision boundary $D_0(\mathbf{x})$ to the origin. Any point \mathbf{x} that satisfies Eq. (38) is on the linear decision boundary $D_0(\mathbf{x})$. All of the points \mathbf{x} on the linear decision boundary $D_0(\mathbf{x})$ reference the constrained primal linear eigenlocus τ .

I will now define the locus equation of the linear decision border $D_{+1}(\mathbf{x})$.

6.0.4 Equation of the $D_{+1}(\mathbf{x})$ Decision Border

Using Eq. (20) and assuming that $D(\mathbf{x}) = 1$, the linear discriminant function can be rewritten as:

$$\frac{\mathbf{x}^T \tau}{\|\tau\|} = -\frac{\tau_0}{\|\tau\|} + \frac{1}{\|\tau\|}, \quad (39)$$

where $\frac{|1-\tau_0|}{\|\tau\|}$ is the distance of the linear decision border $D_{+1}(\mathbf{x})$ to the origin. Any point \mathbf{x} that satisfies Eq. (39) is on the linear decision border $D_{+1}(\mathbf{x})$. All of the points \mathbf{x} on the linear decision border $D_{+1}(\mathbf{x})$ reference the constrained primal linear eigenlocus τ .

I will now define the locus equation of the linear decision border $D_{-1}(\mathbf{x})$.

6.0.5 Equation of the $D_{-1}(\mathbf{x})$ Decision Border

Using Eq. (20) and assuming that $D(\mathbf{x}) = -1$, the linear discriminant function can be rewritten as:

$$\frac{\mathbf{x}^T \tau}{\|\tau\|} = -\frac{\tau_0}{\|\tau\|} - \frac{1}{\|\tau\|}, \quad (40)$$

where $\frac{|-1-\tau_0|}{\|\tau\|}$ is the distance of the linear decision border $D_{-1}(\mathbf{x})$ to the origin. Any point \mathbf{x} that satisfies Eq. (40) is on the linear decision border $D_{-1}(\mathbf{x})$. All of the points \mathbf{x} on the linear decision border $D_{-1}(\mathbf{x})$ reference the constrained primal linear eigenlocus τ .

It is concluded that the constrained linear discriminant function $D(\mathbf{x})$ of Eq. (37) determines three linear curves or surfaces, where all of the points on $D_0(\mathbf{x})$, $D_{+1}(\mathbf{x})$, and $D_{-1}(\mathbf{x})$ exclusively reference τ .

I will now use the locus equations of the linear decision borders to obtain an expression for the distance between the decision borders.

Distance Between Linear Decision Borders

Using Eqs (39) and (40), it follows that the distance between the linear decision borders $D_{+1}(\mathbf{x})$ and $D_{-1}(\mathbf{x})$:

$$\begin{aligned} D_{(D_{+1}(\mathbf{x})-D_{-1}(\mathbf{x}))} &= \left(-\frac{\tau_0}{\|\tau\|} + \frac{1}{\|\tau\|} \right) \\ &\quad - \left(-\frac{\tau_0}{\|\tau\|} - \frac{1}{\|\tau\|} \right), \\ &= \frac{2}{\|\tau\|}, \end{aligned} \tag{41}$$

is inversely proportional to twice the length of the constrained primal linear eigenlocus τ . Therefore, it is concluded that the span of the constrained geometric region between the linear decision borders is regulated by the statistic $2\|\tau\|^{-1}$.

I will now obtain expressions for distances between the linear decision borders and the linear decision boundary.

Distances Between the Decision Borders and Boundary

Using Eqs (38) and (39), it follows that the distance between the linear decision border $D_{+1}(\mathbf{x})$ and the linear decision boundary $D_0(\mathbf{x})$ is $\frac{1}{\|\tau\|}$:

$$\begin{aligned} D_{(D_{+1}(\mathbf{x})-D_0(\mathbf{x}))} &= \left(-\frac{\tau_0}{\|\tau\|} + \frac{1}{\|\tau\|} \right) \\ &\quad - \left(-\frac{\tau_0}{\|\tau\|} \right), \\ &= \frac{1}{\|\tau\|}, \end{aligned} \tag{42}$$

where the linear decision border $D_{+1}(\mathbf{x})$ and the linear decision boundary $D_0(\mathbf{x})$ delineate a constrained geometric region R_1 in \mathbb{R}^d .

Using Eqs (38) and (40), it follows that the distance between the linear decision boundary $D_0(\mathbf{x})$ and the linear decision border $D_{-1}(\mathbf{x})$ is also $\frac{1}{\|\tau\|}$:

$$\begin{aligned} D_{(D_0(\mathbf{x})-D_{-1}(\mathbf{x}))} &= \left(-\frac{\tau_0}{\|\tau\|} \right) \\ &\quad - \left(-\frac{\tau_0}{\|\tau\|} - \frac{1}{\|\tau\|} \right), \\ &= \frac{1}{\|\tau\|}, \end{aligned} \tag{43}$$

where the linear decision border $D_{-1}(\mathbf{x})$ and the linear decision boundary $D_0(\mathbf{x})$ delineate a constrained geometric region R_2 in \mathbb{R}^d .

It follows that the constrained geometric region R_1 between the linear decision border $D_{+1}(\mathbf{x})$ and the linear decision boundary $D_0(\mathbf{x})$ is congruent to the constrained geometric region R_2 between the linear decision boundary $D_0(\mathbf{x})$ and the linear decision border $D_{-1}(\mathbf{x})$: $R_1 \cong R_2$.

The equivalent distance of $\frac{1}{\|\tau\|}$ between each linear decision border and the linear decision boundary reveals that the bilateral symmetry exhibited by the linear decision borders along the linear decision boundary is regulated by the inverted length $\|\tau\|^{-1}$ of τ . It is concluded that the spans of the congruent geometric regions $R_1 \cong R_2$ delineated by the linear decision boundary of Eq. (38) and the linear decision borders of Eqs (39) and (40) are controlled by the statistic $\|\tau\|^{-1}$.

6.1 Eigenaxis of Symmetry

It has been shown that a constrained linear discriminant function $\tau^T \mathbf{x} + \tau_0$ describes three, symmetrical, linear partitioning curves or surfaces, where all of the points on a linear decision boundary $D_0(\mathbf{x})$ and linear decision borders $D_{+1}(\mathbf{x})$, and $D_{-1}(\mathbf{x})$ exclusively reference a constrained primal linear eigenlocus τ . Using Eqs (41), (42), and (43), it follows that τ is an eigenaxis of symmetry which delineates congruent decision regions $Z_1 \cong Z_2$ that are symmetrically partitioned by a linear decision boundary, where the span of both decision regions is regulated by the inverted length $\|\tau\|^{-1}$ of τ . Figure 11 illustrates how a constrained linear discriminant function $\tau^T \mathbf{x} + \tau_0$ describes three, symmetrical, linear partitioning curves or surfaces which delineate congruent decision regions $Z_1 \cong Z_2$ that will be shown to have equal conditional risks $\mathfrak{R}(Z_1) = \mathfrak{R}(Z_2)$.

Let Z denote the decision space determined by the decision regions Z_1 and Z_2 , where $Z \subset \mathbb{R}^d$, $Z = Z_1 + Z_2$, $Z_1 \cong Z_2$, and Z_1 and Z_2 are contiguous. I will now demonstrate that the distance between the loci of the constrained primal linear eigenlocus components τ_1 and τ_2 regulates the span of the decision space Z between the linear decision borders $D_{+1}(\mathbf{x})$ and $D_{-1}(\mathbf{x})$.

6.2 Regulation of Decision Space Z

Substitution of the expression for τ in Eq. (36) into Eq. (41) provides an expression for the span of the decision space Z between the linear decision borders $D_{+1}(\mathbf{x})$ and $D_{-1}(\mathbf{x})$:

$$Z \propto \frac{2}{\|\tau_1 - \tau_2\|}, \quad (44)$$

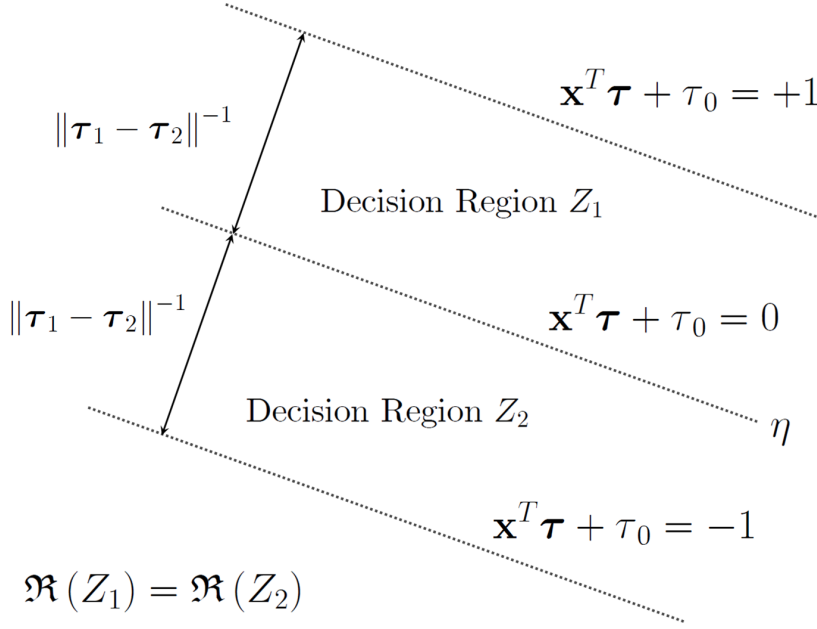


Figure 11: Linear eigenlocus transforms generate a dual locus of principal eigenaxis components and likelihoods $\tau = \tau_1 - \tau_2$ which determines congruent decision regions $Z_1 \cong Z_2$ that have equal conditional risks $\Re(Z_1) = \Re(Z_2)$.

where the constrained width of the decision space Z is inversely proportional to the magnitude of the vector difference of τ_1 and τ_2 . Thus, the span of the decision space Z between the linear borders $D_{+1}(\mathbf{x})$ and $D_{-1}(\mathbf{x})$ is inversely proportional to the distance between the loci of τ_1 and τ_2 . Thus, the distance between the linear decision borders is regulated by the magnitudes and the directions of the constrained primal linear eigenlocus components τ_1 and τ_2 on τ . Using the algebraic and geometric relationships in Eq. (16) depicted in Fig. 7a, it follows that the span of the decision space Z is regulated by the statistic $2(\|\tau_1\| \|\tau_2\| \cos \theta_{\tau_1 \tau_2})^{-1}$, where $\theta_{\tau_1 \tau_2}$ is the angle between τ_1 and τ_2 .

6.3 Regulation of Decision Regions Z_1 and Z_2

The distance between the loci of τ_1 and τ_2 also regulates the span of the decision regions between the linear decision boundary $D_0(\mathbf{x})$ and the linear decision borders $D_{+1}(\mathbf{x})$ and $D_{-1}(\mathbf{x})$. Substitution of the expression for τ in Eq. (36) into Eq. (42) provides an expression for the span of the decision region Z_1 between the linear decision border

$D_{+1}(\mathbf{x})$ and the linear decision boundary $D_0(\mathbf{x})$:

$$\begin{aligned} Z_1 &\propto \left(-\frac{\tau_0}{\|\tau_1 - \tau_2\|} + \frac{1}{\|\tau_1 - \tau_2\|} \right) \\ &\quad - \left(-\frac{\tau_0}{\|\tau_1 - \tau_2\|} \right), \\ &= \frac{1}{\|\tau_1 - \tau_2\|}, \end{aligned} \quad (45)$$

where the span of the decision region Z_1 satisfies the statistic $\|\tau_1 - \tau_2\|^{-1}$.

The span of the decision region Z_2 between the linear decision boundary $D_0(\mathbf{x})$ and the linear decision border $D_{-1}(\mathbf{x})$:

$$\begin{aligned} Z_2 &\propto \left(-\frac{\tau_0}{\|\tau_1 - \tau_2\|} \right) \\ &\quad - \left(-\frac{\tau_0}{\|\tau_1 - \tau_2\|} - \frac{1}{\|\tau_1 - \tau_2\|} \right), \\ &= \frac{1}{\|\tau_1 - \tau_2\|}, \end{aligned} \quad (46)$$

also satisfies the statistic $\|\tau_1 - \tau_2\|^{-1}$. It is concluded that the span of the congruent decision regions Z_1 and Z_2 between the linear decision boundary and the linear decision borders is inversely proportional to the magnitude of the vector difference of τ_1 and τ_2 :

$$\frac{1}{\|\tau_1 - \tau_2\|},$$

where $\|\tau_1 - \tau_2\|$ is the distance between the loci of τ_1 and τ_2 .

I will now derive an equation for the τ_0 term in Eq. (37). I will use the equation to obtain a locus equation that is the basis of a minimax test or an equalizer rule.

6.4 Equation of τ_0

Using the KKT complementary conditions of optimization theory and the KKT condition in Eq. (32), the following set of locus equations must be satisfied:

$$y_i (\mathbf{x}_{i*}^T \tau + \tau_0) - 1 + \xi_i = 0, \quad i = 1, \dots, l,$$

such that an estimate for τ_0 satisfies the locus equation:

$$\begin{aligned} \tau_0 &= \frac{1}{l} \sum_{i=1}^l y_i (1 - \xi_i) - \frac{1}{l} \sum_{i=1}^l \mathbf{x}_{i*}^T \tau, \\ &= \frac{1}{l} \sum_{i=1}^l y_i (1 - \xi_i) - \left(\frac{1}{l} \sum_{i=1}^l \mathbf{x}_{i*} \right)^T \tau. \end{aligned} \quad (47)$$

I will now use the equation for τ_0 to obtain an equation for a linear eigenlocus test that is used to classify unknown pattern vectors.

6.5 The Linear Eigenlocus Test

Substitution of the equation for τ_0 in Eq. (47) into the equation for the discriminant function $D(\mathbf{x})$ in Eq. (37) provides a linear eigenlocus test

$\hat{\Lambda}(\mathbf{x}) \underset{H_2}{\overset{H_1}{\gtrless}} 0$ for classifying an unknown pattern vector \mathbf{x} :

$$\begin{aligned} \hat{\Lambda}(\mathbf{x}) = & (\mathbf{x} - \bar{\mathbf{x}}_{i*})^T \tau \\ & + \frac{1}{l} \sum_{i=1}^l y_i (1 - \xi_i), \end{aligned} \quad (48)$$

where the statistic $\bar{\mathbf{x}}_{i*}$ determines the expected locus (the central location) of a set of extreme points and the statistic $\frac{1}{l} \sum_{i=1}^l y_i (1 - \xi_i)$ accounts for the class membership of the primal principal eigenaxis components on τ_1 and τ_2 .

I will now obtain a locus equation that provides geometric insight into how the linear discriminant function in Eq. (48) makes a decision.

6.5.1 The Decision Locus

Denote a unit linear eigenlocus $\tau / \|\tau\|$ by $\hat{\tau}$. Letting $\tau = \tau / \|\tau\|$ in Eq. (48) provides an expression for a decision locus

$$\begin{aligned} \hat{D}(\mathbf{x}) = & (\mathbf{x} - \bar{\mathbf{x}}_{i*})^T \tau / \|\tau\|, \\ & + \frac{1}{l \|\tau\|} \sum_{i=1}^l y_i (1 - \xi_i), \end{aligned} \quad (49)$$

which is determined by the scalar projection of $\mathbf{x} - \bar{\mathbf{x}}_{i*}$ onto $\hat{\tau}$. Accordingly, the component of $\mathbf{x} - \bar{\mathbf{x}}_{i*}$ along $\hat{\tau}$ determines a signed magnitude $\|\mathbf{x} - \bar{\mathbf{x}}_{i*}\| \cos \theta$ along the axis of $\hat{\tau}$, where θ is the angle between the transformed vector $\mathbf{x} - \bar{\mathbf{x}}_{i*}$ and $\hat{\tau}$.

It follows that the component $\text{comp}_{\hat{\tau}} \left(\overrightarrow{(\mathbf{x} - \bar{\mathbf{x}}_{i*})} \right)$ of the vector transform $\mathbf{x} - \bar{\mathbf{x}}_{i*}$ of an unknown pattern vector \mathbf{x} along the axis of a unit linear eigenlocus $\hat{\tau}$

$$\text{comp}_{\hat{\tau}} \left(\overrightarrow{(\mathbf{x} - \bar{\mathbf{x}}_{i*})} \right) = \|\mathbf{x} - \bar{\mathbf{x}}_{i*}\| \cos \theta,$$

determines a locus $P_{\hat{D}(\mathbf{x})}$ of a category decision, where $P_{\hat{D}(\mathbf{x})}$ is at a distance of $\|\mathbf{x} - \bar{\mathbf{x}}_{i*}\| \cos \theta$ from the origin, along the axis of a linear eigenlocus τ . Figure 12 depicts a decision locus generated by the linear discriminant function $\hat{D}(\mathbf{x})$ in Eq. (49).

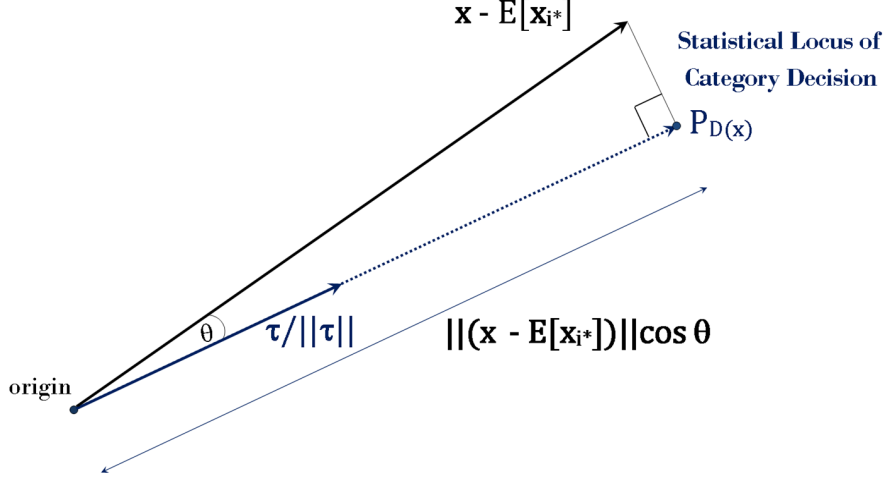


Figure 12: (a) A statistical decision locus $P_{D(\mathbf{x})}$ for an unknown transformed pattern vector $\mathbf{x} - E[\mathbf{x}_{i*}]$ that is projected onto $\tau / \|\tau\|$. The locus of $P_{D(\mathbf{x})}$ involves localized regions $\hat{Z}_1(\mathbf{x}_{i*})$ and $\hat{Z}_2(\mathbf{x}_{i*})$ that have conditional risks $P_e(\hat{Z}_1(\mathbf{x}_{i*}))$ and $P_e(\hat{Z}_2(\mathbf{x}_{i*}))$ determined by central locations and pointwise covariances of individual extreme points \mathbf{x}_{i*} .

The above expression for a decision locus $P_{\hat{D}(\mathbf{x})}$ provides geometric insight into how the linear discriminant function $D(\mathbf{x})$ in Eq. (37) assigns an unknown pattern vector to a pattern class. Using Eqs (38), (39), and (40), it follows that the linear discriminant function $\hat{D}(\mathbf{x})$ in Eq. (49) generates a decision locus $P_{\hat{D}(\mathbf{x})}$ which lies in a geometric region that is either (1) inside one of the decision regions Z_1 and Z_2 depicted in Fig. 11, (2) on the other side of the linear decision border $D_{+1}(\mathbf{x})$, where $\tau^T \mathbf{x} + \tau_0 = +1$, or (3) on the other side of the linear decision border $D_{-1}(\mathbf{x})$, where $\tau^T \mathbf{x} + \tau_0 = -1$.

Returning to Eq. (49), the linear discriminant function

$$\hat{D}(\mathbf{x}) = \text{comp}_{\vec{\tau}} \left(\overrightarrow{(\mathbf{x} - \bar{\mathbf{x}}_{i*})} \right) + \frac{1}{l \|\tau\|} \sum_{i=1}^l y_i (1 - \xi_i),$$

where $\tau = \tau / \|\tau\|$, generates an output based on the decision locus $\text{comp}_{\vec{\tau}}(\mathbf{x} - \bar{\mathbf{x}}_{i*})$ and the class membership statistic $\frac{1}{l \|\tau\|} \sum_{i=1}^l y_i (1 - \xi_i)$.

Substitution of the equation for τ in Eq. (36) into Eq. (48) provides a linear eigenlocus test in terms of the primal eigenlocus components τ_1

and τ_2 :

$$\begin{aligned}\widehat{\Lambda}(\mathbf{x}) &= \left(\mathbf{x} - \frac{1}{l} \sum_{i=1}^l \mathbf{x}_{i*} \right)^T \tau_1 \\ &\quad - \left(\mathbf{x} - \frac{1}{l} \sum_{i=1}^l \mathbf{x}_{i*} \right)^T \tau_2 \\ &\quad + \frac{1}{l} \sum_{i=1}^l y_i (1 - \xi_i) \underset{\omega_2}{\overset{\omega_1}{\geq}} 0.\end{aligned}\tag{50}$$

I will prove that a linear eigenlocus test $\widehat{\Lambda}(\mathbf{x})$ is an equalizer rule:

$$\begin{aligned}\mathfrak{R}_{mm}(Z|\tau) &= \int_{Z_1} p(\widehat{\Lambda}(\mathbf{x})|\omega_2) d\widehat{\Lambda} \\ &= \int_{Z_2} p(\widehat{\Lambda}(\mathbf{x})|\omega_1) d\widehat{\Lambda},\end{aligned}$$

where the conditional probability of error $P(D_2|\omega_1)$ for class ω_2 is equal to the conditional probability of error $P(D_1|\omega_2)$ for class ω_1 , given the linear eigenlocus test $\widehat{\Lambda}(\mathbf{x})$ in Eq. (50) and the congruent $Z_1 \cong Z_2$ decision regions Z_1 and Z_2 delineated by the linear decision boundary $D_0(\mathbf{x})$ in Eq. (38) and the linear decision borders $D_{+1}(\mathbf{x})$ and $D_{-1}(\mathbf{x})$ in Eqs (39) and (40).

A constrained, primal linear eigenlocus τ possesses a property which enables the discriminant function $D(\mathbf{x}) = \tau^T \mathbf{x} + \tau_0$ to satisfy Bayes' minimax risk \mathfrak{R}_{mm} :

$$\begin{aligned}\mathfrak{R}_{mm}(Z|\tau) &= \int_{Z_1} p(\mathbf{x}_{2i*}|\tau_2) d\tau_2 \\ &= \int_{Z_2} p(\mathbf{x}_{1i*}|\tau_1) d\tau_1,\end{aligned}$$

where $p(\mathbf{x}_{2i*}|\tau_2)$ and $p(\mathbf{x}_{1i*}|\tau_1)$ are class-conditional densities for extreme points. I will define this property after I define the fundamental properties possessed by a Wolfe dual linear eigenlocus ψ .

7 The Wolfe Dual Eigenspace

Let there be l principal eigenaxis components $\{\psi_{i*} \vec{\mathbf{e}}_i | \psi_{i*} > 0\}_{i=1}^l$ on a constrained, primal linear eigenlocus within its Wolfe dual eigenspace:

$$\max \Xi(\psi) = \mathbf{1}^T \psi - \frac{\psi^T \mathbf{Q} \psi}{2},$$

where the Wolfe dual linear eigenlocus ψ satisfies the algebraic constraints $\psi^T \mathbf{y} = 0$ and $\psi_{i*} > 0$. Quadratic forms $\psi^T \mathbf{Q} \psi$ describe five

classes of quadratic surfaces that include N -dimensional circles, ellipses, hyperbolae, parabolas, and lines (Hewson, 2009). I will now use Rayleigh's principle (see Strang, 1986) and the theorem for convex duality to define the geometric essence of ψ .

Rayleigh's principle guarantees that the quadratic

$$r(\mathbf{Q}, \mathbf{x}) = \mathbf{x}^T \mathbf{Q} \mathbf{x},$$

is maximized by the largest eigenvector \mathbf{x}_1 , with its maximal value equal to the largest eigenvalue $\lambda_1 = \max_{0 \neq \mathbf{x} \in \mathbb{R}^N} r(\mathbf{Q}, \mathbf{x})$. Raleigh's principle can be used to find principal eigenvectors \mathbf{x}_1 which satisfy additional constraints such as $a_1 x_1 + \dots + a_N x_N = c$, for which

$$\lambda_1 = \max_{a_1 x_1 + \dots + a_N x_N = c} r(\mathbf{Q}, \mathbf{x}).$$

The theorem for convex duality guarantees an equivalence and corresponding symmetry between a constrained primal linear eigenlocus τ and its Wolfe dual ψ . Raleigh's principle and the theorem for convex duality jointly indicate that Eq. (34) provides an estimate of the largest eigenvector ψ of a Gram matrix \mathbf{Q} for which ψ satisfies the constraints $\psi^T \mathbf{y} = 0$ and $\psi_i \geq 0$, such that ψ is a principal eigenaxis of three, symmetrical hyperplane partitioning surfaces associated with the constrained quadratic form $\psi^T \mathbf{Q} \psi$.

I will now show that maximization of the functional $\mathbf{1}^T \psi - \psi^T \mathbf{Q} \psi / 2$ requires that ψ satisfy an eigenenergy constraint which is symmetrically related to the restriction of the primal linear eigenlocus τ to its Wolfe dual eigenspace.

7.1 Eigenenergy Constraint on ψ

Equation (26) and the theorem for convex duality jointly indicate that ψ satisfies an eigenenergy constraint that is symmetrically related to the eigenenergy constraint on τ within its Wolfe dual eigenspace:

$$\|\psi\|_{\min_c}^2 \cong \|\tau\|_{\min_c}^2.$$

It follows that a Wolfe dual linear eigenlocus ψ satisfies an eigenenergy constraint

$$\max \psi^T \mathbf{Q} \psi = \lambda_{\max \psi} \|\psi\|_{\min_c}^2,$$

for which the functional $\mathbf{1}^T \psi - \psi^T \mathbf{Q} \psi / 2$ in Eq. (34) is maximized by the largest eigenvector ψ of \mathbf{Q} , such that the constrained quadratic form $\psi^T \mathbf{Q} \psi / 2$, where $\psi^T \mathbf{y} = 0$ and $\psi_i \geq 0$, reaches its smallest possible value. This indicates that principal eigenaxis components on ψ satisfy minimum length constraints. Principal eigenaxis components on ψ also satisfy an equilibrium constraint.

7.2 Equilibrium Constraint on ψ

The KKT condition in Eq. (29) requires that the magnitudes of the Wolfe dual principal eigenaxis components on ψ satisfy the equation:

$$(y_i = 1) \sum_{i=1}^{l_1} \psi_{1i*} + (y_i = -1) \sum_{i=1}^{l_2} \psi_{2i*} = 0,$$

such that the integrated lengths of the Wolfe dual principal eigenaxis components correlated with each pattern category must balance each other:

$$\sum_{i=1}^{l_1} \psi_{1i*} = \sum_{i=1}^{l_2} \psi_{2i*}. \quad (51)$$

Let $l_1 + l_2 = l$ and express a Wolfe dual linear eigenlocus ψ in terms of l non-orthogonal unit vectors $\{\vec{e}_{1*}, \dots, \vec{e}_{l*}\}$

$$\begin{aligned} \psi &= \sum_{i=1}^l \psi_{i*} \vec{e}_{i*}, \\ &= \sum_{i=1}^{l_1} \psi_{1i*} \vec{e}_{1i*} + \sum_{i=1}^{l_2} \psi_{2i*} \vec{e}_{2i*}, \\ &= \psi_1 + \psi_2, \end{aligned}$$

where each eigen-scaled, non-orthogonal unit vector $\psi_{1i*} \vec{e}_{1i*}$ or $\psi_{2i*} \vec{e}_{2i*}$ is correlated with an extreme vector \mathbf{x}_{1i*} or \mathbf{x}_{2i*} respectively, ψ_1 denotes the eigenlocus component $\sum_{i=1}^{l_1} \psi_{1i*} \vec{e}_{1i*}$ and ψ_2 denotes the eigenlocus component $\sum_{i=1}^{l_2} \psi_{2i*} \vec{e}_{2i*}$.

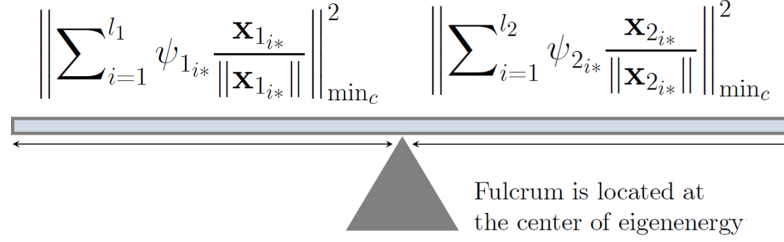
7.3 Symmetrical Balance Exhibited by Axis of ψ

Given Eq. (51), the axis of ψ can be regarded as a lever that has *equal weight on equal sides of a centrally placed fulcrum*. The equilibrium constraint on ψ in Eq. (51) ensures that the total allowed eigenenergies exhibited by the Wolfe dual principal eigenaxis components on ψ_1 and ψ_2 are symmetrically balanced with each other:

$$\left\| \sum_{i=1}^{l_1} \psi_{1i*} \vec{e}_{1i*} \right\|_{\min_c}^2 \equiv \left\| \sum_{i=1}^{l_2} \psi_{2i*} \vec{e}_{2i*} \right\|_{\min_c}^2, \quad (52)$$

about the center of total allowed eigenenergy $\|\psi\|_{\min_c}^2$ which is at the geometric center of ψ . Accordingly, the axis of ψ is a lever that has an equal distribution of eigenenergies on equal sides of a centrally placed fulcrum. Later on, I will show that symmetrically balanced, joint distributions of principal eigenaxis components on ψ and τ are symmetrically distributed over the axes of the Wolfe dual principal eigenaxis components on ψ and the correlated, unconstrained, primal principal eigenaxis components (extreme vectors) on τ .

Equal Wolfe Dual Eigenenergies on Equal Sides of ψ



Axis of ψ is symmetrically balanced
with respect to $\|\psi\|_{\min_c}^2$

Figure 13: The axis of ψ can be regarded as a lever that has an equal distribution of eigenenergies on equal sides of a centrally placed fulcrum located at the center of total allowed eigenenergy $\|\psi\|_{\min_c}^2$ which is at the geometric center of ψ .

Figure **13** depicts how the axis of ψ can be regarded as a lever that has an equal distribution of eigenenergies on equal sides of a centrally placed fulcrum located at the center of total allowed eigenenergy $\|\psi\|_{\min_c}^2$.

The eigenspectrum of \mathbf{Q} plays a fundamental role in describing the hyperplane surfaces which are implicitly delineated by ψ . I will now demonstrate that the eigenspectrum of \mathbf{Q} determines the shapes of the quadratic surfaces described by the constrained quadratic form in Eq. (34).

7.4 Eigenspectrum Shaping of Quadratic Surfaces

Take the standard equation of a quadratic form: $\mathbf{x}^T \mathbf{Q} \mathbf{x} = 1$. Write \mathbf{x} in terms of an orthogonal basis of unit eigenvectors $\{\mathbf{v}_1, \dots, \mathbf{v}_N\}$ so that $\mathbf{x} = \sum_{i=1}^N x_i \mathbf{v}_i$. Substitution of this expression into $\mathbf{x}^T \mathbf{Q} \mathbf{x}$

$$\mathbf{x}^T \mathbf{Q} \mathbf{x} = \left(\sum_{i=1}^N x_i \mathbf{v}_i \right)^T \mathbf{Q} \left(\sum_{j=1}^N x_j \mathbf{v}_j \right)$$

produces a simple coordinate form expression of a quadratic surface:

$$\lambda_1 x_1^2 + \lambda_2 x_2^2 + \dots + \lambda_N x_N^2 = 1, \quad (53)$$

solely in terms of the eigenvalues $\lambda_N \leq \lambda_{N-1} \dots \leq \lambda_1$ of the matrix \mathbf{Q} (Hewson, 2009). Equation (53) reveals that the *geometric shape* of a

quadratic surface is completely determined by the eigenvalues of the matrix associated with a quadratic form. This general property of quadratic forms will lead to far reaching consequences for linear and quadratic eigenlocus transforms.

I will now show that the inner product statistics of a training data collection essentially determine the geometric shapes of the quadratic surfaces described by the constrained quadratic form in Eq. (34).

Consider a Gram or kernel matrix \mathbf{Q} associated with the constrained quadratic form in Eq. (34). Denote the elements of the Gram or kernel matrix \mathbf{Q} by $\varphi(\mathbf{x}_i, \mathbf{x}_j)$, where $\varphi(\mathbf{x}_i, \mathbf{x}_j)$ denotes an inner product relationship between the training vectors \mathbf{x}_i and \mathbf{x}_j . The Cayley-Hamilton theorem provides the result that the eigenvalues $\{\lambda_i\}_{i=1}^N \in \Re$ of \mathbf{Q} satisfy the characteristic equation

$$\det(\mathbf{Q} - \lambda \mathbf{I}) = 0,$$

which is a polynomial of degree N . The roots $p(\lambda) = 0$ of the characteristic polynomial $p(\lambda)$ of \mathbf{Q} :

$$\det \left(\begin{bmatrix} \varphi(\mathbf{x}_1, \mathbf{x}_1) - \lambda_1 & \cdots & \varphi(\mathbf{x}_1, \mathbf{x}_N) \\ \varphi(\mathbf{x}_2, \mathbf{x}_1) & \cdots & \varphi(\mathbf{x}_2, \mathbf{x}_N) \\ \vdots & \ddots & \vdots \\ \varphi(\mathbf{x}_N, \mathbf{x}_1) & \cdots & \varphi(\mathbf{x}_N, \mathbf{x}_N) - \lambda_N \end{bmatrix} \right) = 0,$$

are also the eigenvalues $\lambda_N \leq \lambda_{N-1} \leq \dots \leq \lambda_1$ of \mathbf{Q} (Lathi, 1998). Therefore, given that (1) the roots of a characteristic polynomial $p(\lambda)$ vary continuously with its coefficients and that (2) the coefficients of $p(\lambda)$ can be expressed in terms of sums of principal minors (see Meyer, 2000), it follows that the eigenvalues of \mathbf{Q} vary continuously with the inner product elements $\varphi(\mathbf{x}_i, \mathbf{x}_j)$ of \mathbf{Q} . It is concluded that the eigenvalues $\lambda_N \leq \lambda_{N-1} \leq \dots \leq \lambda_1$ of a Gram or kernel matrix \mathbf{Q} are essentially determined by its inner product elements $\varphi(\mathbf{x}_i, \mathbf{x}_j)$.

7.5 Statistics for Quadratic Partitions

Given Eq. (53) and the continuous functional relationship between the inner product elements and the eigenvalues of a Gram or kernel matrix, it follows that the geometric shapes of the three, symmetrical quadratic partitioning surfaces described by Eqs (33) or (34) are an inherent function of inner product statistics $\varphi(\mathbf{x}_i, \mathbf{x}_j)$ between vectors. Therefore, it is concluded that the algebraic form of the inner product statistics encoded within Gram or kernel matrices essentially determines the shapes of the three, symmetrical quadratic partitioning surfaces described by Eqs (33) or (34).

I have demonstrated that the eigenvalues of a polynomial kernel matrix associated with the constrained quadratic form in Eq. (34), for which matrix elements $\varphi(\mathbf{x}_i, \mathbf{x}_j)$ have the algebraic form of $(\mathbf{x}_i^T \mathbf{x}_j + 1)^2$, describe either $l - 1$ -dimensional circles, ellipses, hyperbolae, or parabolas. Such second-order decision boundary estimates can be produced by solving an inequality constrained optimization problem that is similar in nature to Eq. (25) (see Reeves, 2015).

Let the Gram matrix \mathbf{Q} in Eq. (34) encode inner product statistics $\varphi(\mathbf{x}_i, \mathbf{x}_j) = \mathbf{x}_i^T \mathbf{x}_j$ for a separating hyperplane $H_0(\mathbf{x})$ and hyperplane decision borders $H_{+1}(\mathbf{x})$ and $H_{-1}(\mathbf{x})$ that have bilateral symmetry along $H_0(\mathbf{x})$. I will show that linear eigenlocus transforms map the weighted inner product statistics $\varphi(\mathbf{x}_i, \mathbf{x}_j) = \mathbf{x}_i^T \mathbf{x}_j$ encoded within \mathbf{Q}

$$\mathbf{Q}\psi = \lambda_{\max \psi} \psi$$

into a Wolfe dual linear eigenlocus of principal eigenaxis components

$$\mathbf{Q} \sum_{i=1}^l \psi_{i*} \vec{\mathbf{e}}_{i*} = \lambda_{\max \psi} \sum_{i=1}^l \psi_{i*} \vec{\mathbf{e}}_{i*},$$

formed by l eigen-scaled ψ_{i*} , non-orthogonal unit vectors $\{\vec{\mathbf{e}}_{1*}, \dots, \vec{\mathbf{e}}_{l*}\}$, where the locus of each Wolfe dual principal eigenaxis component $\psi_{i*} \vec{\mathbf{e}}_{i*}$ is determined by the direction and well-proportioned magnitude of a correlated extreme vector \mathbf{x}_{i*} .

By way of motivation, I will now define the fundamental property possessed by τ that enables a constrained, primal linear eigenlocus $\tau^T \mathbf{x} + \tau_0$ to satisfy Bayes' minimax risk $\mathfrak{R}_{mm}(Z|\tau)$.

8 The Property of Symmetrical Balance

I have demonstrated that linear eigenlocus discriminant functions $D(\mathbf{x}) = \tau^T \mathbf{x} + \tau_0$ describe contiguous and congruent $Z_1 \cong Z_2$ decision regions Z_1 and Z_2 that are delineated by linear decision borders $D_{+1}(\mathbf{x})$ and $D_{-1}(\mathbf{x})$ located at equal distances $\frac{2}{\|\tau\|}$ from a linear decision boundary $D_0(\mathbf{x})$, where all of the points \mathbf{x} on $D_{+1}(\mathbf{x})$, $D_{-1}(\mathbf{x})$ and $D_0(\mathbf{x})$ reference τ .

The bilateral symmetry exhibited by linear decision borders $D_{+1}(\mathbf{x})$ and $D_{-1}(\mathbf{x})$ along a linear decision boundary $D_0(\mathbf{x})$ is also known as *symmetrical balance*.

Symmetrical balance can be described as having equal "weight" on equal sides of a centrally placed fulcrum. When elements are arranged equally on either side of a central axis, the result is bilateral symmetry (Jirousek, 1995). As a practical example, consider the general machinery of a fulcrum and a lever, where a lever is any rigid object capable of

turning about some fixed point called a fulcrum. If a fulcrum is placed under directly under a lever's center of gravity, the lever will remain balanced. If a lever is of uniform dimensions and density, then the center of gravity is at the geometric center of the lever. Consider for example, the playground device known as a seesaw or teeter-totter. The center of gravity is at the geometric center of a teeter-totter, which is where the fulcrum of a seesaw is located (Asimov, 1966).

8.0.1 Symmetrical Balance and Bilateral Symmetry

Recall that the axis of ψ can be regarded as a lever that has an equal distribution of eigenenergies on equal sides of a centrally placed fulcrum located at the center of total allowed eigenenergy $\|\psi\|_{\min_c}^2$. Accordingly, the total allowed eigenenergies possessed by the principal eigenaxis components on ψ are symmetrically balanced with each other about the center of total allowed eigenenergy $\|\psi\|_{\min_c}^2$ which is at the geometric center of ψ .

Returning to Eq. (24), recall that the locus of any line, plane, or hyperplane, is determined by the eigenenergy $\|\mathbf{v}\|^2$ of its principal eigenaxis \mathbf{v} . Indeed, the inherent property of a linear locus and its principal eigenaxis \mathbf{v} is the eigenenergy $\|\mathbf{v}\|^2$ exhibited by the principal eigenaxis \mathbf{v} . Accordingly, Eqs (26) and (36) indicate that a constrained primal linear eigenlocus τ satisfies a linear decision boundary $D_0(\mathbf{x})$ and linear decision borders $D_{+1}(\mathbf{x})$ and $D_{-1}(\mathbf{x})$ in terms of its total allowed eigenenergies

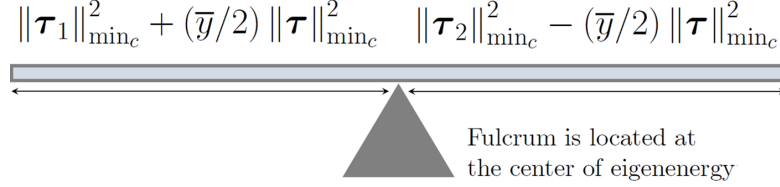
$$\begin{aligned}\|\tau\|_{\min_c}^2 &= \|\tau_1 - \tau_2\|_{\min_c}^2 \\ &\cong \|\tau_1\|_{\min_c}^2 + \|\tau_2\|_{\min_c}^2 - 2\tau_1^T \tau_2,\end{aligned}$$

where $\|\tau_1\|_{\min_c}^2$ is associated with the $D_{+1}(\mathbf{x})$ linear decision border, $\|\tau_2\|_{\min_c}^2$ is associated with the $D_{-1}(\mathbf{x})$ linear decision border, and $\|\tau\|_{\min_c}^2$ is associated with a linear decision boundary $D_0(\mathbf{x})$. It will be shown that the total allowed eigenenergy possessed by each weighted extreme vector describes the probability of observing an extreme point within a localized region.

I will demonstrate that a linear eigenlocus $\tau^T \mathbf{x} + \tau_0$ satisfies Bayes' minimax risk $\mathfrak{R}_{mm}(Z|\tau)$ because the axis of τ is essentially a lever that is symmetrically balanced with respect to the center of eigenenergy $\|\tau_1 - \tau_2\|_{\min_c}^2$ of τ . Figure 14 illustrates the property of symmetrical balance exhibited by τ .

I will show that the total allowed eigenenergies $\|\tau_1 - \tau_2\|_{\min_c}^2$ exhibited by the principal eigenaxis components on a constrained primal linear eigenlocus $\hat{\Lambda}(\mathbf{x}) = \mathbf{x}^T \tau + \tau_0$ are symmetrically balanced with each other in a manner which ensures that the linear discriminant function

Equal Constrained Primal Eigenenergies on Equal Sides of τ



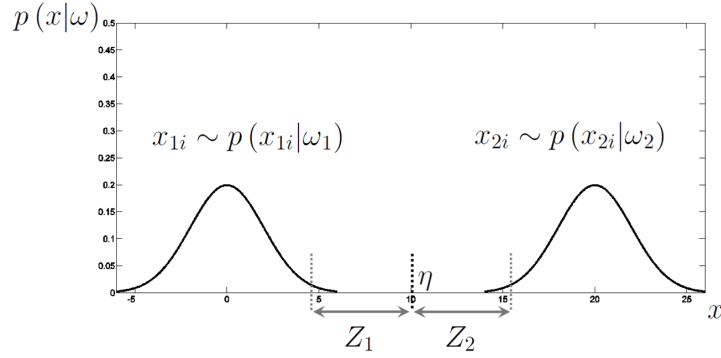
Axis of τ is symmetrically balanced
with respect to $\|\tau_1 - \tau_2\|_{\min_c}^2$

Figure 14: A linear eigenlocus $\tau^T \mathbf{x} + \tau_0$ satisfies Bayes' minimax risk $\mathfrak{R}_{mm}(Z|\tau)$ because the axis of τ is essentially a lever that is symmetrically balanced with respect to the center of eigenenergy $\|\tau_1 - \tau_2\|_{\min_c}^2$ of τ .

$D(\mathbf{x}) = \tau^T \mathbf{x} + \tau_0$ delineates congruent $Z_1 \cong Z_2$ decision regions Z_1 and Z_2 that have equal conditional risks $\mathfrak{R}(Z_1|\tau_2) = \mathfrak{R}(Z_2|\tau_1)$, where τ_2 and τ_1 are class-conditional densities for \mathbf{x}_{2i*} and \mathbf{x}_{1i*} extreme points respectively.

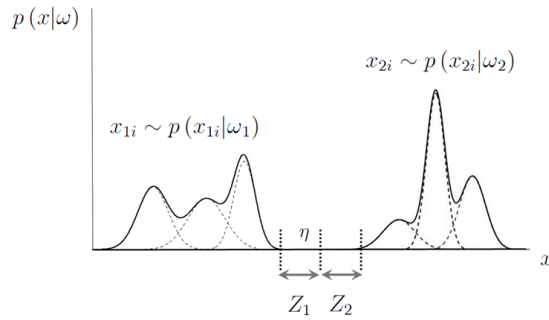
By way of illustration, Figs 15 and 16 illustrate how linear eigenlocus transforms determine decision regions Z_1 and Z_2 that minimize Bayes' risk $\mathfrak{R}_{\mathfrak{B}}(Z|\tau)$, where $\mathfrak{R}(Z_1|\tau_2) = \mathfrak{R}(Z_2|\tau_1) = 0$, for training data drawn from non-overlapping distributions; Fig. 17 illustrates how linear eigenlocus transforms determine decision regions Z_1 and Z_2 that minimize Bayes' risk $\mathfrak{R}_{\mathfrak{B}}(Z|\tau)$, where $\mathfrak{R}(Z_1|\tau_2) = \mathfrak{R}(Z_2|\tau_1)$, for training data drawn from overlapping Gaussian distributions that have similar covariance matrices; Fig. 18 illustrates how linear eigenlocus transforms determine decision regions Z_1 and Z_2 that minimize Bayes' minimax risk $\mathfrak{R}_{mm}(Z|\tau)$, where $\mathfrak{R}(Z_1|\tau_2) = \mathfrak{R}(Z_2|\tau_1)$, for training data drawn from overlapping Gaussian distributions that have dissimilar covariance matrices; Fig. 19 illustrates how linear eigenlocus transforms determine decision regions Z_1 and Z_2 that minimize Bayes' minimax risk $\mathfrak{R}_{mm}(Z|\tau)$, where $\mathfrak{R}(Z_1|\tau_2) = \mathfrak{R}(Z_2|\tau_1)$, for training data drawn from overlapping multimode distributions.

The general course of my argument is outlined below.



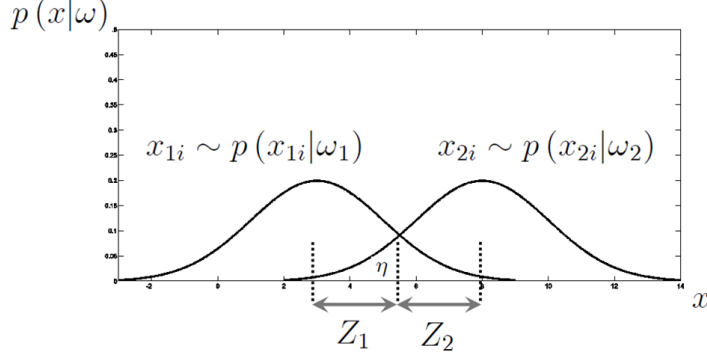
$$\begin{aligned}\mathfrak{R}_{\mathfrak{B}}(Z|\tau) &= \int_{Z_1} p(\mathbf{x}_{2_{i*}}|\tau_2) d\tau_2 \\ &= \int_{Z_2} p(\mathbf{x}_{1_{i*}}|\tau_1) d\tau_1 = 0\end{aligned}$$

Figure 15: Linear eigenlocus transforms determine decision regions Z_1 and Z_2 that minimize Bayes' risk $\mathfrak{R}_{\mathfrak{B}}(Z|\tau)$, where $\mathfrak{R}(Z_1|\tau_2) = \mathfrak{R}(Z_2|\tau_1) = 0$, for training data drawn from non-overlapping Gaussian distributions that have similar covariance matrices.



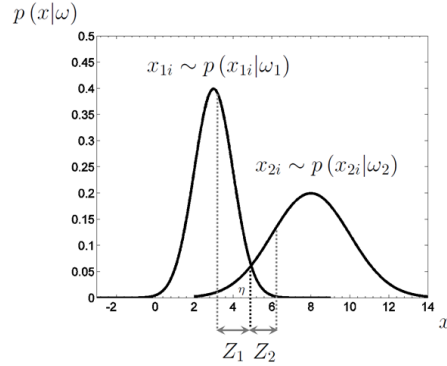
$$\begin{aligned}\mathfrak{R}_{\mathfrak{B}}(Z|\tau) &= \int_{Z_1} p(\mathbf{x}_{2_{i*}}|\tau_2) d\tau_2 \\ &= \int_{Z_2} p(\mathbf{x}_{1_{i*}}|\tau_1) d\tau_1 = 0\end{aligned}$$

Figure 16: Linear eigenlocus transforms determine decision regions Z_1 and Z_2 that minimize Bayes' risk $\mathfrak{R}_{\mathfrak{B}}(Z|\tau)$, where $\mathfrak{R}(Z_1|\tau_2) = \mathfrak{R}(Z_2|\tau_1) = 0$, for training data drawn from non-overlapping multimode distributions.



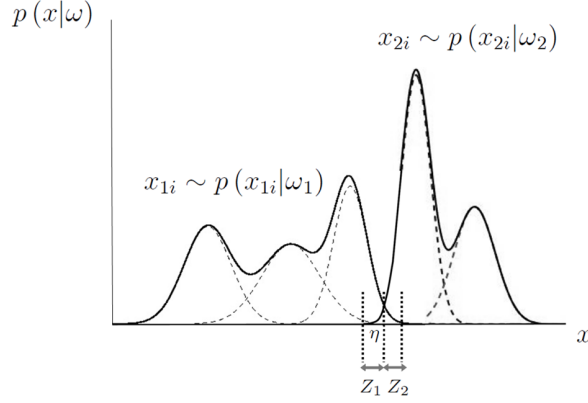
$$\begin{aligned}
\mathfrak{R}_{\mathfrak{B}}(Z|\tau) &= \int_{Z_1} p(\mathbf{x}_{2_{i*}}|\tau_2) d\tau_2 \\
&= \int_{Z_2} p(\mathbf{x}_{1_{i*}}|\tau_1) d\tau_1
\end{aligned}$$

Figure 17: Linear eigenlocus transforms determine decision regions Z_1 and Z_2 that minimize Bayes' risk $\mathfrak{R}_{\mathfrak{B}}(Z|\tau)$, where $\mathfrak{R}(Z_1|\tau_2) = \mathfrak{R}(Z_2|\tau_1)$, for training data drawn from overlapping Gaussian distributions that have similar covariance matrices.



$$\begin{aligned}
\mathfrak{R}_{\text{mm}}(Z|\tau) &= \int_{Z_1} p(\mathbf{x}_{2_{i*}}|\tau_2) d\tau_2 \\
&= \int_{Z_2} p(\mathbf{x}_{1_{i*}}|\tau_1) d\tau_1
\end{aligned}$$

Figure 18: Linear eigenlocus transforms determine decision regions Z_1 and Z_2 that minimize Bayes' minimax risk $\mathfrak{R}_{\text{mm}}(Z|\tau)$, where $\mathfrak{R}(Z_1|\tau_2) = \mathfrak{R}(Z_2|\tau_1)$, for training data drawn from overlapping Gaussian distributions that have dissimilar covariance matrices.



$$\begin{aligned}\mathfrak{R}_{mm}(Z|\tau) &= \int_{Z_1} p(\mathbf{x}_{2i*}|\tau_2) d\tau_2 \\ &= \int_{Z_2} p(\mathbf{x}_{1i*}|\tau_1) d\tau_1\end{aligned}$$

Figure 19: Linear eigenlocus transforms determine decision regions Z_1 and Z_2 that minimize Bayes' minimax risk $\mathfrak{R}_{mm}(Z|\tau)$, where $\mathfrak{R}(Z_1|\tau_2) = \mathfrak{R}(Z_2|\tau_1)$, for training data drawn from overlapping multimode distributions.

General Course of Argument

Using Eq. (13), any given extreme point \mathbf{x}_{i*} is the endpoint on a locus (a position vector) of *random variables*

$$(\|\mathbf{x}_{i*}\| \cos \alpha_{\mathbf{x}_{i*}1}, \|\mathbf{x}_{i*}\| \cos \alpha_{\mathbf{x}_{i*}2}, \dots, \|\mathbf{x}_{i*}\| \cos \alpha_{\mathbf{x}_{i*}d}),$$

where each random variable $\|\mathbf{x}_{i*}\| \cos \alpha_{x_{i*}j}$ is characterized by an expected value $E[\|\mathbf{x}_{i*}\| \cos \alpha_{x_{i*}j}]$ and a variance $\text{var}(\|\mathbf{x}_{i*}\| \cos \alpha_{x_{i*}j})$. Accordingly, an extreme point \mathbf{x}_{i*} is described by a central location (an expected value) and a covariance (a spread).

The function describing the relative likelihood that an extreme point has a given location is a conditional probability density function. The function describing the cumulative probability of given locations for an extreme point, i.e., the probability of finding the extreme point within a localized region, is a conditional probability function.

I will show that each Wolfe dual principal eigenaxis component $\psi_{i*} \vec{\mathbf{e}}_{i*}$ describes a conditional density $p(\mathbf{x}_{i*} | \text{comp}_{\vec{\mathbf{x}}_{i*}}(\vec{\tau}))$ for a correlated extreme point \mathbf{x}_{i*} , such that τ_1 is a parameter vector for a conditional probability density $p(\mathbf{x}_{1i*}|\tau_1)$ for a given set $\{\mathbf{x}_{1i*}\}_{i=1}^{l_1}$ of \mathbf{x}_{1i*} extreme points:

$$\tau_1 = p(\mathbf{x}_{1i*}|\tau_1),$$

and τ_2 is a parameter vector for a conditional probability density $p(\mathbf{x}_{2_{i*}}|\tau_2)$ for a given set $\{\mathbf{x}_{2_{i*}}\}_{i=1}^{l_2}$ of $\mathbf{x}_{2_{i*}}$ extreme points:

$$\tau_2 = p(\mathbf{x}_{2_{i*}}|\tau_2),$$

where the area under each pointwise conditional density $p(\mathbf{x}_{i*}|\text{comp}_{\overrightarrow{\mathbf{x}_{i*}}}(\overrightarrow{\tau}))$ is a conditional probability that an extreme point \mathbf{x}_{i*} will be observed in an Z_1 or Z_2 decision region.

Accordingly, the conditional probability function $P(\mathbf{x}_{1_{i*}}|\tau_1)$ for a given set $\{\mathbf{x}_{1_{i*}}\}_{i=1}^{l_1}$ of $\mathbf{x}_{1_{i*}}$ extreme points is given by the area under the conditional probability density $p(\mathbf{x}_{1_{i*}}|\tau_1)$

$$\begin{aligned} P(\mathbf{x}_{1_{i*}}|\tau_1) &= \int_Z \left(\sum_{i=1}^{l_1} \psi_{1_{i*}} \mathbf{x}_{1_{i*}} \right) d\tau_1 = \int_Z p(\mathbf{x}_{1_{i*}}|\tau_1) d\tau_1, \\ &= \int_Z \tau_1 d\tau_1 = \|\tau_1\|^2 + C_1, \end{aligned}$$

where $\|\tau_1\|^2$ is the *total allowed eigenenergy* of τ_1 .

Likewise, the conditional probability function $P(\mathbf{x}_{2_{i*}}|\tau_2)$ for a given set $\{\mathbf{x}_{2_{i*}}\}_{i=1}^{l_2}$ of $\mathbf{x}_{2_{i*}}$ extreme points is given by the area under the conditional probability density $p(\mathbf{x}_{2_{i*}}|\tau_2)$

$$\begin{aligned} P(\mathbf{x}_{2_{i*}}|\tau_2) &= \int_Z \left(\sum_{i=1}^{l_2} \psi_{2_{i*}} \mathbf{x}_{2_{i*}} \right) d\tau_2 = \int_Z p(\mathbf{x}_{2_{i*}}|\tau_2) d\tau_2, \\ &= \int_Z \tau_2 d\tau_2 = \|\tau_2\|^2 + C_2, \end{aligned}$$

where $\|\tau_2\|^2$ is the *total allowed eigenenergy* of τ_2 .

The property of symmetrical balance exhibited by the principal eigenaxis components on ψ and τ enables linear eigenlocus discriminant functions $\mathbf{x}^T \tau + \tau_0$ to balance the Bayes' risk $\mathfrak{R}_{\mathfrak{B}}$ for any two given sets of feature vectors, where a linear eigenlocus $\hat{\Lambda}(\mathbf{x}) = \mathbf{x}^T \tau + \tau_0$ is an equalizer rule that satisfies Bayes' minimax risk $\mathfrak{R}_{mm}(Z|\tau)$ in Eq. (8). I will demonstrate that the property of symmetrical balance ensures that the conditional probability functions $P(\mathbf{x}_{1_{i*}}|\tau_1)$ and $P(\mathbf{x}_{2_{i*}}|\tau_2)$ for class ω_1 and class ω_2 are equal to each other.

I will define the manner in which the total allowed eigenenergies of τ_1 and τ_2 are symmetrically balanced with each other. I will also define the manner in which the conditional probability functions $P(\mathbf{x}_{1_{i*}}|\tau_1)$ and $P(\mathbf{x}_{2_{i*}}|\tau_2)$ are symmetrically balanced with each other. I will use these results to demonstrate that the conditional probability of decision error

$P(D_2|\omega_1)$ for class ω_1 is given by an error integral

$$\begin{aligned} P(D_2|\omega_1) &= \int_{Z_2} p(\hat{\Lambda}(\mathbf{x})|\omega_1) d\hat{\Lambda}, \\ &= \int_{Z_2} \tau_1 d\tau_1, \\ &= \|\tau_1\|^2 + C_1, \end{aligned}$$

in terms of $\|\tau_1\|^2$ and an integration constant C_1 , where $\|\tau_1\|^2$ is the critical minimum eigenenergy $\|\tau_1\|_{\min_c}^2$ exhibited by τ_1 . Accordingly, the critical minimum eigenenergy $\|\tau_1\|_{\min_c}^2$ exhibited by τ_1 describes how conditional probabilities of classification error $\mathcal{P}_e(\hat{Z}_2(\mathbf{x}_{1_{i*}}))$ for $\mathbf{x}_{1_{i*}}$ extreme points are distributed in the Z_2 decision region.

Likewise, the conditional probability of decision error $P(D_1|\omega_2)$ for class ω_2 is given by an error integral

$$\begin{aligned} P(D_1|\omega_2) &= \int_{Z_1} p(\hat{\Lambda}(\mathbf{x})|\omega_2) d\hat{\Lambda}, \\ &= \int_{Z_1} \tau_2 d\tau_2, \\ &= \|\tau_2\|^2 + C_2, \end{aligned}$$

in terms of $\|\tau_2\|^2$ and an integration constant C_2 , where $\|\tau_2\|^2$ is the critical minimum eigenenergy $\|\tau_2\|_{\min_c}^2$ exhibited by τ_2 . Accordingly, the critical minimum eigenenergy $\|\tau_2\|_{\min_c}^2$ exhibited by τ_2 describes how conditional probabilities of classification error $\mathcal{P}_e(\hat{Z}_1(\mathbf{x}_{2_{i*}}))$ for $\mathbf{x}_{2_{i*}}$ extreme points are distributed in the Z_1 decision region.

In order to demonstrate what is outlined in the general course of my argument, I will develop locus equations in Wolfe dual eigenspace that provide tractable point and coordinate relationships between the weighted, eigen-scaled extreme points on τ_1 and τ_2 and the Wolfe dual principal eigenaxis components on ψ .

I will use these equations to define symmetrical properties possessed by the Wolfe dual and the constrained primal principal eigenaxis components. Next, I will use the equations and identified properties to define conditional probability densities for extreme points. After that, I will use the condition of complementary slackness and the KKT constraint in Eq. (32) to define the manner in which the total allowed eigenenergies of labeled, eigen-scaled extreme vectors are symmetrically balanced with each other. Finally, I will define the manner in which the conditional probability functions are symmetrically balanced with each other.

Thereby, I will conclude that a linear eigenlocus $\hat{\Lambda}(\mathbf{x}) = \mathbf{x}^T \tau + \tau_0$ is an equalizer rule that satisfies Bayes' minimax risk \mathfrak{R}_{mm} in Eq. (8).

Linear eigenlocus transforms involve symmetrically balanced, first and second-order statistical moments of extreme data points. I will begin my analysis by defining first and second-order statistical moments of data points.

8.1 First and Second-Order Statistical Moments

Consider again the Gram matrix \mathbf{Q} associated with the constrained quadratic form in Eq. (34)

$$\mathbf{Q} = \begin{pmatrix} \mathbf{x}_1^T \mathbf{x}_1 & \mathbf{x}_1^T \mathbf{x}_2 & \cdots & -\mathbf{x}_1^T \mathbf{x}_N \\ \mathbf{x}_2^T \mathbf{x}_1 & \mathbf{x}_2^T \mathbf{x}_2 & \cdots & -\mathbf{x}_2^T \mathbf{x}_N \\ \vdots & \vdots & \ddots & \vdots \\ -\mathbf{x}_N^T \mathbf{x}_1 & -\mathbf{x}_N^T \mathbf{x}_2 & \cdots & \mathbf{x}_N^T \mathbf{x}_N \end{pmatrix}, \quad (54)$$

where $\mathbf{Q} \triangleq \tilde{\mathbf{X}} \tilde{\mathbf{X}}^T$, $\tilde{\mathbf{X}} \triangleq \mathbf{D}_y \mathbf{X}$, \mathbf{D}_y is a $N \times N$ diagonal matrix of training labels y_i and the $N \times d$ data matrix is $\mathbf{X} = (\mathbf{x}_1, \mathbf{x}_2, \dots, \mathbf{x}_N)^T$. Without loss of generality (WLOG), assume that N is an even number, let the first $N/2$ vectors have the label $y_i = 1$ and let the last $N/2$ vectors have the label $y_i = -1$. WLOG, the analysis that follows does not take label information into account.

Using Eq. (17), let the inner product statistic $\mathbf{x}_i^T \mathbf{x}_j$ be interpreted as $\|\mathbf{x}_i\|$ times the scalar projection $\|\mathbf{x}_j\| \cos \theta_{\mathbf{x}_i \mathbf{x}_j}$ of \mathbf{x}_j onto \mathbf{x}_i . It follows that row $\mathbf{Q}(i, :)$ in Eq. (54) encodes uniformly weighted $\|\mathbf{x}_i\|$ scalar projections $\|\mathbf{x}_j\| \cos \theta_{\mathbf{x}_i \mathbf{x}_j}$ for each of the N vectors $\{\mathbf{x}_j\}_{j=1}^N$ onto the vector \mathbf{x}_i :

$$\tilde{\mathbf{Q}} = \begin{pmatrix} \|\mathbf{x}_1\| \|\mathbf{x}_1\| \cos \theta_{\mathbf{x}_1 \mathbf{x}_1} & \cdots & -\|\mathbf{x}_1\| \|\mathbf{x}_N\| \cos \theta_{\mathbf{x}_1 \mathbf{x}_N} \\ \|\mathbf{x}_2\| \|\mathbf{x}_1\| \cos \theta_{\mathbf{x}_2 \mathbf{x}_1} & \cdots & -\|\mathbf{x}_2\| \|\mathbf{x}_N\| \cos \theta_{\mathbf{x}_2 \mathbf{x}_N} \\ \vdots & \ddots & \vdots \\ -\|\mathbf{x}_N\| \|\mathbf{x}_1\| \cos \theta_{\mathbf{x}_N \mathbf{x}_1} & \cdots & \|\mathbf{x}_N\| \|\mathbf{x}_N\| \cos \theta_{\mathbf{x}_N \mathbf{x}_N} \end{pmatrix}, \quad (55)$$

where $0 < \theta_{\mathbf{x}_i \mathbf{x}_j} \leq \frac{\pi}{2}$ or $\frac{\pi}{2} < \theta_{\mathbf{x}_i \mathbf{x}_j} \leq \pi$. Alternatively, column $\mathbf{Q}(:, j)$ in Eq. (54) encodes weighted $\|\mathbf{x}_i\|$ scalar projections $\|\mathbf{x}_j\| \cos \theta_{\mathbf{x}_i \mathbf{x}_j}$ for the vector \mathbf{x}_j onto each of the N vectors $\{\mathbf{x}_i\}_{i=1}^N$.

Now consider the i th row $\tilde{\mathbf{Q}}(i, :)$ of $\tilde{\mathbf{Q}}$ in Eq. (55). Again using Eq. (17), it follows that element $\tilde{\mathbf{Q}}(i, j)$ of row $\tilde{\mathbf{Q}}(i, :)$ encodes the length $\|\mathbf{x}_i\|$ of the vector \mathbf{x}_i multiplied by the scalar projection $\|\mathbf{x}_j\| \cos \theta_{\mathbf{x}_i \mathbf{x}_j}$ of \mathbf{x}_j onto \mathbf{x}_i :

$$\tilde{\mathbf{Q}}(i, j) = \|\mathbf{x}_i\| [\|\mathbf{x}_j\| \cos \theta_{\mathbf{x}_i \mathbf{x}_j}],$$

where the signed magnitude of the vector projection of \mathbf{x}_j along the axis of \mathbf{x}_i

$$\text{comp}_{\vec{\mathbf{x}}_i}(\vec{\mathbf{x}}_j) = \|\mathbf{x}_j\| \cos \theta_{\mathbf{x}_i \mathbf{x}_j} = \mathbf{x}_j^T \left(\frac{\mathbf{x}_i}{\|\mathbf{x}_i\|} \right),$$

provides a measure $\widehat{\mathbf{x}}_j$ of the first degree components of the vector \mathbf{x}_j

$$\mathbf{x}_j = (x_{j1}, x_{j2}, \dots, x_{jd})^T,$$

along the axis of the vector \mathbf{x}_i

$$\mathbf{x}_i = (x_{i1}, x_{i2}, \dots, x_{id})^T.$$

Accordingly, the signed magnitude $\|\mathbf{x}_j\| \cos \theta_{\mathbf{x}_i \mathbf{x}_j}$ provides an estimate $\widehat{\mathbf{x}}_i$ for the amount of first degree components of the vector \mathbf{x}_i that are distributed over the axis of the vector \mathbf{x}_j . This indicates that signed magnitudes $\|\mathbf{x}_j\| \cos \theta_{\mathbf{x}_i \mathbf{x}_j}$ encoded with $\widetilde{\mathbf{Q}}$ account for how a data point \mathbf{x}_i is distributed along axes of vectors \mathbf{x}_j within Euclidean space.

Using the above assumptions and notation, for any given row $\widetilde{\mathbf{Q}}(i, :)$ of Eq. (55), it follows that the statistic denoted by $E_{\widehat{\mathbf{x}}_i} \left[\mathbf{x}_i | \{\mathbf{x}_j\}_{j=1}^N \right]$

$$\begin{aligned} E_{\widehat{\mathbf{x}}_i} \left[\mathbf{x}_i | \{\mathbf{x}_j\}_{j=1}^N \right] &= \|\mathbf{x}_i\| \sum_j \text{comp}_{\vec{\mathbf{x}}_i}(\vec{\mathbf{x}}_j) \\ &= \|\mathbf{x}_i\| \sum_j \|\mathbf{x}_j\| \cos \theta_{\mathbf{x}_i \mathbf{x}_j}, \end{aligned} \quad (56)$$

provides an estimate $E_{\widehat{\mathbf{x}}_i} \left[\mathbf{x}_i | \{\mathbf{x}_j\}_{j=1}^N \right]$ for the amount of first degree components of a vector \mathbf{x}_i that are distributed over the axes of a set of vectors $\{\mathbf{x}_j\}_{j=1}^N$, where labels have not been taken into account. Therefore, Eq. (56) describes a distribution of first degree coordinates for a vector \mathbf{x}_i in a data collection.

Given that Eq. (56) involves signed magnitudes of vector projections along the axis of a fixed vector \mathbf{x}_i , the distribution of first degree vector coordinates described by Eq. (56) is said to determine a first-order statistical moment about the locus of a data point \mathbf{x}_i . Because the statistic $E_{\widehat{\mathbf{x}}_i} \left[\mathbf{x}_i | \{\mathbf{x}_j\}_{j=1}^N \right]$ depends on the uniform direction of a fixed vector \mathbf{x}_i , the statistic $E_{\widehat{\mathbf{x}}_i} \left[\mathbf{x}_i | \{\mathbf{x}_j\}_{j=1}^N \right]$ is said to be unidirectional. In the next section, I will define pointwise covariance statistics that provide unidirectional estimates of covariance along a fixed reference axis.

8.2 Unidirectional Covariance Statistics

Classical covariance statistics provide omnidirectional estimates of covariance along N axes of N vectors. I will now argue that such omnidirectional statistics provide non-coherent estimates of covariance.

8.2.1 Omnidirectional Covariance Statistics

Take the data matrix $\mathbf{X} = (\mathbf{x}_1, \mathbf{x}_2, \dots, \mathbf{x}_N)^T$ and consider the classical covariance statistic:

$$\begin{aligned}\widehat{\text{cov}}(\mathbf{X}) &= \frac{1}{N} \sum_i (\mathbf{x}_i - \bar{\mathbf{x}})^2, \\ &= \frac{1}{N} \sum_i \left(\mathbf{x}_i - \left(\frac{1}{N} \sum_i \mathbf{x}_i \right) \right)^2,\end{aligned}$$

written in vector notation. The statistic $\widehat{\text{cov}}(\mathbf{X})$ measures the square of the Euclidean distance between a common mean vector $\bar{\mathbf{x}}$ and each of the vectors \mathbf{x}_i in a collection of data $\{\mathbf{x}_i\}_{i=1}^N$ (Ash, 1993; Flury, 1997).

Because the statistic $\widehat{\text{cov}}(\mathbf{X})$ depends on N directions of N training vectors, the statistic $\widehat{\text{cov}}(\mathbf{X})$ is said to be omnidirectional and is considered to be a non-coherent estimate of covariance. Accordingly, the statistic $\widehat{\text{cov}}(\mathbf{X})$ provides an omnidirectional, non-coherent estimate of the joint variations of the $d \times N$ random variables of a collection of N random vectors $\{\mathbf{x}_i\}_{i=1}^N$ about the d random variables of the mean vector $\bar{\mathbf{x}}$.

I will now develop pointwise covariance statistics $\widehat{\text{cov}}_{up}(\mathbf{x}_i)$ for individual vectors. Pointwise covariance statistics are unidirectional statistics that provide coherent estimates of covariance along a fixed reference axis. WLOG, label information is not taken into consideration.

8.2.2 Pointwise Covariance Statistics

Take any row $\tilde{\mathbf{Q}}(i, :)$ of the matrix $\tilde{\mathbf{Q}}$ in Eq. (55) and consider the inner product statistic $\|\mathbf{x}_i\| \|\mathbf{x}_j\| \cos \theta_{\mathbf{x}_i \mathbf{x}_j}$ in element $\tilde{\mathbf{Q}}(i, j)$. Using Eqs (13) and (16), it follows that element $\tilde{\mathbf{Q}}(i, j)$ in row $\tilde{\mathbf{Q}}(i, :)$ encodes the joint variations $\text{cov}(\mathbf{x}_i, \mathbf{x}_j)$

$$\text{cov}(\mathbf{x}_i, \mathbf{x}_j) = \|\mathbf{x}_i\| \|\mathbf{x}_j\| \cos \theta_{\mathbf{x}_i \mathbf{x}_j},$$

between the components of the vector \mathbf{x}_i

$$(\|\mathbf{x}_i\| \cos \alpha_{\mathbf{x}_{i1}1}, \|\mathbf{x}_i\| \cos \alpha_{\mathbf{x}_{i2}2}, \dots, \|\mathbf{x}_i\| \cos \alpha_{\mathbf{x}_{id}d}),$$

and the components of the vector \mathbf{x}_j

$$(\|\mathbf{x}_j\| \cos \alpha_{\mathbf{x}_{j1}1}, \|\mathbf{x}_j\| \cos \alpha_{\mathbf{x}_{j2}2}, \dots, \|\mathbf{x}_j\| \cos \alpha_{\mathbf{x}_{jd}d}),$$

where the d components $\{\|\mathbf{x}\| \cos \alpha_{x_i i}\}_{i=1}^d$ of any given vector \mathbf{x} are random variables, each of which is characterized by an expected value $E[\|\mathbf{x}\| \cos \alpha_{x_i i}]$ and a variance $\text{var}(\|\mathbf{x}\| \cos \alpha_{x_i i})$. It follows that the j th

element $\tilde{\mathbf{Q}}(i, j)$ of row $\tilde{\mathbf{Q}}(i, :)$ encodes the joint variations of the d random variables of a vector \mathbf{x}_j about the d random variables of the vector \mathbf{x}_i . Thus, row $\tilde{\mathbf{Q}}(i, :)$ encodes the joint variations between the random variables of a fixed vector \mathbf{x}_i and the random variables of an entire collection of data.

Again take any row $\tilde{\mathbf{Q}}(i, :)$ of the matrix $\tilde{\mathbf{Q}}$ in Eq. (55). Using the definition of the scalar project statistic in Eq. (17), it follows that the statistic $\widehat{\text{cov}}_{up}(\mathbf{x}_i)$:

$$\begin{aligned}\widehat{\text{cov}}_{up}(\mathbf{x}_i) &= \sum_{j=1}^N \|\mathbf{x}_i\| \|\mathbf{x}_j\| \cos \theta_{\mathbf{x}_i \mathbf{x}_j}, \\ &= \sum_{j=1}^N \mathbf{x}_i^T \mathbf{x}_j = \mathbf{x}_i^T \left(\sum_{j=1}^N \mathbf{x}_j \right), \\ &= \|\mathbf{x}_i\| \sum_{j=1}^N \|\mathbf{x}_j\| \cos \theta_{\mathbf{x}_i \mathbf{x}_j},\end{aligned}\tag{57}$$

provides a unidirectional estimate of the joint variations of the d random variables of each of the N vectors of a data collection $\{\mathbf{x}_j\}_{j=1}^N$, as well as the d random variables of the common mean $\sum_{j=1}^N \mathbf{x}_j$ of the data, about the d random variables of a fixed vector \mathbf{x}_i , along the axis of the fixed vector \mathbf{x}_i . Thereby, the statistic $\widehat{\text{cov}}_{up}(\mathbf{x}_i)$ encodes the direction of a vector \mathbf{x}_i and a signed magnitude along the axis of the vector \mathbf{x}_i .

The statistic $\widehat{\text{cov}}_{up}(\mathbf{x}_i)$ in Eq. (57) is defined to be a pointwise covariance estimate for a data point \mathbf{x}_i , where the statistic $\widehat{\text{cov}}_{up}(\mathbf{x}_i)$ provides a unidirectional estimate of the joint variations between the random variables of each vector \mathbf{x}_j in a data collection and the random variables of a fixed vector \mathbf{x}_i , as well as a unidirectional estimate of the joint variations between the random variables of the mean vector $\sum_{j=1}^N \mathbf{x}_j$ and the fixed vector \mathbf{x}_i . Given that the joint variations estimated by the statistic $\widehat{\text{cov}}_{up}(\mathbf{x}_i)$ are derived from second-order distance statistics $\|\mathbf{x}_i - \mathbf{x}_j\|^2$ which involve signed magnitudes of vector projections along the common axis of a fixed vector \mathbf{x}_i , a pointwise covariance estimate $\widehat{\text{cov}}_{up}(\mathbf{x}_i)$ is said to determine a second-order statistical moment about the locus of a data point \mathbf{x}_i . Using Eq. (56), Eq. (57) also encodes a distribution of first order coordinates for a given vector \mathbf{x}_i which determines a first-order statistical moment about the locus of the data point \mathbf{x}_i .

I will now demonstrate that pointwise covariance statistics can be used to discover extreme points.

8.2.3 Discovery of Extreme Data Points

The Gram matrix associated with the constrained quadratic form in Eq. (34) encodes inner product statistics for two labeled collections of data.

Denote those data points that belong to class ω_1 by \mathbf{x}_{1_i} and those that belong to class ω_2 by \mathbf{x}_{2_i} . Let $\bar{\mathbf{x}}_1$ and $\bar{\mathbf{x}}_2$ denote the mean vectors of class ω_1 and class ω_2 . Let $i = 1 : n_1$ where the vector \mathbf{x}_{1_i} has the label $y_i = 1$, and let $i = n_1 + 1 : n_1 + n_2$ where the vector \mathbf{x}_{2_i} has the label $y_i = -1$. Using label information, Eq. (57) can be rewritten as

$$\widehat{\text{cov}}_{up}(\mathbf{x}_{1_i}) = \mathbf{x}_{1_i}^T \left(\sum_{j=1}^{n_1} \mathbf{x}_{1_j} - \sum_{j=n_1+1}^{n_1+n_2} \mathbf{x}_{2_j} \right),$$

and

$$\widehat{\text{cov}}_{up}(\mathbf{x}_{2_i}) = \mathbf{x}_{2_i}^T \left(\sum_{j=n_1+1}^{n_1+n_2} \mathbf{x}_{2_j} - \sum_{j=1}^{n_1} \mathbf{x}_{1_j} \right).$$

I will now show that extreme points possess large pointwise covariances relative to the non-extreme points in each respective pattern class. Recall that an extreme point is located relatively far from its distribution mean, relatively close to the mean of the other distribution, and relatively close to other extreme points. Denote an extreme point by $\mathbf{x}_{1_{i*}}$ or $\mathbf{x}_{2_{i*}}$ and a non-extreme point by \mathbf{x}_{1_i} or \mathbf{x}_{2_i} .

Take any extreme point $\mathbf{x}_{1_{i*}}$ and any non-extreme point \mathbf{x}_{1_i} that belong to class ω_1 , and consider the pointwise covariance estimates for $\mathbf{x}_{1_{i*}}$:

$$\widehat{\text{cov}}_{up}(\mathbf{x}_{1_{i*}}) = \mathbf{x}_{1_{i*}}^T \bar{\mathbf{x}}_1 - \mathbf{x}_{1_{i*}}^T \bar{\mathbf{x}}_2,$$

and for \mathbf{x}_{1_i} :

$$\widehat{\text{cov}}_{up}(\mathbf{x}_{1_i}) = \mathbf{x}_{1_i}^T \bar{\mathbf{x}}_1 - \mathbf{x}_{1_i}^T \bar{\mathbf{x}}_2.$$

Because $\mathbf{x}_{1_{i*}}$ is an extreme point, it follows that $\mathbf{x}_{1_{i*}}^T \bar{\mathbf{x}}_1 > \mathbf{x}_{1_i}^T \bar{\mathbf{x}}_1$ and that $\mathbf{x}_{1_{i*}}^T \bar{\mathbf{x}}_2 < \mathbf{x}_{1_i}^T \bar{\mathbf{x}}_2$; so $\widehat{\text{cov}}_{up}(\mathbf{x}_{1_{i*}}) > \widehat{\text{cov}}_{up}(\mathbf{x}_{1_i})$. Therefore, each extreme point $\mathbf{x}_{1_{i*}}$ exhibits a pointwise covariance $\widehat{\text{cov}}_{up}(\mathbf{x}_{1_{i*}})$ that exceeds the pointwise covariance $\widehat{\text{cov}}_{up}(\mathbf{x}_{1_i})$ of all of the non-extreme points \mathbf{x}_{1_i} in class ω_1 .

Now take any extreme point $\mathbf{x}_{2_{i*}}$ and any non-extreme point \mathbf{x}_{2_i} that belong to class ω_2 , and consider the pointwise covariance estimates for $\mathbf{x}_{2_{i*}}$:

$$\widehat{\text{cov}}_{up}(\mathbf{x}_{2_{i*}}) = \mathbf{x}_{2_{i*}}^T \bar{\mathbf{x}}_2 - \mathbf{x}_{2_{i*}}^T \bar{\mathbf{x}}_1,$$

and for \mathbf{x}_{2_i} :

$$\widehat{\text{cov}}_{up}(\mathbf{x}_{2_i}) = \mathbf{x}_{2_i}^T \bar{\mathbf{x}}_2 - \mathbf{x}_{2_i}^T \bar{\mathbf{x}}_1.$$

Because $\mathbf{x}_{2_{i*}}$ is an extreme point, it follows that $\mathbf{x}_{2_{i*}}^T \bar{\mathbf{x}}_2 > \mathbf{x}_{2_i}^T \bar{\mathbf{x}}_2$ and that $\mathbf{x}_{2_{i*}}^T \bar{\mathbf{x}}_1 < \mathbf{x}_{2_i}^T \bar{\mathbf{x}}_1$; so $\widehat{\text{cov}}_{up}(\mathbf{x}_{2_{i*}}) > \widehat{\text{cov}}_{up}(\mathbf{x}_{2_i})$. Therefore, each extreme point $\mathbf{x}_{2_{i*}}$ exhibits a pointwise covariance $\widehat{\text{cov}}_{up}(\mathbf{x}_{2_{i*}})$ that exceeds the pointwise covariance $\widehat{\text{cov}}_{up}(\mathbf{x}_{2_i})$ of all of the non-extreme points \mathbf{x}_{2_i} in class ω_2 . It follows that extreme points possess large pointwise covariances relative to non-extreme points in their respective pattern class. It also follows that the pointwise covariance $\widehat{\text{cov}}_{up}(\mathbf{x}_{1_{i*}})$ or $\widehat{\text{cov}}_{up}(\mathbf{x}_{2_{i*}})$

exhibited by any given extreme point \mathbf{x}_{1i*} or \mathbf{x}_{2i*} may exceed pointwise covariances of other extreme points in each respective pattern class.

It will be assumed that each extreme point \mathbf{x}_{1i*} or \mathbf{x}_{2i*} exhibits a critical first and second-order statistical moment $\widehat{\text{cov}}_{up}(\mathbf{x}_{1i*})$ or $\widehat{\text{cov}}_{up}(\mathbf{x}_{2i*})$ that exceeds some threshold ϱ , for which each corresponding eigen-scale ψ_{1i*} or ψ_{2i*} exhibits a critical value that exceeds zero $\psi_{1i*} > 0$ or $\psi_{2i*} > 0$. Accordingly, first and second-order statistical moments $\widehat{\text{cov}}_{up}(\mathbf{x}_{1i})$ or $\widehat{\text{cov}}_{up}(\mathbf{x}_{2i})$ about the loci of non-extreme points \mathbf{x}_{1i} or \mathbf{x}_{2i} do not exceed the threshold ϱ , and their corresponding eigen-scales ψ_{1i} or ψ_{2i} are effectively zero $\psi_{1i} = 0$ or $\psi_{2i} = 0$.

I will now develop an expression for a principal eigen-decomposition of the Gram matrix \mathbf{Q} denoted in Eqs (54) and (55) that describes tractable point and coordinate relationships between the eigen-scaled extreme points on τ_1 and τ_2 and the Wolfe dual principal eigenaxis components on ψ .

9 Inside the Wolfe Dual Eigenspace

Take the Gram matrix \mathbf{Q} associated with the quadratic form in Eq (34). Let \mathbf{q}_j denote the j th column of \mathbf{Q} , which is an N -vector. Let λ_{\max_ψ} and ψ denote the largest eigenvalue and largest eigenvector of \mathbf{Q} respectively. Using this notation (see Trefethen and Bau, 1998), the principal eigen-decomposition of \mathbf{Q}

$$\mathbf{Q}\psi = \lambda_{\max_\psi}\psi,$$

can be rewritten as

$$\lambda_{\max_\psi}\psi = \sum_{j=1}^N \psi_j \mathbf{q}_j,$$

so that the principal eigenaxis ψ of \mathbf{Q} is expressed as a linear combination of eigen-transformed vectors $\frac{\psi_j}{\lambda_{\max_\psi}}\mathbf{q}_j$:

$$\begin{bmatrix} \psi \end{bmatrix} = \frac{\psi_1}{\lambda_{\max_\psi}} \begin{bmatrix} \mathbf{q}_1 \end{bmatrix} + \frac{\psi_2}{\lambda_{\max_\psi}} \begin{bmatrix} \mathbf{q}_2 \end{bmatrix} + \cdots + \frac{\psi_N}{\lambda_{\max_\psi}} \begin{bmatrix} \mathbf{q}_N \end{bmatrix}, \quad (58)$$

where the i th element of the vector \mathbf{q}_j encodes inner product statistics $\mathbf{x}_i^T \mathbf{x}_j$ between the vectors \mathbf{x}_i and \mathbf{x}_j .

Using Eqs (54) and (58), a Wolfe dual linear eigenlocus $(\psi_1, \dots, \psi_N)^T$

can be written as:

$$\begin{aligned} \psi = & \frac{\psi_1}{\lambda_{\max_\psi}} \begin{pmatrix} \mathbf{x}_1^T \mathbf{x}_1 \\ \mathbf{x}_2^T \mathbf{x}_1 \\ \vdots \\ -\mathbf{x}_N^T \mathbf{x}_1 \end{pmatrix} + \frac{\psi_2}{\lambda_{\max_\psi}} \begin{pmatrix} \mathbf{x}_1^T \mathbf{x}_2 \\ \mathbf{x}_2^T \mathbf{x}_2 \\ \vdots \\ -\mathbf{x}_N^T \mathbf{x}_2 \end{pmatrix} + \dots \\ & \dots + \frac{\psi_{N-1}}{\lambda_{\max_\psi}} \begin{pmatrix} -\mathbf{x}_1^T \mathbf{x}_{N-1} \\ -\mathbf{x}_2^T \mathbf{x}_{N-1} \\ \vdots \\ \mathbf{x}_N^T \mathbf{x}_{N-1} \end{pmatrix} + \frac{\psi_N}{\lambda_{\max_\psi}} \begin{pmatrix} -\mathbf{x}_1^T \mathbf{x}_N \\ -\mathbf{x}_2^T \mathbf{x}_N \\ \vdots \\ \mathbf{x}_N^T \mathbf{x}_N \end{pmatrix}, \end{aligned} \quad (59)$$

which illustrates that the magnitude ψ_j of the j^{th} Wolfe dual principal eigenaxis component $\psi_j \vec{\mathbf{e}}_j$ is correlated with joint variations of labeled vectors \mathbf{x}_i about the vector \mathbf{x}_j .

Alternatively, using Eqs (55) and (58), a Wolfe dual linear eigenlocus ψ can be written as:

$$\begin{aligned} \psi = & \frac{\psi_1}{\lambda_{\max_\psi}} \begin{pmatrix} \|\mathbf{x}_1\| \|\mathbf{x}_1\| \cos \theta_{\mathbf{x}_1^T \mathbf{x}_1} \\ \|\mathbf{x}_2\| \|\mathbf{x}_1\| \cos \theta_{\mathbf{x}_2^T \mathbf{x}_1} \\ \vdots \\ -\|\mathbf{x}_N\| \|\mathbf{x}_1\| \cos \theta_{\mathbf{x}_N^T \mathbf{x}_1} \end{pmatrix} + \dots \\ & \dots + \frac{\psi_N}{\lambda_{\max_\psi}} \begin{pmatrix} -\|\mathbf{x}_1\| \|\mathbf{x}_N\| \cos \theta_{\mathbf{x}_1^T \mathbf{x}_N} \\ -\|\mathbf{x}_2\| \|\mathbf{x}_N\| \cos \theta_{\mathbf{x}_2^T \mathbf{x}_N} \\ \vdots \\ \|\mathbf{x}_N\| \|\mathbf{x}_N\| \cos \theta_{\mathbf{x}_N^T \mathbf{x}_N} \end{pmatrix}, \end{aligned} \quad (60)$$

which illustrates that the magnitude ψ_j of the j^{th} Wolfe dual principal eigenaxis component $\psi_j \vec{\mathbf{e}}_j$ on ψ is correlated with scalar projections $\|\mathbf{x}_j\| \cos \theta_{\mathbf{x}_i \mathbf{x}_j}$ of the vector \mathbf{x}_j onto labeled vectors \mathbf{x}_i .

Equations (59) and (60) both indicate that the magnitude ψ_j of the j^{th} Wolfe dual principal eigenaxis component $\psi_j \vec{\mathbf{e}}_j$ on ψ is correlated with a first and second-order statistical moment about the locus of the data point \mathbf{x}_j .

Assumptions

It will be assumed that each extreme point \mathbf{x}_{1i*} or \mathbf{x}_{2i*} exhibits a critical first and second-order statistical moment $\widehat{\text{cov}}_{up}(\mathbf{x}_{1i*})$ or $\widehat{\text{cov}}_{up}(\mathbf{x}_{2i*})$ that exceeds some threshold ϱ , for which each corresponding eigen-scale ψ_{1i*} or ψ_{2i*} exhibits a critical value that exceeds zero $\psi_{1i*} > 0$ or $\psi_{2i*} > 0$. It will also be assumed that first and second-order statistical moments $\widehat{\text{cov}}_{up}(\mathbf{x}_{1i})$ or $\widehat{\text{cov}}_{up}(\mathbf{x}_{2i})$ about the loci of non-extreme points \mathbf{x}_{1i} or \mathbf{x}_{2i}

do not exceed the threshold ϱ and that the corresponding eigen-scales ψ_{1i} or ψ_{2i} are effectively zero $\psi_{1i} = 0$ or $\psi_{2i} = 0$.

Express a Wolfe dual linear eigenlocus ψ in terms of l non-orthogonal unit vectors $\{\vec{e}_{1*}, \dots, \vec{e}_{l*}\}$

$$\begin{aligned}\psi &= \sum_{i=1}^l \psi_{i*} \vec{e}_{i*}, \\ &= \sum_{i=1}^{l_1} \psi_{1i*} \vec{e}_{1i*} + \sum_{i=1}^{l_2} \psi_{2i*} \vec{e}_{2i*},\end{aligned}\tag{61}$$

where each eigen-scaled, non-orthogonal unit vector denoted by $\psi_{1i*} \vec{e}_{1i*}$ or $\psi_{2i*} \vec{e}_{2i*}$ is correlated with an extreme vector \mathbf{x}_{1i*} or \mathbf{x}_{2i*} respectively. Accordingly, each Wolfe dual principal eigenaxis component $\psi_{1i*} \vec{e}_{1i*}$ or $\psi_{2i*} \vec{e}_{2i*}$ is an eigen-scaled, non-orthogonal unit vector that contributes to the estimation of ψ and τ .

WLOG, indices do not indicate locations of data in Eq. (60).

Extreme Point Notation

Denote the extreme points that belong to class ω_1 and ω_2 by \mathbf{x}_{1i*} and \mathbf{x}_{2i*} with weights (labels) $y_i = 1$ and $y_i = -1$ respectively. Let there be l_1 extreme points \mathbf{x}_{1i*} from class ω_1 and l_2 extreme points \mathbf{x}_{2i*} from class ω_2 .

Let there be l_1 principal eigenaxis components $\psi_{1i*} \vec{e}_{1i*}$, where each eigen-scale ψ_{1i*} is correlated with the extreme vector \mathbf{x}_{1i*} . Let there be l_2 principal eigenaxis components $\psi_{2i*} \vec{e}_{2i*}$, where each eigen-scale ψ_{2i*} is correlated with the extreme vector \mathbf{x}_{2i*} . Let $l_1 + l_2 = l$.

I will now define symmetrically balanced, pointwise covariance statistics. The geometric nature of the statistics is outlined first.

9.1 Symmetrically Balanced Covariance Statistics

Take two labeled sets of extreme vectors, where each extreme vector is correlated with an eigen-scale that determines eigen-scaled, signed magnitudes, i.e., eigen-scaled components of the eigen-scaled extreme vector, along the axes of the extreme vectors in each pattern class, such that the integrated eigen-scales from each pattern class balance each other.

Generally speaking, for any given set of extreme vectors, all of the eigen-scaled, signed magnitudes along the axis of any given extreme vector from a given pattern class, which are determined by vector projections of eigen-scaled extreme vectors from the *other* pattern class, *are distributed in opposite directions*. Thereby, for two labeled sets of extreme vectors, where each extreme vector is correlated with an eigen-scale and the integrated eigen-scales from each pattern class balance each other, eigen-scaled, signed magnitudes along the axis of any given

extreme vector, which are determined by vector projections of eigen-scaled extreme vectors from the *other* pattern class, *are distributed on the opposite side of the origin*. Accordingly, eigen-scaled, signed magnitudes along the axes of all of the extreme vectors are distributed in a symmetrically balanced manner, where each eigen-scale encodes a symmetrically balanced distribution for an extreme point which ensures that the components of an extreme vector are distributed over the axes of a given collection of extreme vectors in a symmetrically balanced and well-proportioned manner.

Using Eqs (51) and (57), along with the notation and assumptions outlined above, it follows that summation over the l components of ψ in Eq. (60), provides symmetrically balanced covariance statistics for the \mathbf{x}_{1i*} extreme vectors, where each extreme point \mathbf{x}_{1i*} exhibits a symmetrically balanced, first and second-order statistical moment $\widehat{\text{cov}}_{up\uparrow}(\mathbf{x}_{1i*})$

$$\begin{aligned} \widehat{\text{cov}}_{up\uparrow}(\mathbf{x}_{1i*}) &= \|\mathbf{x}_{1i*}\| \sum_{j=1}^{l_1} \psi_{1j*} \|\mathbf{x}_{1j*}\| \cos \theta_{\mathbf{x}_{1i*}\mathbf{x}_{1j*}} \\ &\quad - \|\mathbf{x}_{1i*}\| \sum_{j=1}^{l_2} \psi_{2j*} \|\mathbf{x}_{2j*}\| \cos \theta_{\mathbf{x}_{1i*}\mathbf{x}_{2j*}}, \end{aligned} \quad (62)$$

relative to l symmetrically balanced, eigen-scaled, signed magnitudes determined by vector projections of eigen-scaled extreme vectors in each respective pattern class.

Likewise, summation over the l components of ψ in Eq. (60), provides symmetrically balanced covariance statistics for the \mathbf{x}_{2i*} extreme vectors, where each extreme point \mathbf{x}_{2i*} exhibits a symmetrically balanced, first and second-order statistical moment $\widehat{\text{cov}}_{up\uparrow}(\mathbf{x}_{2i*})$

$$\begin{aligned} \widehat{\text{cov}}_{up\uparrow}(\mathbf{x}_{2i*}) &= \|\mathbf{x}_{2i*}\| \sum_{j=1}^{l_2} \psi_{2j*} \|\mathbf{x}_{2j*}\| \cos \theta_{\mathbf{x}_{2i*}\mathbf{x}_{2j*}} \\ &\quad - \|\mathbf{x}_{2i*}\| \sum_{j=1}^{l_1} \psi_{1j*} \|\mathbf{x}_{1j*}\| \cos \theta_{\mathbf{x}_{1i*}\mathbf{x}_{2j*}}, \end{aligned} \quad (63)$$

relative to l symmetrically balanced, eigen-scaled, signed magnitudes determined by vector projections of eigen-scaled extreme vectors in each respective pattern class.

I will use Eqs (62) and (63) to define symmetrical geometric and statistical properties possessed by principal eigenaxis components on τ and ψ .

Loci of the $\psi_{1i*} \vec{\mathbf{e}}_{1i*}$ Components

Let $i = 1 : l_1$, where each extreme vector \mathbf{x}_{1i*} is correlated with a Wolfe principal eigenaxis component $\psi_{1i*} \vec{\mathbf{e}}_{1i*}$. Using Eqs (60) and (61), the locus of the i^{th} principal eigenaxis component $\psi_{1i*} \vec{\mathbf{e}}_{1i*}$ on ψ is a function

of the expression:

$$\begin{aligned} \psi_{1i*} &= \lambda_{\max_\psi}^{-1} \|\mathbf{x}_{1i*}\| \sum_{j=1}^{l_1} \psi_{1j*} \|\mathbf{x}_{1j*}\| \cos \theta_{\mathbf{x}_{1i*} \mathbf{x}_{1j*}} \\ &\quad - \lambda_{\max_\psi}^{-1} \|\mathbf{x}_{1i*}\| \sum_{j=1}^{l_2} \psi_{2j*} \|\mathbf{x}_{2j*}\| \cos \theta_{\mathbf{x}_{1i*} \mathbf{x}_{2j*}}, \end{aligned} \quad (64)$$

where ψ_{1i*} provides an eigen-scaling for the non-orthogonal unit vector $\vec{\mathbf{e}}_{1i*}$. Geometric and statistical explanations for the eigenlocus statistics

$$\psi_{1j*} \|\mathbf{x}_{1j*}\| \cos \theta_{\mathbf{x}_{1i*} \mathbf{x}_{1j*}} \text{ and } \psi_{2j*} \|\mathbf{x}_{2j*}\| \cos \theta_{\mathbf{x}_{1i*} \mathbf{x}_{2j*}}, \quad (65)$$

in Eq. (64) are considered next.

Geometric and Statistical Nature of Eigenlocus Statistics

The first geometric interpretation of the eigenlocus statistics in Eq. (65) defines ψ_{1j*} and ψ_{2j*} to be eigen-scales for the signed magnitudes of the vector projections

$$\|\mathbf{x}_{1j*}\| \cos \theta_{\mathbf{x}_{1i*} \mathbf{x}_{1j*}} \text{ and } \|\mathbf{x}_{2j*}\| \cos \theta_{\mathbf{x}_{1i*} \mathbf{x}_{2j*}},$$

of the eigen-scaled extreme vectors $\psi_{1j*} \mathbf{x}_{1j*}$ and $\psi_{2j*} \mathbf{x}_{2j*}$ along the axis of the extreme vector \mathbf{x}_{1i*} , where $\cos \theta_{\mathbf{x}_{1i*} \mathbf{x}_{1j*}}$ and $\cos \theta_{\mathbf{x}_{1i*} \mathbf{x}_{2j*}}$ are the respective angles between the axes of the eigen-scaled extreme vectors $\psi_{1j*} \mathbf{x}_{1j*}$ and $\psi_{2j*} \mathbf{x}_{2j*}$ and the axis of the extreme vector \mathbf{x}_{1i*} . Note that the signed magnitude $\psi_{2j*} \|\mathbf{x}_{2j*}\| \cos \theta_{\mathbf{x}_{1i*} \mathbf{x}_{2j*}}$ is distributed in the opposite direction, so that the locus of $\psi_{2j*} \|\mathbf{x}_{2j*}\| \cos \theta_{\mathbf{x}_{1i*} \mathbf{x}_{2j*}}$ is on the opposite side of the origin, along the axis of the extreme vector \mathbf{x}_{1i*} .

Figure 20 illustrates the geometric and statistical nature of the eigenlocus statistics in Eq. (65), where any given eigen-scaled, signed magnitude $\psi_{1j*} \|\mathbf{x}_{1j*}\| \cos \theta_{\mathbf{x}_{1i*} \mathbf{x}_{1j*}}$ or $\psi_{2j*} \|\mathbf{x}_{2j*}\| \cos \theta_{\mathbf{x}_{1i*} \mathbf{x}_{2j*}}$ may be positive or negative (see Fig. 20a and 20b.)

Alternative Geometric Interpretation

An alternative geometric explanation for the eigenlocus statistics in Eq. (65) accounts for the representation of τ_1 and τ_2 within the Wolfe dual eigenspace. Consider the algebraic relationships

$$\psi_{1j*} \|\mathbf{x}_{1j*}\| = \|\psi_{1j*} \mathbf{x}_{1j*}\| = \|\tau_1(j)\|,$$

and

$$\psi_{2j*} \|\mathbf{x}_{2j*}\| = \|\psi_{2j*} \mathbf{x}_{2j*}\| = \|\tau_2(j)\|,$$

where $\tau_1(j)$ and $\tau_2(j)$ are the j th constrained, primal principal eigenaxis components on τ_1 and τ_2 . It follows that the eigen-scaled ψ_{1j*} signed

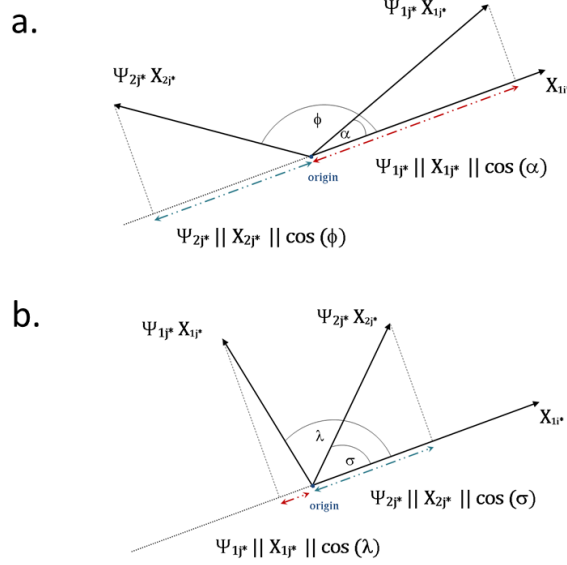


Figure 20: Examples of positive and negative, eigen-scaled, signed magnitudes of vector projections of eigen-scaled extreme vectors $\psi_{1j^*} \mathbf{x}_{1j^*}$ and $\psi_{2j^*} \mathbf{x}_{2j^*}$, along the axis of an extreme vector \mathbf{x}_{1i^*} which is correlated with a Wolfe dual principal eigenaxis component $\psi_{1i^*} \vec{\mathbf{e}}_{1i^*}$.

magnitude $\|\mathbf{x}_{1j^*}\| \cos \theta_{\mathbf{x}_{1i^*} \mathbf{x}_{1j^*}}$ of the vector projection of the eigen-scaled extreme vector $\psi_{1j^*} \mathbf{x}_{1j^*}$ along the axis of the extreme vector \mathbf{x}_{1i^*}

$$\psi_{1j^*} \|\mathbf{x}_{1j^*}\| \cos \theta_{\mathbf{x}_{1i^*} \mathbf{x}_{1j^*}},$$

encodes the cosine-scaled $\cos \theta_{\mathbf{x}_{1i^*} \mathbf{x}_{1j^*}}$ length of the j th constrained primal principal eigenaxis component $\tau_1(j)$ on τ_1

$$\cos \theta_{\mathbf{x}_{1i^*} \mathbf{x}_{1j^*}} \|\tau_1(j)\|,$$

where ψ_{1j^*} is the length of the $\psi_{1j^*} \vec{\mathbf{e}}_{1j^*}$ Wolfe dual principal eigenaxis component and $\cos \theta_{\mathbf{x}_{1i^*} \mathbf{x}_{1j^*}}$ encodes the angle between the extreme vectors \mathbf{x}_{1i^*} and \mathbf{x}_{1j^*} .

Likewise, the eigen-scaled ψ_{2j^*} signed magnitude $\|\mathbf{x}_{2j^*}\| \cos \theta_{\mathbf{x}_{1i^*} \mathbf{x}_{2j^*}}$ of the vector projection of the eigen-scaled extreme vector $\psi_{2j^*} \mathbf{x}_{2j^*}$ along the axis of the extreme vector \mathbf{x}_{1i^*}

$$\psi_{2j^*} \|\mathbf{x}_{2j^*}\| \cos \theta_{\mathbf{x}_{1i^*} \mathbf{x}_{2j^*}},$$

encodes the cosine-scaled $\cos \theta_{\mathbf{x}_{1i^*} \mathbf{x}_{2j^*}}$ length of the j th constrained primal principal eigenaxis component $\tau_2(j)$ on τ_2

$$\cos \theta_{\mathbf{x}_{1i^*} \mathbf{x}_{2j^*}} \|\tau_2(j)\|,$$

where ψ_{2j*} is the length of the $\psi_{2j*} \vec{e}_{2j*}$ Wolfe dual principal eigenaxis component and $\cos \theta_{\mathbf{x}_{1i*} \mathbf{x}_{2j*}}$ encodes the angle between the extreme vectors \mathbf{x}_{1i*} and \mathbf{x}_{2j*} .

It follows that the locus of each Wolfe dual principal eigenaxis component $\psi_{1i*} \vec{e}_{1i*}$ is a function of the constrained, primal principal eigenaxis components on τ_1 and τ_2 :

$$\begin{aligned} \psi_{1i*} = & \lambda_{\max \psi}^{-1} \|\mathbf{x}_{1i*}\| \sum_{j=1}^{l_1} \cos \theta_{\mathbf{x}_{1i*} \mathbf{x}_{1j*}} \|\tau_1(j)\| \\ & - \lambda_{\max \psi}^{-1} \|\mathbf{x}_{1i*}\| \sum_{j=1}^{l_2} \cos \theta_{\mathbf{x}_{1i*} \mathbf{x}_{2j*}} \|\tau_2(j)\|, \end{aligned} \quad (66)$$

where the angle between each principal eigenaxis component $\tau_1(j)$ and $\tau_2(j)$ and the extreme vector \mathbf{x}_{1i*} is fixed.

I will now examine how similar geometric and statistical properties which are jointly exhibited by Wolfe dual $\psi_{1i*} \vec{e}_{1i*}$ and constrained primal $\psi_{1i*} \mathbf{x}_{1i*}$ principal eigenaxis components regulate the symmetric partitioning of a feature space Z .

Similar Geometric and Statistical Properties

Using the definition of Eq. (62), Eq. (64) indicates that the locus of the principal eigenaxis component $\psi_{1i*} \vec{e}_{1i*}$ is determined by a symmetrically balanced, signed magnitude along the axis of an extreme vector \mathbf{x}_{1i*} , relative to symmetrically balanced, eigen-scaled, signed magnitudes of extreme vector projections in each respective pattern class.

Symmetrically Balanced Signed Magnitudes

Let $\text{comp}_{\vec{\mathbf{x}}_{1i*}} \left(\overrightarrow{\tilde{\psi}_{1i*} \|\tilde{\mathbf{x}}_{*}\|_{1i*}} \right)$ denote the symmetrically balanced, signed magnitude

$$\begin{aligned} \text{comp}_{\vec{\mathbf{x}}_{1i*}} \left(\overrightarrow{\tilde{\psi}_{1i*} \|\tilde{\mathbf{x}}_{*}\|_{1i*}} \right) = & \sum_{j=1}^{l_1} \psi_{1j*} \\ & \times \left[\|\mathbf{x}_{1j*}\| \cos \theta_{\mathbf{x}_{1i*} \mathbf{x}_{1j*}} \right] \\ & - \sum_{j=1}^{l_2} \psi_{2j*} \\ & \times \left[\|\mathbf{x}_{2j*}\| \cos \theta_{\mathbf{x}_{1i*} \mathbf{x}_{2j*}} \right], \end{aligned} \quad (67)$$

along the axis of the extreme vector \mathbf{x}_{1i*} that is correlated with the Wolfe dual principal eigenaxis component $\psi_{1i*} \vec{e}_{1i*}$.

Symmetrically Balanced Distributions and Statistical Moments

Using the definitions of Eqs (57) and (62), it follows that Eq. (67) determines a symmetrically balanced distribution of eigen-scaled, first

degree coordinates of extreme vectors along the axis of \mathbf{x}_{1i*} , where each eigen-scale ψ_{1j*} or ψ_{2j*} determines how the extreme vector \mathbf{x}_{1j*} or \mathbf{x}_{2j*} is distributed along the axis of \mathbf{x}_{1i*} and each eigen-scale ψ_{1j*} or ψ_{2j*} encodes a symmetrically balanced distribution of eigen-scaled, first degree coordinates of extreme vectors $\{\psi_{j*}\mathbf{x}_{j*}\}_{j=1}^l$ along the axis of the extreme vector \mathbf{x}_{1j*} or \mathbf{x}_{2j*} .

It follows that each eigen-scaled, signed magnitude $\psi_{1j*} \|\mathbf{x}_{1j*}\| \cos \theta_{\mathbf{x}_{1i*}, \mathbf{x}_{1j*}}$ or $\psi_{2j*} \|\mathbf{x}_{2j*}\| \cos \theta_{\mathbf{x}_{1i*}, \mathbf{x}_{2j*}}$ provides an estimate for how the components of the extreme vector \mathbf{x}_{1i*} are symmetrically distributed over the axis of an eigen-scaled extreme vector $\psi_{1j*}\mathbf{x}_{1j*}$ or $\psi_{2j*}\mathbf{x}_{2j*}$, where each eigen-scale ψ_{1j*} or ψ_{2j*} encodes a symmetrically balanced distribution of eigen-scaled, first degree coordinates of extreme vectors $\{\psi_{j*}\mathbf{x}_{j*}\}_{j=1}^l$ along the axis of the extreme vector \mathbf{x}_{1j*} or \mathbf{x}_{2j*} .

Again using Eqs (57 and (62), it follows that Eq. (67) determines a symmetrically balanced, first and second-order statistical moment about the locus of \mathbf{x}_{1i*} , where each eigen-scale ψ_{1j*} or ψ_{1j*} determines how the components of an extreme vector \mathbf{x}_{1j*} or \mathbf{x}_{2j*} are distributed along the axis of \mathbf{x}_{1i*} , and each eigen-scale ψ_{1j*} or ψ_{1j*} encodes a symmetrically balanced distribution for the extreme vector \mathbf{x}_{1j*} or \mathbf{x}_{2j*} .

Symmetrically Balanced Distributions of Eigenaxis Components

Using Eqs (51), (64), and (67), it follows that symmetrically balanced, joint distributions of the principal eigenaxis components on ψ and τ are distributed over the axis of the extreme vector \mathbf{x}_{1i*} .

Again using Eq. (64), it follows that identical, symmetrically balanced, joint distributions of the principal eigenaxis components on ψ and τ are distributed over the axis of the Wolfe dual principal eigenaxis component $\psi_{1i*}\vec{\mathbf{e}}_{1i*}$. Thereby, symmetrically balanced, joint distributions of the principal eigenaxis components on ψ and τ are identically and symmetrically distributed over the respective axes of each Wolfe dual principal eigenaxis component $\psi_{1i*}\vec{\mathbf{e}}_{1i*}$ and correlated extreme vector \mathbf{x}_{1i*} .

Alternatively, using Eq. (66), the symmetrically balanced, signed magnitude in Eq. (67) depends upon the difference between integrated cosine-scaled lengths of the constrained primal principal eigenaxis components on τ_1 and τ_2 :

$$\begin{aligned} \text{comp}_{\vec{\mathbf{x}}_{1i*}} \left(\overrightarrow{\widetilde{\psi}_{1i*} \|\widetilde{\mathbf{x}}_{*}\|_{1i*}} \right) &= \sum_{j=1}^{l_1} \cos \theta_{\mathbf{x}_{1i*}, \mathbf{x}_{1j*}} \|\tau_1(j)\| \\ &\quad - \sum_{j=1}^{l_2} \cos \theta_{\mathbf{x}_{1i*}, \mathbf{x}_{2j*}} \|\tau_2(j)\|, \end{aligned} \quad (68)$$

which also shows that symmetrically balanced, joint distributions of the

principal eigenaxis components on ψ and τ are identically and symmetrically distributed along the respective axes of each Wolfe dual principal eigenaxis component $\psi_{1i*} \vec{e}_{1i*}$ and correlated extreme vector \mathbf{x}_{1i*} .

Using Eqs (64) and (67), it follows that the length ψ_{1i*} of each Wolfe dual principal eigenaxis component $\psi_{1i*} \vec{e}_{1i*}$ is determined by the weighted length of a correlated extreme vector \mathbf{x}_{1i*}

$$\psi_{1i*} = \left[\lambda_{\max_\psi}^{-1} \times \text{comp}_{\mathbf{x}_{1i*}} \left(\overrightarrow{\tilde{\psi}_{1i*} \|\tilde{\mathbf{x}}_*\|_{1i*}} \right) \right] \|\mathbf{x}_{1i*}\|, \quad (69)$$

where the weighting factor encodes an eigenvalue $\lambda_{\max_\psi}^{-1}$ scaling of a symmetrically balanced, signed magnitude $\text{comp}_{\mathbf{x}_{1i*}} \left(\overrightarrow{\tilde{\psi}_{1i*} \|\tilde{\mathbf{x}}_*\|_{1i*}} \right)$ along the axis of \mathbf{x}_{1i*} .

Symmetrically Balanced Lengths

Given that $\psi_{1i*} > 0$, $\lambda_{\max_\psi}^{-1} > 0$, and $\|\mathbf{x}_{1i*}\| > 0$, it follows that the symmetrically balanced, signed magnitude along the axis of each extreme vector \mathbf{x}_{1i*} is a positive number

$$\text{comp}_{\mathbf{x}_{1i*}} \left(\overrightarrow{\tilde{\psi}_{1i*} \|\tilde{\mathbf{x}}_*\|_{1i*}} \right) > 0,$$

which indicates that the weighting factor in Eq. (69) determines a well-proportioned length

$$\lambda_{\max_\psi}^{-1} \text{comp}_{\mathbf{x}_{1i*}} \left(\overrightarrow{\tilde{\psi}_{1i*} \|\tilde{\mathbf{x}}_*\|_{1i*}} \right) \|\mathbf{x}_{1i*}\|,$$

for an extreme vector \mathbf{x}_{1i*} . Thereby, the length ψ_{1i*} of each Wolfe dual principal eigenaxis component $\psi_{1i*} \vec{e}_{1i*}$ is determined by a well-proportioned length of a correlated extreme vector \mathbf{x}_{1i*} .

Returning to Eqs (62) and (64), it follows that the length ψ_{1i*} of each Wolfe dual principal eigenaxis component $\psi_{1i*} \vec{e}_{1i*}$ on ψ

$$\psi_{1i*} = \lambda_{\max_\psi}^{-1} \text{comp}_{\mathbf{x}_{1i*}} \left(\overrightarrow{\tilde{\psi}_{1i*} \|\tilde{\mathbf{x}}_*\|_{1i*}} \right) \|\mathbf{x}_{1i*}\|,$$

is shaped by a symmetrically balanced, first and second-order statistical moment about the locus of a correlated extreme vector \mathbf{x}_{1i*} .

Now, take any given correlated pair $\{\psi_{1i*} \vec{e}_{1i*}, \psi_{1i*} \mathbf{x}_{1i*}\}$ of Wolfe dual $\psi_{1i*} \vec{e}_{1i*}$ and constrained primal $\psi_{1i*} \mathbf{x}_{1i*}$ principal eigenaxis components. I will now show that the direction of $\psi_{1i*} \vec{e}_{1i*}$ is identical to the direction of $\psi_{1i*} \mathbf{x}_{1i*}$.

Directional Symmetries

The vector direction of each Wolfe dual principal eigenaxis component $\psi_{1i*} \vec{\mathbf{e}}_{1i*}$ is implicitly specified by Eq. (64), where it has been assumed that ψ_{1i*} provides an eigen-scaling for a non-orthogonal unit vector $\vec{\mathbf{e}}_{1i*}$. Using the definitions of Eqs (57) and (62), it follows that the symmetrically balanced, pointwise covariance statistic in Eq. (64) encodes the direction of a correlated extreme vector \mathbf{x}_{1i*} and a well-proportioned magnitude along the axis of the extreme vector \mathbf{x}_{1i*} .

Returning to Eqs (67), (68), and (69), take any given Wolfe dual principal eigenaxis component $\psi_{1i*} \vec{\mathbf{e}}_{1i*}$ that is correlated with an extreme vector \mathbf{x}_{1i*} . Given that the magnitude ψ_{1i*} of each Wolfe dual principal eigenaxis component $\psi_{1i*} \vec{\mathbf{e}}_{1i*}$ is determined by a well-proportioned magnitude of a correlated extreme vector \mathbf{x}_{1i*}

$$\psi_{1i*} = \lambda_{\max_\psi}^{-1} \text{comp}_{\vec{\mathbf{x}}_{1i*}} \left(\overrightarrow{\widetilde{\psi}_{1i*} \|\widetilde{\mathbf{x}}_{*}\|_{1i*}} \right) \|\mathbf{x}_{1i*}\|,$$

it follows that each non-orthogonal unit vector $\vec{\mathbf{e}}_{1i*}$ has the same direction as an extreme vector \mathbf{x}_{1i*}

$$\vec{\mathbf{e}}_{1i*} \equiv \frac{\mathbf{x}_{1i*}}{\|\mathbf{x}_{1i*}\|}.$$

Therefore, the direction of each Wolfe dual principal eigenaxis component $\psi_{1i*} \vec{\mathbf{e}}_{1i*}$ on ψ is identical to the direction of a correlated, constrained primal principal eigenaxis component $\psi_{1i*} \mathbf{x}_{1i*}$ on τ_1 which is determined by the direction of an eigen-scaled ψ_{1i*} extreme vector \mathbf{x}_{1i*} . Each Wolfe dual $\psi_{1i*} \vec{\mathbf{e}}_{1i*}$ and correlated constrained primal $\psi_{1i*} \mathbf{x}_{1i*}$ principal eigenaxis component are said to exhibit directional symmetry.

Directions of Large Covariance

It is concluded that the uniform directions of the Wolfe dual $\psi_{1i*} \vec{\mathbf{e}}_{1i*}$ and the correlated constrained primal $\psi_{1i*} \mathbf{x}_{1i*}$ principal eigenaxis components determine directions of large covariance which contribute to a symmetric partitioning of a minimal geometric region of constant width that spans a region of large covariance between two data distributions. It is also concluded that each of the correlated principal eigenaxis components on ψ_1 and τ_1 possess well-proportioned magnitudes for which the constrained linear discriminant function $D(\mathbf{x}) = \mathbf{x}^T \tau + \tau_0$ delineates centrally located, bipartite, symmetric regions of large covariance between any two data distributions.

Loci of the $\psi_{2i*} \vec{\mathbf{e}}_{2i*}$ Components

Let $i = 1 : l_2$, where each extreme vector \mathbf{x}_{2i*} is correlated with a Wolfe dual principal eigenaxis component $\psi_{2i*} \vec{\mathbf{e}}_{2i*}$. Using Eqs (60) and (61),

the locus of the i^{th} Wolfe dual principal eigenaxis component $\psi_{2i*} \vec{e}_{2i*}$ on ψ is a function of the expression:

$$\begin{aligned} \psi_{2i*} &= \lambda_{\max_\psi}^{-1} \|\mathbf{x}_{2i*}\| \sum_{j=1}^{l_2} \psi_{2j*} \|\mathbf{x}_{2j*}\| \cos \theta_{\mathbf{x}_{2i*} \mathbf{x}_{2j*}} \\ &\quad - \lambda_{\max_\psi}^{-1} \|\mathbf{x}_{2i*}\| \sum_{j=1}^{l_1} \psi_{1j*} \|\mathbf{x}_{1j*}\| \cos \theta_{\mathbf{x}_{2i*} \mathbf{x}_{1j*}}, \end{aligned} \quad (70)$$

where ψ_{2i*} provides an eigen-scaling for the non-orthogonal unit vector \vec{e}_{2i*} .

Results obtained from the above analysis are readily generalized to the Wolfe dual $\psi_{2i*} \vec{e}_{2i*}$ and the constrained primal $\psi_{2i*} \mathbf{x}_{2i*}$ principal eigenaxis components, so the analysis will not be replicated. However, the counterpart to Eq. (67) is necessary for a future argument. Let $i = l_1 + 1 : l_1 + l_2$, where each extreme vector \mathbf{x}_{2i*} is correlated with a Wolfe principal eigenaxis component $\psi_{2i*} \vec{e}_{2i*}$. Accordingly, let $\text{comp}_{\vec{\mathbf{x}}_{2i*}} \left(\overrightarrow{\psi_{2i*} \|\tilde{\mathbf{x}}_*\|_{2i*}} \right)$ denote the symmetrically balanced, signed magnitude

$$\begin{aligned} \text{comp}_{\vec{\mathbf{x}}_{2i*}} \left(\overrightarrow{\psi_{2i*} \|\tilde{\mathbf{x}}_*\|_{2i*}} \right) &= \sum_{j=1}^{l_2} \psi_{2j*} \\ &\quad \times \left[\|\mathbf{x}_{2j*}\| \cos \theta_{\mathbf{x}_{2i*} \mathbf{x}_{2j*}} \right] \\ &\quad - \sum_{j=1}^{l_1} \psi_{1j*} \\ &\quad \times \left[\|\mathbf{x}_{1j*}\| \cos \theta_{\mathbf{x}_{2i*} \mathbf{x}_{1j*}} \right], \end{aligned} \quad (71)$$

along the axis of the extreme vector \mathbf{x}_{2i*} that is correlated with the Wolfe dual principal eigenaxis component $\psi_{2i*} \vec{e}_{2i*}$.

9.2 Similar Properties Exhibited by ψ and τ

I will now identify similar geometric and statistical properties which are jointly exhibited by the Wolfe dual principal eigenaxis components on ψ and the correlated, constrained primal principal eigenaxis components on τ . The properties are summarized below.

Directional Symmetry

1. The direction of each Wolfe dual principal eigenaxis component $\psi_{1i*} \vec{e}_{1i*}$ on $\psi_1 \in \mathbb{R}^l$ is identical to the direction of a correlated, constrained, primal principal eigenaxis component $\psi_{1i*} \mathbf{x}_{1i*}$ on $\tau_1 \in \mathbb{R}^d$.
2. The direction of each Wolfe dual principal eigenaxis component $\psi_{2i*} \vec{e}_{2i*}$ on $\psi_2 \in \mathbb{R}^l$ is identical to the direction of a correlated, constrained, primal principal eigenaxis component $\psi_{2i*} \mathbf{x}_{2i*}$ on $\tau_2 \in \mathbb{R}^d$.

Symmetrically Balanced Lengths

1. The lengths of each Wolfe dual principal eigenaxis component $\psi_{1i*} \vec{e}_{1i*}$ on $\psi_1 \in \mathbb{R}^l$ and each correlated, constrained, primal principal eigenaxis component $\psi_{1i*} \mathbf{x}_{1i*}$ on $\tau_1 \in \mathbb{R}^d$ are shaped by identical, symmetrically balanced, joint distributions of the principal eigenaxis components on ψ and τ .
2. The lengths of each Wolfe dual principal eigenaxis component $\psi_{2i*} \vec{e}_{2i*}$ on $\psi_2 \in \mathbb{R}^l$ and each correlated, constrained, primal principal eigenaxis component $\psi_{2i*} \mathbf{x}_{2i*}$ on $\tau_2 \in \mathbb{R}^d$ are shaped by identical, symmetrically balanced, joint distributions of the principal eigenaxis components on ψ and τ .

Symmetrically Balanced Pointwise Covariance Statistics

1. The magnitude ψ_{1i*} of each Wolfe dual principal eigenaxis component $\psi_{1i*} \vec{e}_{1i*}$ on $\psi_1 \in \mathbb{R}^l$

$$\psi_{1i*} = \lambda_{\max_\psi}^{-1} \text{comp}_{\mathbf{x}_{1i*}} \left(\overrightarrow{\tilde{\psi}_{1i*} \|\tilde{\mathbf{x}}_*\|_{1i*}} \right) \|\mathbf{x}_{1i*}\|,$$

is determined by a symmetrically balanced, pointwise covariance estimate

$$\begin{aligned} \widehat{\text{cov}}_{up\downarrow}(\mathbf{x}_{1i*}) &= \lambda_{\max_\psi}^{-1} \|\mathbf{x}_{1i*}\| \\ &\times \sum_{j=1}^{l_1} \psi_{1j*} \|\mathbf{x}_{1j*}\| \cos \theta_{\mathbf{x}_{1i*} \mathbf{x}_{1j*}} \\ &- \lambda_{\max_\psi}^{-1} \|\mathbf{x}_{1i*}\| \\ &\times \sum_{j=1}^{l_2} \psi_{2j*} \|\mathbf{x}_{2j*}\| \cos \theta_{\mathbf{x}_{1i*} \mathbf{x}_{2j*}}, \end{aligned}$$

for a correlated extreme vector $\mathbf{x}_{1i*} \in \mathbb{R}^d$, such that the locus of each constrained, primal principal eigenaxis component $\psi_{1i*} \mathbf{x}_{1i*}$ on $\tau_1 \in \mathbb{R}^d$ provides a maximum covariance estimate in a principal location \mathbf{x}_{1i*} , in the form of a symmetrically balanced, first and second-order statistical moment about the locus of an extreme data point \mathbf{x}_{1i*} .

2. The magnitude ψ_{2i*} of each Wolfe dual principal eigenaxis component $\psi_{2i*} \vec{e}_{2i*}$ on $\psi_2 \in \mathbb{R}^l$

$$\psi_{2i*} = \lambda_{\max_\psi}^{-1} \text{comp}_{\mathbf{x}_{2i*}} \left(\overrightarrow{\tilde{\psi}_{2i*} \|\tilde{\mathbf{x}}_*\|_{2i*}} \right) \|\mathbf{x}_{2i*}\|,$$

is determined by a symmetrically balanced, pointwise covariance estimate

$$\begin{aligned}\widehat{\text{cov}}_{up\uparrow}(\mathbf{x}_{2i*}) &= \lambda_{\max\psi}^{-1} \|\mathbf{x}_{2i*}\| \\ &\times \sum_{j=1}^{l_2} \psi_{2j*} \|\mathbf{x}_{2j*}\| \cos \theta_{\mathbf{x}_{2i*} \mathbf{x}_{2j*}} \\ &- \lambda_{\max\psi}^{-1} \|\mathbf{x}_{2i*}\| \\ &\times \sum_{j=1}^{l_1} \psi_{1j*} \|\mathbf{x}_{1j*}\| \cos \theta_{\mathbf{x}_{2i*} \mathbf{x}_{1j*}},\end{aligned}$$

for a correlated extreme vector $\mathbf{x}_{2i*} \in \mathbb{R}^d$, such that the locus of each constrained, primal principal eigenaxis component $\psi_{2i*} \mathbf{x}_{2i*}$ on $\tau_2 \in \mathbb{R}^d$ provides a maximum covariance estimate in a principal location \mathbf{x}_{2i*} , in the form of a symmetrically balanced, first and second-order statistical moment about the locus of an extreme point \mathbf{x}_{2i*} .

Symmetrically Balanced Statistical Moments

1. Each Wolfe dual principal eigenaxis component $\psi_{1i*} \vec{\mathbf{e}}_{1i*}$ on ψ_1 encodes a symmetrically balanced, first and second-order statistical moment about the locus of a correlated extreme point \mathbf{x}_{1i*} , relative to the loci of all of the eigen-scaled extreme points which determines the locus of the constrained, primal principal eigenaxis component $\psi_{1i*} \mathbf{x}_{1i*}$ on τ_1 .
2. Each Wolfe dual principal eigenaxis component $\psi_{2i*} \vec{\mathbf{e}}_{1i*}$ on ψ_2 encodes a symmetrically balanced, first and second-order statistical moment about the locus of a correlated extreme point \mathbf{x}_{2i*} , relative to the loci of all of the eigen-scaled extreme points which determines the locus of the constrained, primal principal eigenaxis component $\psi_{2i*} \mathbf{x}_{2i*}$ on τ_2 .

Symmetrically Balanced Distributions of Extreme Point Coordinates

1. Any given maximum covariance estimate $\widehat{\text{cov}}_{up\uparrow}(\mathbf{x}_{1i*})$ describes how the components of l eigen-scaled extreme vectors $\{\psi_{1j*} \mathbf{x}_{1j*}\}_{j=1}^{l_1}$ and $\{\psi_{2j*} \mathbf{x}_{2j*}\}_{j=1}^{l_2}$ are distributed along the axis of an extreme vector \mathbf{x}_{1i*} , where each eigen-scale ψ_{1j*} or ψ_{2j*} encodes a symmetrically balanced distribution of l eigen-scaled extreme vectors along the axis of an extreme vector \mathbf{x}_{1j*} or \mathbf{x}_{2j*} , such that a pointwise covariance estimate $\widehat{\text{cov}}_{up\uparrow}(\mathbf{x}_{1i*})$ provides an estimate for how

the components of the extreme vector $\mathbf{x}_{1_{i*}}$ are symmetrically distributed over the axes of the l eigen-scaled extreme vectors. Thus, $\widehat{\text{cov}}_{up\downarrow}(\mathbf{x}_{1_{i*}})$ describes a distribution of first degree coordinates for $\mathbf{x}_{1_{i*}}$.

2. Any given maximum covariance estimate $\widehat{\text{cov}}_{up\downarrow}(\mathbf{x}_{2_{i*}})$ describes how the components of l eigen-scaled extreme vectors $\{\psi_{1_{j*}}\mathbf{x}_{1_{j*}}\}_{j=1}^{l_1}$ and $\{\psi_{2_{j*}}\mathbf{x}_{2_{j*}}\}_{j=1}^{l_2}$ are distributed along the axis of an extreme vector $\mathbf{x}_{2_{i*}}$, where each eigen-scale $\psi_{1_{j*}}$ or $\psi_{2_{j*}}$ encodes a symmetrically balanced distribution of l eigen-scaled extreme vectors along the axis of an extreme vector $\mathbf{x}_{1_{j*}}$ or $\mathbf{x}_{2_{j*}}$, such that a point-wise covariance estimate $\widehat{\text{cov}}_{up\downarrow}(\mathbf{x}_{2_{i*}})$ provides an estimate for how the components of the extreme vector $\mathbf{x}_{2_{i*}}$ are symmetrically distributed over the axes of the l eigen-scaled extreme vectors. Thus, $\widehat{\text{cov}}_{up\downarrow}(\mathbf{x}_{2_{i*}})$ describes a distribution of first degree coordinates for $\mathbf{x}_{2_{i*}}$.

I will now define the equivalence between the total allowed eigenenergies of ψ and τ .

9.3 Equivalence Between Eigenenergies of ψ and τ

The inner product between the integrated Wolf dual principal eigenaxis components on ψ

$$\begin{aligned} \|\psi\|_{\min_c}^2 &= \left(\sum_{i=1}^{l_1} \psi_{1_{i*}} \frac{\mathbf{x}_{1_{i*}}^T}{\|\mathbf{x}_{1_{i*}}\|} + \sum_{i=1}^{l_2} \psi_{2_{i*}} \frac{\mathbf{x}_{2_{i*}}^T}{\|\mathbf{x}_{2_{i*}}\|} \right) \\ &\quad \times \left(\sum_{i=1}^{l_1} \psi_{1_{i*}} \frac{\mathbf{x}_{1_{i*}}}{\|\mathbf{x}_{1_{i*}}\|} + \sum_{i=1}^{l_2} \psi_{2_{i*}} \frac{\mathbf{x}_{2_{i*}}}{\|\mathbf{x}_{2_{i*}}\|} \right), \end{aligned}$$

determines the total allowed eigenenergy $\|\psi\|_{\min_c}^2$ of ψ which is symmetrically equivalent with the critical minimum eigenenergy $\|\tau\|_{\min_c}^2$ of τ within its Wolfe dual eigenspace

$$\begin{aligned} \|\tau\|_{\min_c}^2 &= \left(\sum_{i=1}^{l_1} \psi_{1_{i*}} \mathbf{x}_{1_{i*}}^T - \sum_{i=1}^{l_2} \psi_{2_{i*}} \mathbf{x}_{2_{i*}}^T \right) \\ &\quad \times \left(\sum_{i=1}^{l_1} \psi_{1_{i*}} \mathbf{x}_{1_{i*}} - \sum_{i=1}^{l_2} \psi_{2_{i*}} \mathbf{x}_{2_{i*}} \right). \end{aligned}$$

I will now argue that equivalence $\|\psi\|_{\min_c}^2 \simeq \|\tau\|_{\min_c}^2$ between the total allowed eigenenergies of ψ and τ involves symmetrically balanced, joint eigenenergy distributions with respect to the principal eigenaxis components on ψ and τ .

Symmetrical Equivalence of Eigenenergy Distributions Equations (51), (64), (67), and (71) show that identical, symmetrically balanced, joint distributions of principal eigenaxis components on ψ and τ are symmetrically distributed over the axes of the Wolfe dual principal eigenaxis components on ψ and the correlated, unconstrained primal principal eigenaxis components (extreme vectors) on τ . Therefore, correlated, constrained primal and Wolfe dual principal eigenaxis components are formed by equivalent, symmetrically balanced, joint distributions of principal eigenaxis components on ψ and τ . Thereby, symmetrically balanced, joint distributions of principal eigenaxis components on ψ and τ are symmetrically distributed over the axes of all of the Wolfe dual principal eigenaxis components $\{\psi_{1i*} \vec{e}_{1i*}\}_{i=1}^{l_1}$ and $\{\psi_{2i*} \vec{e}_{2i*}\}_{i=1}^{l_2}$ on ψ_1 and ψ_2 and all of the constrained primal principal eigenaxis components $\{\psi_{1i*} \mathbf{x}_{1i*}\}_{i=1}^{l_1}$ and $\{\psi_{2i*} \mathbf{x}_{2i*}\}_{i=1}^{l_2}$ on τ_1 and τ_2 , where $\vec{e}_{1i*} = \frac{\mathbf{x}_{1i*}}{\|\mathbf{x}_{1i*}\|}$ and $\vec{e}_{2i*} = \frac{\mathbf{x}_{2i*}}{\|\mathbf{x}_{2i*}\|}$.

It follows that the distribution of eigenenergies with respect to the Wolfe dual principal eigenaxis components on ψ is symmetrically equivalent to the distribution of eigenenergies with respect to the constrained primal principal eigenaxis components on τ , such that the total allowed eigenenergies $\|\psi\|_{\min_c}^2$ and $\|\tau\|_{\min_c}^2$ exhibited by ψ and τ satisfy symmetrically balanced, joint eigenenergy distributions with respect to the principal eigenaxis components on ψ and τ . Therefore, all of the constrained primal principal eigenaxis components on $\tau_1 - \tau_2$ possess eigenenergies that satisfy symmetrically balanced, joint eigenenergy distributions with respect to the principal eigenaxis components on ψ and τ .

I will show that the critical minimum eigenenergies exhibited by the eigen-scaled extreme vectors describe conditional probabilities of classification error for extreme points, where any given extreme point has a conditional risk that is described by a measure of central location and a measure of spread described by a conditional probability density.

In the next section, I will show that each Wolfe dual principal eigenaxis component describes a conditional probability density for an extreme point. By way of motivation, an overview of Bayesian estimates for parameter vectors θ of unknown probability densities $p(\mathbf{x})$ is presented next.

9.4 Parameter Vectors θ of Probability Densities

Take any given class of feature vectors \mathbf{x} that are described by an unknown probability density function $p(\mathbf{x})$. Let the unknown density function $p(\mathbf{x})$ have a known parametric form in terms of a parameter vector θ , where the unknowns are the components of θ . Any information about

θ prior to observing a set of data samples is assumed to be contained in a known prior density $p(\theta)$, where observation of a set of data samples produces a posterior density $p(\theta|D)$ which is sharply peaked about the true value of θ if $\hat{\theta} \simeq \theta$.

Given these assumptions, $p(\mathbf{x}|D)$ can be computed by integrating the joint density $p(\mathbf{x}, \theta|D)$ over θ

$$p(\mathbf{x}|D) = \int p(\mathbf{x}, \theta|D) d\theta.$$

Write $p(\mathbf{x}, \theta|D)$ as $p(\mathbf{x}|\theta)p(\theta|D)$. If $p(\theta|D)$ peaks sharply about some value $\hat{\theta}$, then the integral

$$p(\mathbf{x}|D) = \int p(\mathbf{x}|\theta)p(\theta|D) d\theta \simeq p(\mathbf{x}|\hat{\theta}),$$

produces an estimate $\hat{\theta}$ for the desired parameter vector θ (Duda et al., 2001). Accordingly, unknown probability density functions $p(\mathbf{x})$ can be determined by Bayesian estimation of a parameter vector θ with a known prior density $p(\theta)$.

Learning an Unknown Vector $\hat{\theta}$ of Two Conditional Densities

Given the previous assumptions for Bayesian estimation of parameter vectors θ , it is reasonable to assume that information about an unknown probability density function $p(\mathbf{x})$ is distributed over the components of a parameter vector $\hat{\theta}$. It has been demonstrated that symmetrically balanced, joint distributions of principal eigenaxis components on ψ and τ are symmetrically distributed over the axes of all of the Wolfe dual principal eigenaxis components on ψ and all of the constrained primal principal eigenaxis components on τ . I will show that information for two unknown conditional density functions $p(\mathbf{x}_{1i*}|\hat{\theta}_1)$ and $p(\mathbf{x}_{2i*}|\hat{\theta}_2)$ is distributed over the eigen-scaled extreme points on $\tau_1 - \tau_2$, where τ is an unknown parameter vector $\hat{\theta}$ that contains information about the unknown conditional densities $\hat{\theta} = \hat{\theta}_1 - \hat{\theta}_2$. In the next analysis, I will define pointwise conditional densities described by the components of a constrained, primal linear eigenlocus $\tau = \tau_1 - \tau_2$, where each conditional density $p(\mathbf{x}_{1i*} | \text{comp}_{\overrightarrow{\mathbf{x}_{1i*}}}(\overrightarrow{\tau}))$ or $p(\mathbf{x}_{2i*} | \text{comp}_{\overrightarrow{\mathbf{x}_{2i*}}}(\overrightarrow{\tau}))$ for an \mathbf{x}_{1i*} or \mathbf{x}_{2i*} extreme point is given by components $\text{comp}_{\overrightarrow{\mathbf{x}_{1i*}}}(\overrightarrow{\tau})$ or $\text{comp}_{\overrightarrow{\mathbf{x}_{2i*}}}(\overrightarrow{\tau})$ of τ along the corresponding extreme vector \mathbf{x}_{1i*} or \mathbf{x}_{2i*} .

9.5 Pointwise Conditional Densities

Consider again the equations for the loci of the $\psi_{1i*} \overrightarrow{\mathbf{e}}_{1i*}$ and $\psi_{2i*} \overrightarrow{\mathbf{e}}_{2i*}$ Wolfe dual principal eigenaxis components in Eqs (64) and (70). It has

been demonstrated that any given Wolfe dual principal eigenaxis component $\psi_{1i*} \vec{e}_{1i*}$ correlated with an \mathbf{x}_{1i*} extreme point and any given Wolfe dual principal eigenaxis component $\psi_{2i*} \vec{e}_{2i*}$ correlated with an \mathbf{x}_{2i*} extreme point provides an estimate for how the components of l eigen-scaled extreme vectors $\{\psi_{j*} \mathbf{x}_{j*}\}_{j=1}^l$ are symmetrically distributed along the axis of a correlated extreme vector \mathbf{x}_{1i*} or \mathbf{x}_{2i*} , where components of eigen-scaled extreme vectors $\psi_{j*} \mathbf{x}_{j*}$ are symmetrically distributed according to class labels ± 1 , signed magnitudes $\|\mathbf{x}_{j*}\| \cos \theta_{\mathbf{x}_{1i*} \mathbf{x}_{j*}}$ or $\|\mathbf{x}_{j*}\| \cos \theta_{\mathbf{x}_{2i*} \mathbf{x}_{j*}}$, and symmetrically balanced distributions of eigen-scaled extreme vectors $\{\psi_{j*} \mathbf{x}_{j*}\}_{j=1}^l$ encoded within eigen-scales ψ_{j*} .

Thereby, symmetrically balanced distributions of all of the extreme points are symmetrically distributed along the axes of all of the extreme vectors, where all of the eigen-scales satisfy the equivalence relation $\sum_{j=1}^{l_1} \psi_{1j*} = \sum_{j=1}^{l_2} \psi_{2j*}$. Accordingly, principal eigenaxis components $\psi_{1i*} \vec{e}_{1i*}$ or $\psi_{2i*} \vec{e}_{2i*}$ describe distributions of first degree coordinates for extreme points \mathbf{x}_{1i*} or \mathbf{x}_{2i*} .

Therefore, for any given extreme vector \mathbf{x}_{1i*} , the relative likelihood that the extreme point \mathbf{x}_{1i*} has a given location is described by the locus of the Wolfe dual principal eigenaxis component $\psi_{1i*} \vec{e}_{1i*}$:

$$\begin{aligned} \psi_{1i*} \vec{e}_{1i*} &= \lambda_{\max_\psi}^{-1} \|\mathbf{x}_{1i*}\| \sum_{j=1}^{l_1} \psi_{1j*} \|\mathbf{x}_{1j*}\| \cos \theta_{\mathbf{x}_{1i*} \mathbf{x}_{1j*}} \\ &\quad - \lambda_{\max_\psi}^{-1} \|\mathbf{x}_{1i*}\| \sum_{j=1}^{l_2} \psi_{2j*} \|\mathbf{x}_{2j*}\| \cos \theta_{\mathbf{x}_{1i*} \mathbf{x}_{2j*}}, \end{aligned}$$

where $\psi_{1i*} \vec{e}_{1i*}$ describes a conditional expectation (a measure of central location) and a conditional covariance (a measure of spread) for the extreme point \mathbf{x}_{1i*} . Thereby, it is concluded that the principal eigenaxis component $\psi_{1i*} \vec{e}_{1i*}$ describes a conditional density $p(\mathbf{x}_{1i*} | \text{comp}_{\vec{\mathbf{x}_{1i*}}}(\vec{\tau}))$ for the extreme point \mathbf{x}_{1i*} .

Likewise, for any given extreme vector \mathbf{x}_{2i*} , the relative likelihood that the extreme point \mathbf{x}_{2i*} has a given location is described by the locus of the Wolfe dual principal eigenaxis component $\psi_{2i*} \vec{e}_{2i*}$:

$$\begin{aligned} \psi_{2i*} \vec{e}_{2i*} &= \lambda_{\max_\psi}^{-1} \|\mathbf{x}_{2i*}\| \sum_{j=1}^{l_2} \psi_{2j*} \|\mathbf{x}_{2j*}\| \cos \theta_{\mathbf{x}_{2i*} \mathbf{x}_{2j*}} \\ &\quad - \lambda_{\max_\psi}^{-1} \|\mathbf{x}_{2i*}\| \sum_{j=1}^{l_1} \psi_{1j*} \|\mathbf{x}_{1j*}\| \cos \theta_{\mathbf{x}_{2i*} \mathbf{x}_{1j*}}, \end{aligned}$$

where $\psi_{2i*} \vec{e}_{2i*}$ describes a conditional expectation (a measure of central location) and a conditional covariance (a measure of spread) for the extreme point \mathbf{x}_{2i*} . Thereby, it is concluded that the principal eigenaxis component $\psi_{2i*} \vec{e}_{2i*}$ describes a conditional density $p(\mathbf{x}_{2i*} | \text{comp}_{\vec{\mathbf{x}_{2i*}}}(\vec{\tau}))$ for the extreme point \mathbf{x}_{2i*} .

Using Eq. (52), it follows that the conditional densities encoded within the Wolfe dual principal eigenaxis components for class ω_1 and class ω_2 are symmetrically balanced with each other.

I will now show that a linear eigenlocus $\tau = \tau_1 - \tau_2$ is a parameter vector for class-conditional probability density functions $p(\mathbf{x}_{1i*}|\omega_1)$ and $p(\mathbf{x}_{2i*}|\omega_2)$.

9.6 Class-conditional Probability Densities

Given that each Wolfe dual principal eigenaxis component $\psi_{1i*} \vec{\mathbf{e}}_{1i*}$ describes a conditional density $p(\mathbf{x}_{1i*} | \text{comp}_{\vec{\mathbf{x}}_{1i*}}(\vec{\tau}))$ for a correlated extreme point \mathbf{x}_{1i*} , it follows that conditional densities for the \mathbf{x}_{1i*} extreme points are distributed over the principal eigenaxis components of τ_1

$$\begin{aligned} \tau_1 &= \sum_{i=1}^{l_1} p(\mathbf{x}_{1i*} | \text{comp}_{\vec{\mathbf{x}}_{1i*}}(\vec{\tau})) \mathbf{x}_{1i*}, \\ &= \sum_{i=1}^{l_1} \psi_{1i*} \mathbf{x}_{1i*}, \end{aligned} \quad (72)$$

where $\psi_{1i*} \mathbf{x}_{1i*}$ describes a conditional density for \mathbf{x}_{1i*} , such that τ_1 is a parameter vector for a class-conditional probability density $p(\mathbf{x}_{1i*}|\tau_1)$ for a given set $\{\mathbf{x}_{1i*}\}_{i=1}^{l_1}$ of \mathbf{x}_{1i*} extreme points:

$$\tau_1 = p(\mathbf{x}_{1i*}|\tau_1).$$

Given that each Wolfe dual principal eigenaxis component $\psi_{2i*} \vec{\mathbf{e}}_{2i*}$ describes a conditional density $p(\mathbf{x}_{2i*} | \text{comp}_{\vec{\mathbf{x}}_{2i*}}(\vec{\tau}))$ for a correlated extreme point \mathbf{x}_{2i*} , it follows that conditional densities for the \mathbf{x}_{2i*} extreme points are distributed over the principal eigenaxis components of τ_2

$$\begin{aligned} \tau_2 &= \sum_{i=1}^{l_2} p(\mathbf{x}_{2i*} | \text{comp}_{\vec{\mathbf{x}}_{2i*}}(\vec{\tau})) \mathbf{x}_{2i*}, \\ &= \sum_{i=1}^{l_2} \psi_{2i*} \mathbf{x}_{2i*}, \end{aligned} \quad (73)$$

where $\psi_{2i*} \mathbf{x}_{2i*}$ describes a conditional density for \mathbf{x}_{2i*} , such that τ_2 is a parameter vector for a class-conditional probability density $p(\mathbf{x}_{2i*}|\tau_2)$ for a given set $\{\mathbf{x}_{2i*}\}_{i=1}^{l_2}$ of \mathbf{x}_{2i*} extreme points:

$$\tau_2 = p(\mathbf{x}_{2i*}|\tau_2).$$

I will now show that the conditional probabilities of decision error $P(D_2|\omega_1)$ and $P(D_1|\omega_2)$ for class ω_1 and class ω_2 are functions of the decision regions Z_1 and Z_2 and the class-conditional densities $p(\mathbf{x}_{1i*}|\tau_1)$ and $p(\mathbf{x}_{2i*}|\tau_2)$.

9.7 Conditional Probability of Decision Error $P(D_2|\omega_1)$

A linear eigenlocus $\tau = \sum_{i=1}^{l_1} \psi_{1i*} \mathbf{x}_{1i*} - \sum_{i=1}^{l_2} \psi_{2i*} \mathbf{x}_{2i*}$ partitions any given feature space into congruent decision regions $Z_1 \cong Z_2$, such that for any two overlapping data distributions, an \mathbf{x}_{1i*} or \mathbf{x}_{2i*} extreme point lies in either region Z_1 or region Z_2 . Therefore, the area under each pointwise conditional density in Eq. (72)

$$\int_{Z_1} p(\mathbf{x}_{1i*} | \text{comp}_{\mathbf{x}_{1i*}}(\vec{\tau})) d\tau_1(\mathbf{x}_{1i*}) \text{ or } \int_{Z_2} p(\mathbf{x}_{1i*} | \text{comp}_{\mathbf{x}_{1i*}}(\vec{\tau})) d\tau_1(\mathbf{x}_{1i*}),$$

is a conditional probability that an \mathbf{x}_{1i*} extreme point will be observed in region Z_1 or region Z_2 , where pointwise conditional densities $\psi_{1i*} \mathbf{x}_{1i*}$ for \mathbf{x}_{1i*} extreme points that lie in region Z_1 have minimal or no effect on the cost or risk of making a decision error.

The area $P(\mathbf{x}_{1i*}|\tau_1)$ under the class-conditional density $p(\mathbf{x}_{1i*}|\tau_1)$ in Eq. (72)

$$\begin{aligned} P(\mathbf{x}_{1i*}|\tau_1) &= \int_Z \left(\sum_{i=1}^{l_1} p(\mathbf{x}_{1i*} | \text{comp}_{\mathbf{x}_{1i*}}(\vec{\tau})) \mathbf{x}_{1i*} \right) d\tau_1, \quad (74) \\ &= \int_Z \left(\sum_{i=1}^{l_1} \psi_{1i*} \mathbf{x}_{1i*} \right) d\tau_1 = \int_Z p(\mathbf{x}_{1i*}|\tau_1) d\tau_1, \\ &= \int_Z \tau_1 d\tau_1 = \frac{1}{2} \|\tau_1\|^2 + C = \|\tau_1\|^2 + C_1, \end{aligned}$$

describes the conditional probability of observing the \mathbf{x}_{1i*} extreme points $\{\mathbf{x}_{1i*}\}_{i=1}^{l_1}$ within localized regions of the decision space Z , where conditional densities $\psi_{1i*} \mathbf{x}_{1i*}$ for \mathbf{x}_{1i*} extreme points that lie in the Z_2 decision region *contribute* to the cost or risk of making a decision error, and conditional densities $\psi_{1i*} \mathbf{x}_{1i*}$ for \mathbf{x}_{1i*} extreme points that lie in the Z_1 decision region *have minimal or no effect* on the cost or risk of making a decision error.

It follows that integration over the components of τ_1

$$\begin{aligned} \|\tau_1\|^2 &= \left(\sum_{i=1}^{l_1} p(\mathbf{x}_{1i*} | \text{comp}_{\mathbf{x}_{1i*}}(\vec{\tau})) \mathbf{x}_{1i*} \right)^T \\ &\quad \times \left(\sum_{i=1}^{l_1} p(\mathbf{x}_{1i*} | \text{comp}_{\mathbf{x}_{1i*}}(\vec{\tau})) \mathbf{x}_{1i*} \right), \end{aligned}$$

determines regions of likelihood $\hat{Z}_1(\mathbf{x}_{1i*})$ or $\hat{Z}_2(\mathbf{x}_{1i*})$ for the \mathbf{x}_{1i*} extreme points, where any given region of likelihood $\hat{Z}_2(\mathbf{x}_{1i*})$ in the Z_2 decision region is a localized region that has a conditional risk $\mathfrak{R}(\hat{Z}_2(\mathbf{x}_{1i*}))$, where Bayes' error $\mathcal{P}_e(\hat{Z}_2(\mathbf{x}_{1i*}))$ is determined by the central location (expected value) and the spread (covariance) of an \mathbf{x}_{1i*} extreme

point. Any given region of likelihood $\widehat{Z}_1(\mathbf{x}_{1_{i*}})$ in the Z_1 decision region describes a localized region that has a conditional risk of zero $\Re(\widehat{Z}_1(\mathbf{x}_{1_{i*}})) = 0$ because Bayes' error $\mathcal{P}_e(\widehat{Z}_1(\mathbf{x}_{1_{i*}})) = 0$.

It follows the conditional probability of decision error $P(D_2|\omega_1)$ for class ω_1 is given by an error integral

$$\begin{aligned} P(D_2|\omega_1) &= \int_{Z_2} p(\widehat{\Lambda}(\mathbf{x})|\omega_1) d\widehat{\Lambda}, \\ &= \int_{Z_2} \tau_1 d\tau_1, \\ &= \|\tau_1\|^2 + C_1, \end{aligned} \quad (75)$$

in terms of $\|\tau_1\|^2$ and an integration constant C_1 , where $\|\tau_1\|^2$ is the critical minimum eigenenergy $\|\tau_1\|_{\min_c}^2$ exhibited by τ_1 . Accordingly, the critical minimum eigenenergy $\|\tau_1\|_{\min_c}^2$ exhibited by τ_1 describes how conditional probabilities of classification error $\mathcal{P}_e(\widehat{Z}_2(\mathbf{x}_{1_{i*}}))$ for $\mathbf{x}_{1_{i*}}$ extreme points are distributed in the Z_2 decision region.

9.8 Conditional Probability of Decision Error $P(D_1|\omega_2)$

The area under each pointwise conditional density in Eq. (73)

$$\int_{Z_1} p(\mathbf{x}_{2_{i*}} | \text{comp}_{\overrightarrow{\mathbf{x}_{2_{i*}}}(\vec{\tau}))} d\tau_2(\mathbf{x}_{2_{i*}}) \text{ or } \int_{Z_2} p(\mathbf{x}_{2_{i*}} | \text{comp}_{\overrightarrow{\mathbf{x}_{2_{i*}}}(\vec{\tau}))} d\tau_2(\mathbf{x}_{2_{i*}}),$$

is a conditional probability that an $\mathbf{x}_{2_{i*}}$ extreme point will be observed in region Z_1 or region Z_2 , where pointwise conditional densities $\psi_{2_{i*}} \mathbf{x}_{2_{i*}}$ for $\mathbf{x}_{2_{i*}}$ extreme points that lie in region Z_2 have minimal or no effect on the cost or risk of making a decision error.

The area $P(\mathbf{x}_{2_{i*}}|\tau_2)$ under the conditional density $p(\mathbf{x}_{2_{i*}}|\tau_2)$ in Eq. (73)

$$\begin{aligned} P(\mathbf{x}_{2_{i*}}|\tau_2) &= \int_Z \left(\sum_{i=1}^{l_2} p(\mathbf{x}_{2_{i*}} | \text{comp}_{\overrightarrow{\mathbf{x}_{2_{i*}}}(\vec{\tau}))} \mathbf{x}_{1_{i*}} \right) d\tau_1, \\ &= \int_Z \left(\sum_{i=1}^{l_2} \psi_{2_{i*}} \mathbf{x}_{2_{i*}} \right) d\tau_2 = \int_Z p(\mathbf{x}_{2_{i*}}|\tau_2) d\tau_2, \\ &= \int_Z \tau_2 d\tau_2 = \frac{1}{2} \|\tau_2\|^2 + C = \|\tau_2\|^2 + C_2, \end{aligned} \quad (76)$$

describes the conditional probability of observing the $\mathbf{x}_{2_{i*}}$ extreme points $\{\mathbf{x}_{2_{i*}}\}_{i=1}^{l_2}$ within localized regions of the decision space Z , where conditional densities $\psi_{2_{i*}} \mathbf{x}_{2_{i*}}$ for $\mathbf{x}_{2_{i*}}$ extreme points that lie in the Z_1 decision region *contribute* to the cost or risk of making a decision error, and conditional densities $\psi_{2_{i*}} \mathbf{x}_{2_{i*}}$ for $\mathbf{x}_{2_{i*}}$ extreme points that lie in the Z_2 decision

region *have minimal or no effect* on the cost or risk of making a decision error.

It follows that integration over the components of τ_2

$$\begin{aligned} \|\tau_2\|^2 &= \left(\sum_{i=1}^{l_2} p(\mathbf{x}_{2_{i*}} | \text{comp}_{\overrightarrow{\mathbf{x}_{2_{i*}}}(\vec{\tau}))}(\vec{\tau})) \mathbf{x}_{2_{i*}} \right)^T \\ &\quad \times \left(\sum_{i=1}^{l_2} p(\mathbf{x}_{2_{i*}} | \text{comp}_{\overrightarrow{\mathbf{x}_{2_{i*}}}(\vec{\tau}))}(\vec{\tau})) \mathbf{x}_{2_{i*}} \right), \end{aligned}$$

determines regions of likelihood $\hat{Z}_1(\mathbf{x}_{2_{i*}})$ or $\hat{Z}_2(\mathbf{x}_{2_{i*}})$ for the $\mathbf{x}_{2_{i*}}$ extreme points, where any given region of likelihood $\hat{Z}_1(\mathbf{x}_{2_{i*}})$ in the Z_1 decision region is a localized region that has a conditional risk $\Re(\hat{Z}_1(\mathbf{x}_{2_{i*}}))$, where Bayes' error $\mathcal{P}_e(\hat{Z}_1(\mathbf{x}_{2_{i*}}))$ is determined by the central location (expected value) and the spread (covariance) of an $\mathbf{x}_{2_{i*}}$ extreme point. Any given region of likelihood $\hat{Z}_2(\mathbf{x}_{2_{i*}})$ in the Z_2 decision region describes a localized region that has a conditional risk of zero $\Re(\hat{Z}_2(\mathbf{x}_{2_{i*}})) = 0$ because Bayes' error $\mathcal{P}_e(\hat{Z}_2(\mathbf{x}_{2_{i*}})) = 0$.

It follows the conditional probability of decision error $P(D_1|\omega_2)$ for class ω_2 is given by an error integral.

$$\begin{aligned} P(D_1|\omega_2) &= \int_{Z_1} p(\hat{\Lambda}(\mathbf{x})|\omega_2) d\hat{\Lambda}, \\ &= \int_{Z_1} \tau_2 d\tau_2, \\ &= \|\tau_2\|^2 + C_2, \end{aligned} \tag{77}$$

in terms of $\|\tau_2\|^2$ and an integration constant C_2 , where $\|\tau_2\|^2$ is the critical minimum eigenenergy $\|\tau_2\|_{\min_c}^2$ exhibited by τ_2 . Accordingly, the critical minimum eigenenergy $\|\tau_2\|_{\min_c}^2$ exhibited by τ_2 describes how conditional probabilities of classification error $\mathcal{P}_e(\hat{Z}_1(\mathbf{x}_{2_{i*}}))$ for $\mathbf{x}_{2_{i*}}$ extreme points are distributed in the Z_1 decision region.

Recall that extreme points are located somewhere within overlapping regions or tail regions between two data distributions. Given that a linear eigenlocus τ is an eigenaxis of symmetry which delineates congruent decision regions $Z_1 \cong Z_2$ that are symmetrically partitioned by a linear decision boundary, it follows that, for any given overlapping data distributions and decision threshold η (linear decision boundary), the extreme points $\mathbf{x}_{1_{i*}}$ and $\mathbf{x}_{2_{i*}}$ from class ω_1 and class ω_2 are located on both sides of the decision threshold η . This indicates that linear eigenlocus transforms routinely accomplish an elegant statistical balancing feat that involves finding the right mix of principal eigenaxis components on ψ and τ . The

fundamental problem involves determining the eigen-scales $\{\psi_{i*}\}_{i=1}^l$ of the Wolfe dual principal eigenaxis components $\{\psi_{i*} \vec{e}_i | \psi_{i*} > 0\}_{i=1}^l$ on ψ .

9.9 Finding the Right Mix of Component Lengths

It has been demonstrated that the directions of the constrained primal and the Wolfe dual principal eigenaxis components are fixed, along with the angles between all of the extreme vectors. I will now argue that the lengths of the Wolfe dual principal eigenaxis components on ψ must satisfy critical magnitude constraints.

Using Eq. (64), the integrated lengths $\sum_{i=1}^{l_1} \psi_{1i*}$ of the $\psi_{1i*} \vec{e}_{1i*}$ components on ψ_1 must satisfy the equation:

$$\begin{aligned} \sum_{i=1}^{l_1} \psi_{1i*} &= \lambda_{\max_\psi}^{-1} \sum_{i=1}^{l_1} \|\mathbf{x}_{1i*}\| \\ &\times \sum_{j=1}^{l_1} \psi_{1j*} \|\mathbf{x}_{1j*}\| \cos \theta_{\mathbf{x}_{1i*} \mathbf{x}_{1j*}} \\ &- \lambda_{\max_\psi}^{-1} \sum_{i=1}^{l_1} \|\mathbf{x}_{1i*}\| \\ &\times \sum_{j=1}^{l_2} \psi_{2j*} \|\mathbf{x}_{2j*}\| \cos \theta_{\mathbf{x}_{1i*} \mathbf{x}_{2j*}}. \end{aligned} \quad (78)$$

Using Eq. (70), the integrated lengths $\sum_{i=1}^{l_2} \psi_{2i*}$ of the $\psi_{2i*} \vec{e}_{2i*}$ components on ψ_2 must satisfy the equation:

$$\begin{aligned} \sum_{i=1}^{l_2} \psi_{2i*} &= \lambda_{\max_\psi}^{-1} \sum_{i=1}^{l_2} \|\mathbf{x}_{2i*}\| \\ &\times \sum_{j=1}^{l_2} \psi_{2j*} \|\mathbf{x}_{2j*}\| \cos \theta_{\mathbf{x}_{2i*} \mathbf{x}_{2j*}} \\ &- \lambda_{\max_\psi}^{-1} \sum_{i=1}^{l_2} \|\mathbf{x}_{2i*}\| \\ &\times \sum_{j=1}^{l_1} \psi_{1j*} \|\mathbf{x}_{1j*}\| \cos \theta_{\mathbf{x}_{2i*} \mathbf{x}_{1j*}}. \end{aligned} \quad (79)$$

I will now argue that Eqs (78) and (79) determine a balanced eigenlocus equation, where RHS Eq. (78) = RHS Eq. (79).

9.10 Balanced Eigenlocus Equations

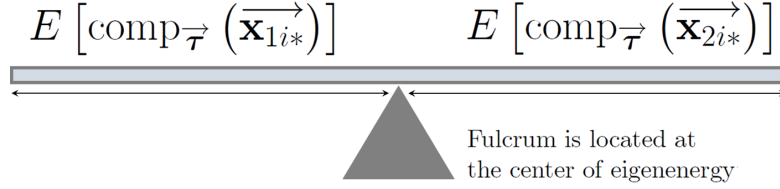
Returning now to Eq. (51), the equilibrium constraint $\sum_{i=1}^{l_1} \psi_{1i*} = \sum_{i=1}^{l_2} \psi_{2i*}$ on the component lengths of ψ indicates that the RHS of Eq. (78) must equal the RHS of Eq. (79). It follows that

$$\bar{\mathbf{x}}_{1i*}^T (\tau_1 - \tau_2) = \bar{\mathbf{x}}_{2i*}^T (\tau_2 - \tau_1). \quad (80)$$

Therefore, the component of $\bar{\mathbf{x}}_{1i*}$ along τ is symmetrically balanced with the component of $\bar{\mathbf{x}}_{2i*}$ along $-\tau$

$$\text{comp}_{\vec{\tau}} \left(\overrightarrow{\bar{\mathbf{x}}_{1i*}} \right) = \text{comp}_{-\vec{\tau}} \left(\overrightarrow{\bar{\mathbf{x}}_{2i*}} \right),$$

Equal Expected Components on Equal Sides of τ



Axis of τ is in a state of statistical equilibrium

Figure 21: The axis of τ satisfies a state of statistical equilibrium in which two equal weights $E [\text{comp}_{\vec{\tau}} (\vec{x}_{1i*})]$ and $E [\text{comp}_{\vec{\tau}} (\vec{x}_{2i*})]$ are placed on opposite sides of the fulcrum of τ .

where

$$\|\vec{x}_{1i*}\| \cos \theta_{\vec{x}_{1i*}\tau} = \|\vec{x}_{2i*}\| \cos 180 - \theta_{\vec{x}_{2i*}\tau},$$

so that the *expected components* $E [\text{comp}_{\vec{\tau}} (\vec{x}_{1i*})]$ and $E [\text{comp}_{\vec{\tau}} (\vec{x}_{2i*})]$ of the extreme vectors from each pattern class have equal magnitudes on opposite sides of the axis of τ .

State of Statistical Equilibrium Given Eq. (80), it follows that the axis of τ is a lever of uniform density, where the center of τ is $\|\tau\|_{\min_c}^2$, for which two equal weights $E [\text{comp}_{\vec{\tau}} (\vec{x}_{1i*})]$ and $E [\text{comp}_{\vec{\tau}} (\vec{x}_{2i*})]$ are placed on opposite sides of the fulcrum of τ , so that the axis of τ is in a state of *statistical equilibrium*. Figure 21 illustrates the state of statistical equilibrium which is satisfied by the axis of τ .

9.10.1 Critical Magnitude Constraints

Equation (80) indicates that the lengths

$$\{\psi_{1i*} | \psi_{1i*} > 0\}_{i=1}^{l_1} \text{ and } \{\psi_{2i*} | \psi_{2i*} > 0\}_{i=1}^{l_2},$$

of the l Wolfe dual principal eigenaxis components on ψ satisfy critical magnitude constraints, such that the highly interconnected sets of inner product relationships amongst the Wolfe dual and the constrained primal principal eigenaxis components in Eqs (78) and (79) determine well-proportioned lengths ψ_{1i*} or ψ_{2i*} for each Wolfe dual principal eigenaxis component $\psi_{1i*} \vec{e}_{1i*}$ or $\psi_{2i*} \vec{e}_{2i*}$, which essentially determine a

well-proportioned length for each correlated, constrained primal principal eigenaxis component $\psi_{1i*} \mathbf{x}_{1i*}$ or $\psi_{2i*} \mathbf{x}_{2i*}$ on τ_1 or τ_2 . I will demonstrate that the state of equilibrium $\sum_{i=1}^{l_1} \psi_{1i*} = \sum_{i=1}^{l_2} \psi_{2i*}$ satisfied by ψ determines a point of statistical equilibrium $\tau = \tau_1 - \tau_2$ for which a linear eigenlocus $\tau^T \mathbf{x} + \tau_0$ satisfies Bayes' minimax risk $\mathfrak{R}_{mm}(Z|\tau)$.

I will now define the manner in which the principal eigenaxis τ of a linear eigenlocus $\tau^T \mathbf{x} + \tau_0$ is a lever that is symmetrically balanced with respect to the center of eigenenergy $\|\tau_1 - \tau_2\|_{\min_c}^2$ of τ , such that the total allowed eigenenergies of labeled, eigen-scaled extreme vectors on $\tau_1 - \tau_2$ are symmetrically balanced about the fulcrum $\|\tau_1 - \tau_2\|_{\min_c}^2$.

10 Risk Minimization

I will show that the conditional probability of decision error $P(D_2|\omega_1)$ for class ω_1 is given by the error integral

$$P(D_2|\omega_1) = \int_{Z_2} \tau_1 d\tau_1 = \|\tau_1\|_{\min_c}^2 + C_1,$$

and that the conditional probability of decision error $P(D_1|\omega_2)$ for class ω_2 is given by the error integral

$$P(D_1|\omega_2) = \int_{Z_1} \tau_2 d\tau_2 = \|\tau_2\|_{\min_c}^2 + C_2,$$

where C_1 and C_2 are integration constants for τ_1 and τ_2 , $\|\tau_1\|_{\min_c}^2$ is the total allowed eigenenergy exhibited by τ_1 which describes how Bayes' error $\mathcal{P}_e(\hat{Z}_2(\mathbf{x}_{1i*}))$ for \mathbf{x}_{1i*} extreme points is distributed in the Z_2 decision region, and $\|\tau_2\|_{\min_c}^2$ is the total allowed eigenenergy exhibited by τ_2 which describes how Bayes' error $\mathcal{P}_e(\hat{Z}_1(\mathbf{x}_{2i*}))$ for \mathbf{x}_{2i*} extreme points is distributed in the Z_1 decision region.

I will now develop locus equations for which all of the eigen-scaled extreme points on a linear eigenlocus $\tau^T \mathbf{x} + \tau_0$ satisfy Bayes' minimax risk $\mathfrak{R}_{mm}(Z|\tau)$, where $\mathfrak{R}(Z_2|\tau_1) = \mathfrak{R}(Z_1|\tau_2)$. I will begin by developing locus equations for the total allowed eigenenergies $\|\tau_1\|_{\min_c}^2$ and $\|\tau_2\|_{\min_c}^2$ exhibited by τ_1 and τ_2 .

10.1 Equations for Total Allowed Eigenenergies

Let there be l weighted, eigen-scaled, extreme points on a linear eigenlocus τ . Given the theorem of Karush, Kuhn and Tucker and the KKT condition in Eq. (32), it follows that a Wolf dual linear eigenlocus ψ exists, where

$$\{\psi_{i*} > 0\}_{i=1}^l,$$

such that the l constrained, primal principal eigenaxis components $\{\psi_{i*} \mathbf{x}_{i*}\}_{i=1}^l$ on τ satisfy an algebraic system of l locus equations satisfied as strict equalities:

$$\psi_{i*} [y_i (\mathbf{x}_{i*}^T \tau + \tau_0) - 1 + \xi_i] = 0, \quad i = 1, \dots, l. \quad (81)$$

I will now use Eq. (81) to define critical minimum eigenenergy constraints on τ_1 and τ_2 . The analysis begins with the critical minimum eigenenergy constraint on τ_1 .

10.1.1 The Total Allowed Eigenenergy of τ_1

Take any eigen-scaled extreme vector $\psi_{1i*} \mathbf{x}_{1i*}$ that belongs to class ω_1 . Using Eq. (81) and letting $y_i = +1$, it follows that the constrained, primal principal eigenaxis component $\psi_{1i*} \mathbf{x}_{1i*}$ on τ_1 is determined by an equation satisfied as a strict equality:

$$\psi_{1i*} \mathbf{x}_{1i*}^T \tau = \psi_{1i*} (1 - \xi_i - \tau_0),$$

which is part of an algebraic system of l_1 eigenlocus equations. Therefore, each constrained, primal principal eigenaxis component $\psi_{1i*} \mathbf{x}_{1i*}$ on τ_1 satisfies the above eigenlocus equation.

Now take all of the l_1 eigen-scaled extreme vectors $\{\psi_{1i*} \mathbf{x}_{1i*}\}_{i=1}^{l_1}$ that belong to class ω_1 . Again using Eq. (81) and letting $y_i = +1$, it follows that the complete set of l_1 constrained, primal principal eigenaxis components $\{\psi_{1i*} \mathbf{x}_{1i*}\}_{i=1}^{l_1}$ on τ_1 is determined by the algebraic system of l_1 equations satisfied as strict equalities:

$$\psi_{1i*} \mathbf{x}_{1i*}^T \tau = \psi_{1i*} (1 - \xi_i - \tau_0), \quad i = 1, \dots, l_1. \quad (82)$$

Using the above expression, it follows that the entire set of $l_1 \times d$ eigen-transformed, extreme vector coordinates of $\{\psi_{1i*} \mathbf{x}_{1i*}\}_{i=1}^{l_1}$ satisfies the algebraic system of eigenlocus equations:

$$(1) \quad \psi_{11*} \mathbf{x}_{11*}^T \tau = \psi_{11*} (1 - \xi_1 - \tau_0),$$

$$(2) \quad \psi_{12*} \mathbf{x}_{12*}^T \tau = \psi_{12*} (1 - \xi_2 - \tau_0),$$

$$\vdots$$

$$(l_1) \quad \psi_{1l_*} \mathbf{x}_{1l_*}^T \tau = \psi_{1l_*} (1 - \xi_{l_*} - \tau_0),$$

where each constrained primal principal eigenaxis component $\psi_{1i*} \mathbf{x}_{1i*}$ on τ_1 satisfies the identity:

$$\psi_{1i*} \mathbf{x}_{1i*}^T \tau \equiv \psi_{1i*} (1 - \xi_i - \tau_0).$$

I will now develop an identity for the total allowed eigenenergy of τ_1 . Let E_{τ_1} denote the functional of the total allowed eigenenergy $\|\tau_1\|_{\min_c}^2$ of τ_1 and let $\tau = \tau_1 - \tau_2$. Summation over the above algebraic system of l_1 eigenlocus equations produces the following expression for the total allowed eigenenergy $\|\tau_1\|_{\min_c}^2$ of τ_1 :

$$\left(\sum_{i=1}^{l_1} \psi_{1_{i*}} \mathbf{x}_{1_{i*}}^T \right) (\tau_1 - \tau_2) \equiv \sum_{i=1}^{l_1} \psi_{1_{i*}} (1 - \xi_i - \tau_0),$$

which reduces to

$$\tau_1^T \tau_1 - \tau_1^T \tau_2 \equiv \sum_{i=1}^{l_1} \psi_{1_{i*}} (1 - \xi_i - \tau_0),$$

so that the functional E_{τ_1} satisfies the identity

$$\|\tau_1\|_{\min_c}^2 - \tau_1^T \tau_2 \equiv \sum_{i=1}^{l_1} \psi_{1_{i*}} (1 - \xi_i - \tau_0).$$

It follows that the total allowed eigenenergy $\|\tau_1\|_{\min_c}^2$ of the constrained, primal principal eigenlocus component τ_1 is described by the identity

$$\|\tau_1\|_{\min_c}^2 - \|\tau_1\| \|\tau_2\| \cos \theta_{\tau_1 \tau_2} \equiv \sum_{i=1}^{l_1} \psi_{1_{i*}} (1 - \xi_i - \tau_0), \quad (83)$$

where the functional E_{τ_1} of the total allowed eigenenergy $\|\tau_1\|_{\min_c}^2$ of τ_1

$$E_{\tau_1} = \|\tau_1\|_{\min_c}^2 - \|\tau_1\| \|\tau_2\| \cos \theta_{\tau_1 \tau_2},$$

is equivalent to the functional E_{ψ_1}

$$E_{\psi_1} = \sum_{i=1}^{l_1} \psi_{1_{i*}} (1 - \xi_i - \tau_0),$$

of integrated magnitudes $\sum_{i=1}^{l_1} \psi_{1_{i*}}$ of Wolfe dual principal eigenaxis components $\psi_{1_{i*}} \frac{\mathbf{x}_{1_{i*}}}{\|\mathbf{x}_{1_{i*}}\|}$ and the τ_0 statistic. The critical minimum eigenenergy constraint on τ_2 is examined next.

10.1.2 The Total Allowed Eigenenergy of τ_2

Take any eigen-scaled extreme vector $\psi_{2_{i*}} \mathbf{x}_{2_{i*}}$ that belongs to class ω_2 . Using Eq. (81) and letting $y_i = -1$, it follows that the constrained, primal principal eigenaxis component $\psi_{2_{i*}} \mathbf{x}_{2_{i*}}$ on τ_2 is determined by an equation satisfied as a strict equality:

$$-\psi_{2_{i*}} \mathbf{x}_{2_{i*}}^T \tau = \psi_{2_{i*}} (1 - \xi_i + \tau_0),$$

which is part of an algebraic system of l_2 eigenlocus equations. Therefore, each constrained, primal principal eigenaxis component $\psi_{2_{i*}} \mathbf{x}_{2_{i*}}$ on τ_2 satisfies the above eigenlocus equation.

Now take all of the l_2 eigen-scaled, extreme vectors $\{\psi_{2_{i*}} \mathbf{x}_{2_{i*}}\}_{i=1}^{l_2}$ that belong to class ω_2 . Again using Eq. (81) and letting $y_i = -1$, it follows that the complete set of l_2 constrained, primal principal eigenaxis components $\{\psi_{2_{i*}} \mathbf{x}_{2_{i*}}\}_{i=1}^{l_2}$ on τ_2 is determined by the algebraic system of l_2 eigenlocus equations satisfied as strict equalities:

$$-\psi_{2_{i*}} \mathbf{x}_{2_{i*}}^T \tau = \psi_{2_{i*}} (1 - \xi_i + \tau_0), \quad i = 1, \dots, l_2. \quad (84)$$

Using the above expression, it follows that the entire set of $l_2 \times d$ eigen-transformed, extreme vector coordinates of $\{\psi_{2_{i*}} \mathbf{x}_{2_{i*}}\}_{i=1}^{l_2}$ satisfies the algebraic system of eigenlocus equations:

$$\begin{aligned} (1) \quad & -\psi_{2_{1*}} \mathbf{x}_{2_{1*}}^T \tau = \psi_{2_{1*}} (1 - \xi_i + \tau_0), \\ (2) \quad & -\psi_{2_{2*}} \mathbf{x}_{2_{2*}}^T \tau = \psi_{2_{2*}} (1 - \xi_i + \tau_0), \\ & \vdots \\ (l_2) \quad & -\psi_{2_{l_2*}} \mathbf{x}_{2_{l_2*}}^T \tau = \psi_{2_{l_2*}} (1 - \xi_i + \tau_0), \end{aligned}$$

where each constrained, primal principal eigenaxis component $\psi_{2_{i*}} \mathbf{x}_{2_{i*}}$ on τ_2 satisfies the identity:

$$-\psi_{2_{i*}} \mathbf{x}_{2_{i*}}^T \tau \equiv \psi_{2_{i*}} (1 - \xi_i + \tau_0).$$

I will now develop an identity for the total allowed eigenenergy of τ_2 . Let E_{τ_2} denote the functional of the total allowed eigenenergy $\|\tau_2\|_{\min_c}^2$ of τ_2 and let $\tau = \tau_1 - \tau_2$. Summation over the above algebraic system of l_2 eigenlocus equations produces the following expression for the total allowed eigenenergy $\|\tau_2\|_{\min_c}^2$ of τ_2 :

$$-\left(\sum_{i=1}^{l_2} \psi_{2_{i*}} \mathbf{x}_{2_{i*}}^T\right) (\tau_1 - \tau_2) \equiv \sum_{i=1}^{l_2} \psi_{2_{i*}} (1 - \xi_i + \tau_0),$$

which reduces to

$$\tau_2^T \tau_2 - \tau_2^T \tau_1 \equiv \sum_{i=1}^{l_2} \psi_{2_{i*}} (1 - \xi_i + \tau_0),$$

so that the functional E_{τ_2} satisfies the identity

$$\|\tau_2\|_{\min_c}^2 - \tau_2^T \tau_1 \equiv \sum_{i=1}^{l_2} \psi_{2_{i*}} (1 - \xi_i + \tau_0).$$

It follows that the total allowed eigenenergy $\|\tau_2\|_{\min_c}^2$ of the constrained, primal eigenlocus component τ_2 is described by the identity

$$\|\tau_2\|_{\min_c}^2 - \|\tau_2\| \|\tau_1\| \cos \theta_{\tau_2 \tau_1} \equiv \sum_{i=1}^{l_2} \psi_{2_{i*}} (1 - \xi_i + \tau_0), \quad (85)$$

where the functional E_{τ_2} of the total allowed eigenenergy $\|\tau_2\|_{\min_c}^2$ of τ_2

$$E_{\tau_2} = \|\tau_2\|_{\min_c}^2 - \|\tau_2\| \|\tau_1\| \cos \theta_{\tau_2 \tau_1},$$

is equivalent to the functional E_{ψ_2}

$$E_{\psi_2} = \sum_{i=1}^{l_2} \psi_{2i_*} (1 - \xi_i + \tau_0),$$

of the integrated magnitudes $\sum_{i=1}^{l_2} \psi_{2i_*}$ of the Wolfe dual principal eigenaxis components $\psi_{2i_*} \frac{\mathbf{x}_{2i_*}}{\|\mathbf{x}_{2i_*}\|}$ and the τ_0 statistic. The critical minimum eigenenergy constraint on τ is examined next.

10.1.3 The Total Allowed Eigenenergy of τ

I will now develop an identity for the total allowed eigenenergy of a constrained, primal linear eigenlocus τ . Let E_τ denote the functional satisfied by the total allowed eigenenergy $\|\tau\|_{\min_c}^2$ of τ .

Summation over the complete algebraic system of eigenlocus equations satisfied by τ_1

$$\left(\sum_{i=1}^{l_1} \psi_{1i_*} \mathbf{x}_{1i_*}^T \right) \tau \equiv \sum_{i=1}^{l_1} \psi_{1i_*} (1 - \xi_i - \tau_0),$$

and by τ_2

$$\left(- \sum_{i=1}^{l_2} \psi_{2i_*} \mathbf{x}_{2i_*}^T \right) \tau \equiv \sum_{i=1}^{l_2} \psi_{2i_*} (1 - \xi_i + \tau_0),$$

produces the following identity for the functional E_τ satisfied by the total allowed eigenenergy $\|\tau\|_{\min_c}^2$ of τ

$$\begin{aligned} & \left(\sum_{i=1}^{l_1} \psi_{1i_*} \mathbf{x}_{1i_*}^T - \sum_{i=1}^{l_2} \psi_{2i_*} \mathbf{x}_{2i_*}^T \right) \tau \\ & \equiv \sum_{i=1}^{l_1} \psi_{1i_*} (1 - \xi_i - \tau_0) + \sum_{i=1}^{l_2} \psi_{2i_*} (1 - \xi_i + \tau_0), \end{aligned}$$

which reduces to

$$\begin{aligned} (\tau_1 - \tau_2)^T \tau & \equiv \sum_{i=1}^{l_1} \psi_{1i_*} (1 - \xi_i - \tau_0) \\ & + \sum_{i=1}^{l_2} \psi_{2i_*} (1 - \xi_i + \tau_0), \\ & \equiv \sum_{i=1}^l \psi_{i_*} (1 - \xi_i). \end{aligned} \tag{86}$$

It follows that the functional E_τ of the total allowed eigenenergy $\|\tau\|_{\min_c}^2$ of τ

$$\begin{aligned} E_\tau & = (\tau_1 - \tau_2)^T \tau \\ & = \|\tau\|_{\min_c}^2, \end{aligned}$$

is equivalent to the functional E_ψ

$$E_\psi = \sum_{i=1}^l \psi_{i*} (1 - \xi_i),$$

solely in terms of the integrated magnitudes $\sum_{i=1}^l \psi_{i*}$ of the Wolfe dual principal eigenaxis components on ψ . Therefore, the total allowed eigenenergy $\|\tau\|_{\min_c}^2$ of a constrained, primal linear eigenlocus τ is described by the integrated magnitudes ψ_{i*} of the Wolfe dual principal eigenaxis components $\psi_{i*} \frac{\mathbf{x}_{i*}}{\|\mathbf{x}_{i*}\|}$ on ψ

$$\begin{aligned} \|\tau\|_{\min_c}^2 &\equiv \sum_{i=1}^l \psi_{i*} (1 - \xi_i) \\ &\equiv \sum_{i=1}^l \psi_{i*} - \sum_{i=1}^l \psi_{i*} \xi_i, \end{aligned} \quad (87)$$

where the regularization parameters $\xi_i = \xi \ll 1$ are seen to determine negligible constraints on $\|\tau\|_{\min_c}^2$. It is concluded that the total allowed eigenenergy $\|\tau\|_{\min_c}^2$ exhibited by a constrained, primal linear eigenlocus τ is equivalent to the integrated magnitudes $\sum_{i=1}^l \psi_{i*}$ of the Wolfe dual principal eigenaxis components $\psi_{i*} \frac{\mathbf{x}_{i*}}{\|\mathbf{x}_{i*}\|}$ on ψ .

Given Eqs (83), (85), and (86), it follows that the total allowed eigenenergies exhibited by τ_1 , τ_2 , and τ satisfy the eigenlocus equation

$$\begin{aligned} \|\tau\|_{\min_c}^2 &= \|\tau_1\|_{\min_c}^2 - \|\tau_1\| \|\tau_2\| \cos \theta_{\tau_1 \tau_2} \\ &\quad + \|\tau_2\|_{\min_c}^2 - \|\tau_2\| \|\tau_1\| \cos \theta_{\tau_2 \tau_1}, \end{aligned}$$

where the linear discriminant function $D(\mathbf{x}) = \tau^T \mathbf{x} + \tau_0$ in Eq. (37) satisfies a linear decision boundary in terms of the total allowed eigenenergy $\|\tau\|_{\min_c}^2$ exhibited by τ .

I will now define the manner in which the linear discriminant function $D(\mathbf{x}) = \tau^T \mathbf{x} + \tau_0$ in Eq. (37) minimizes the Bayes' minimax risk \mathfrak{R}_{mm} in Eq. (8). The solution involves a surprising statistical balancing feat in decision space Z which hinges on an elegant statistical balancing feat in eigenspace \tilde{Z} .

10.2 The Statistical Balancing Feat in Eigenspace

A linear eigenlocus

$$\tau = \tau_1 - \tau_2,$$

formed by a dual locus of weighted (+1 or -1), eigen-scaled (ψ_{1i*} or ψ_{2i*}) extreme vectors (\mathbf{x}_{1i*} or \mathbf{x}_{2i*})

$$\tau = \sum_{i=1}^{l_1} \psi_{1i*} \mathbf{x}_{1i*} - \sum_{i=1}^{l_2} \psi_{2i*} \mathbf{x}_{2i*},$$

has a dual nature, where each eigen-scale $\psi_{1_{i*}}$ or $\psi_{2_{i*}}$ determines the total allowed eigenenergy $\|\psi_{1_{i*}} \mathbf{x}_{1_{i*}}\|_{\min_c}^2$ or $\|\psi_{2_{i*}} \mathbf{x}_{2_{i*}}\|_{\min_c}^2$ of a principal eigenaxis component $\psi_{1_{i*}} \mathbf{x}_{1_{i*}}$ or $\psi_{2_{i*}} \mathbf{x}_{2_{i*}}$ on $\tau_1 - \tau_2$ and determines a conditional density $p(\mathbf{x}_{1_{i*}} | \text{comp}_{\overrightarrow{\mathbf{x}_{1_{i*}}}}(\vec{\tau})) \mathbf{x}_{1_{i*}}$ or $p(\mathbf{x}_{2_{i*}} | \text{comp}_{\overrightarrow{\mathbf{x}_{2_{i*}}}}(\vec{\tau})) \mathbf{x}_{2_{i*}}$ for an extreme point $\mathbf{x}_{1_{i*}}$ or $\mathbf{x}_{2_{i*}}$, such that $\tau = \tau_1 - \tau_2$ is a parameter vector of likelihoods

$$\begin{aligned} \hat{\Lambda}(\mathbf{x}) &= \sum_{i=1}^{l_1} p(\mathbf{x}_{1_{i*}} | \text{comp}_{\overrightarrow{\mathbf{x}_{1_{i*}}}}(\vec{\tau})) \mathbf{x}_{1_{i*}} \\ &\quad - \sum_{i=1}^{l_2} p(\mathbf{x}_{2_{i*}} | \text{comp}_{\overrightarrow{\mathbf{x}_{2_{i*}}}}(\vec{\tau})) \mathbf{x}_{2_{i*}}. \end{aligned}$$

The dual nature of τ enables the linear discriminant function

$$D(\mathbf{x}) = \tau^T \mathbf{x} + \tau_0,$$

to satisfy the minimax criterion

$$\begin{aligned} \mathfrak{R}_{mm}(Z|\tau) &= \int_{Z_1} p(\mathbf{x}_{2_{i*}} | \tau_2) d\tau_2 \\ &= \int_{Z_2} p(\mathbf{x}_{1_{i*}} | \tau_1) d\tau_1, \end{aligned}$$

by means of an elegant statistical balancing feat in eigenspace for which the functional E_{τ_1} of $\|\tau_1\|_{\min_c}^2$ in Eq. (83) and the functional E_{τ_2} of $\|\tau_2\|_{\min_c}^2$ in Eq. (85) are constrained to be equal to each other by means of a symmetric equalizer statistic $\nabla_{eq} = \frac{\tau_0}{2} \sum_{i=1}^l \psi_{i*}$.

I have shown that each of the constrained, primal principal eigenaxis components $\psi_{1_{i*}} \mathbf{x}_{1_{i*}}$ or $\psi_{2_{i*}} \mathbf{x}_{2_{i*}}$ on $\tau = \tau_1 - \tau_2$ have such magnitudes and directions that a linear eigenlocus $\tau^T \mathbf{x} + \tau_0$ partitions any given feature space into congruent decision regions $Z_1 \cong Z_2$ which are symmetrically partitioned by a linear decision boundary by means of three, symmetrical linear loci, all of which reference τ .

I will now show that linear eigenlocus transforms determine decision regions that have equal conditional risks. I will demonstrate that balancing Bayes' risk \mathfrak{R}_{mm} hinges on balancing the eigenenergies of $\tau_1 - \tau_2$.

10.2.1 Balancing the Eigenenergies of $\tau_1 - \tau_2$

Using Eq. (83) and the equilibrium constraint on ψ in Eq. (51)

$$\begin{aligned} \|\tau_1\|_{\min_c}^2 - \|\tau_1\| \|\tau_2\| \cos \theta_{\tau_1 \tau_2} &\equiv \sum_{i=1}^{l_1} \psi_{1_{i*}} (1 - \xi_i - \tau_0), \\ &\equiv \frac{1}{2} \sum_{i=1}^l \psi_{i*} (1 - \xi_i - \tau_0), \end{aligned}$$

it follows that the functional E_{τ_1} of the total allowed eigenenergy $\|\tau_1\|_{\min_c}^2$ of τ_1

$$E_{\tau_1} = \|\tau_1\|_{\min_c}^2 - \|\tau_1\| \|\tau_2\| \cos \theta_{\tau_1 \tau_2},$$

is equivalent to the functional E_{ψ_1} :

$$E_{\psi_1} = \frac{1}{2} \sum_{i=1}^l \psi_{i*} (1 - \xi_i) - \tau_0 \sum_{i=1}^{l_1} \psi_{1i*}. \quad (88)$$

Using Eq. (85) and the equilibrium constraint on ψ in Eq. (51)

$$\begin{aligned} \|\tau_2\|_{\min_c}^2 - \|\tau_2\| \|\tau_1\| \cos \theta_{\tau_2 \tau_1} &\equiv \sum_{i=1}^{l_2} \psi_{2i*} (1 - \xi_i + \tau_0), \\ &\equiv \frac{1}{2} \sum_{i=1}^l \psi_{i*} (1 - \xi_i + \tau_0), \end{aligned}$$

it follows that the functional E_{τ_2} of the total allowed eigenenergy $\|\tau_2\|_{\min_c}^2$ of τ_2

$$E_{\tau_2} = \|\tau_2\|_{\min_c}^2 - \|\tau_2\| \|\tau_1\| \cos \theta_{\tau_2 \tau_1},$$

is equivalent to the functional E_{ψ_2} :

$$E_{\psi_2} = \frac{1}{2} \sum_{i=1}^l \psi_{i*} (1 - \xi_i) + \tau_0 \sum_{i=1}^{l_2} \psi_{2i*}. \quad (89)$$

Now use the identity for $\|\tau\|_{\min_c}^2$ in Eq. (87)

$$\|\tau\|_{\min_c}^2 \equiv \sum_{i=1}^l \psi_{i*} (1 - \xi_i),$$

to rewrite E_{ψ_1}

$$\begin{aligned} E_{\psi_1} &= \frac{1}{2} \sum_{i=1}^l \psi_{i*} (1 - \xi_i) - \tau_0 \sum_{i=1}^{l_1} \psi_{1i*}, \\ &\equiv \frac{1}{2} \|\tau\|_{\min_c}^2 - \tau_0 \sum_{i=1}^{l_1} \psi_{1i*}, \end{aligned}$$

and E_{ψ_2}

$$\begin{aligned} E_{\psi_2} &= \frac{1}{2} \sum_{i=1}^l \psi_{i*} (1 - \xi_i) + \tau_0 \sum_{i=1}^{l_2} \psi_{2i*}, \\ &\equiv \frac{1}{2} \|\tau\|_{\min_c}^2 + \tau_0 \sum_{i=1}^{l_2} \psi_{2i*}, \end{aligned}$$

in terms of $\frac{1}{2} \|\tau\|_{\min_c}^2$ and an equalizer statistic.

Substituting the expressions for E_{ψ_1} and E_{ψ_2} into Eqs (83) and (85), it follows that

$$(\|\tau_1\|_{\min_c}^2 - \|\tau_1\| \|\tau_2\| \cos \theta_{\tau_1 \tau_2}) + \tau_0 \sum_{i=1}^{l_1} \psi_{1i*} \equiv \frac{1}{2} \|\tau\|_{\min_c}^2,$$

and that

$$(\|\tau_2\|_{\min_c}^2 - \|\tau_2\| \|\tau_1\| \cos \theta_{\tau_2 \tau_1}) - \tau_0 \sum_{i=1}^{l_2} \psi_{2_{i*}} \equiv \frac{1}{2} \|\tau\|_{\min_c}^2,$$

where the terms $\tau_0 \sum_{i=1}^{l_1} \psi_{1_{i*}}$ and $-\tau_0 \sum_{i=1}^{l_2} \psi_{2_{i*}}$ provide a symmetric equalizer statistic ∇_{eq} for the conditional probability functions $P(\mathbf{x}_{1_{i*}}|\tau_1)$ and $P(\mathbf{x}_{2_{i*}}|\tau_2)$.

Let ∇_{eq} denote $\tau_0 \sum_{i=1}^{l_1} \psi_{1_{i*}}$ and $\tau_0 \sum_{i=1}^{l_2} \psi_{2_{i*}}$, where

$$\nabla_{eq} \triangleq \frac{\tau_0}{2} \sum_{i=1}^l \psi_{i*}.$$

It follows that the parameter vectors τ_1 and τ_2 satisfy the eigenlocus equations

$$\|\tau_1\|_{\min_c}^2 - \|\tau_1\| \|\tau_2\| \cos \theta_{\tau_1 \tau_2} + \nabla_{eq} \equiv \frac{1}{2} \|\tau\|_{\min_c}^2, \quad (90)$$

and

$$\|\tau_2\|_{\min_c}^2 - \|\tau_2\| \|\tau_1\| \cos \theta_{\tau_2 \tau_1} - \nabla_{eq} \equiv \frac{1}{2} \|\tau\|_{\min_c}^2, \quad (91)$$

where $\nabla_{eq} \triangleq \frac{\tau_0}{2} \sum_{i=1}^l \psi_{i*}$. I will now examine the algebraic and geometric properties of the equalizer statistic ∇_{eq} in eigenspace.

10.2.2 Properties of ∇_{eq} in Eigenspace

Substituting the equation $\tau = \sum_{i=1}^{l_1} \psi_{1_{i*}} \mathbf{x}_{1_{i*}} - \sum_{i=1}^{l_2} \psi_{2_{i*}} \mathbf{x}_{2_{i*}}$ for τ in Eq. (36) into the equation for τ_0 in Eq. (47) produces the statistic for τ_0 :

$$\begin{aligned} \tau_0 = & -\frac{1}{l} \sum_{i=1}^l \mathbf{x}_{i*}^T \sum_{j=1}^{l_1} \psi_{1_{j*}} \mathbf{x}_{1_{j*}} \\ & + \frac{1}{l} \sum_{i=1}^l \mathbf{x}_{i*}^T \sum_{j=1}^{l_2} \psi_{2_{j*}} \mathbf{x}_{2_{j*}} + \frac{1}{l} \sum_{i=1}^l y_i (1 - \xi_i). \end{aligned} \quad (92)$$

Substituting the statistic for τ_0 in Eq. (92) into the equation for ∇_{eq} produces the statistic for ∇_{eq} :

$$\begin{aligned} \nabla_{eq} = & \frac{\tau_0}{2} \sum_{i=1}^l \psi_{i*}, \\ = & -\left(\frac{1}{l} \sum_{i=1}^l \mathbf{x}_{i*}^T \tau_1\right) \frac{1}{2} \sum_{i=1}^l \psi_{i*} \\ & + \left(\frac{1}{l} \sum_{i=1}^l \mathbf{x}_{i*}^T \tau_2\right) \frac{1}{2} \sum_{i=1}^l \psi_{i*} + \delta(y) \frac{1}{2} \sum_{i=1}^l \psi_{i*}, \end{aligned}$$

where $\delta(y) \triangleq \frac{1}{l} \sum_{i=1}^l y_i (1 - \xi_i)$.

It follows that τ_0 regulates a symmetrical balancing act for components of $\bar{\mathbf{x}}_{i*}$ along τ_1 and τ_2 , where the statistic ∇_{eq} can be written as

$$+\nabla_{eq} = \left(\text{comp}_{\vec{\tau}_2} \left(\overrightarrow{\bar{\mathbf{x}}_{i*}} \right) - \text{comp}_{\vec{\tau}_1} \left(\overrightarrow{\bar{\mathbf{x}}_{i*}} \right) + \delta(y) \right) \frac{1}{2} \sum_{i=1}^l \psi_{i*},$$

and

$$-\nabla_{eq} = \left(\text{comp}_{\vec{\tau}_1} \left(\overrightarrow{\bar{\mathbf{x}}_{i*}} \right) - \text{comp}_{\vec{\tau}_2} \left(\overrightarrow{\bar{\mathbf{x}}_{i*}} \right) - \delta(y) \right) \frac{1}{2} \sum_{i=1}^l \psi_{i*}.$$

Returning now to Eq. (80):

$$\bar{\mathbf{x}}_{1i*}^T (\tau_1 - \tau_2) = \bar{\mathbf{x}}_{2i*}^T (\tau_2 - \tau_1),$$

given that components of $\bar{\mathbf{x}}_{1i*}$ and $\bar{\mathbf{x}}_{2i*}$ along τ_1 and τ_2 satisfy the state of statistical equilibrium

$$\text{comp}_{\vec{\tau}_1} \left(\overrightarrow{\bar{\mathbf{x}}_{1i*}} \right) - \text{comp}_{\vec{\tau}_2} \left(\overrightarrow{\bar{\mathbf{x}}_{1i*}} \right) = \text{comp}_{\vec{\tau}_2} \left(\overrightarrow{\bar{\mathbf{x}}_{2i*}} \right) - \text{comp}_{\vec{\tau}_1} \left(\overrightarrow{\bar{\mathbf{x}}_{2i*}} \right),$$

it follows that

$$+\nabla_{eq} = \delta(y) \frac{1}{2} \sum_{i=1}^l \psi_{i*} = \delta(y) \frac{1}{2} \|\tau\|_{\min_c}^2,$$

and that

$$-\nabla_{eq} = -\delta(y) \frac{1}{2} \sum_{i=1}^l \psi_{i*} = -\delta(y) \frac{1}{2} \|\tau\|_{\min_c}^2.$$

Substituting the expression for $+\nabla_{eq}$ into Eq. (90) produces an equation that describes conditional probabilities of locations for the \mathbf{x}_{1i*} extreme points $\{\mathbf{x}_{1i*}\}_{i=1}^{l_1}$ within the decision space Z :

$$P(\mathbf{x}_{1i*} | \tau_1) = \|\tau_1\|_{\min_c}^2 - \|\tau_1\| \|\tau_2\| \cos \theta_{\tau_1 \tau_2} + \delta(y) \frac{1}{2} \|\tau\|_{\min_c}^2 \equiv \frac{1}{2} \|\tau\|_{\min_c}^2,$$

and substituting the expression for $-\nabla_{eq}$ into (91) produces an equation that describes conditional probabilities of locations for the \mathbf{x}_{2i*} extreme points $\{\mathbf{x}_{2i*}\}_{i=1}^{l_2}$ within the decision space Z :

$$P(\mathbf{x}_{2i*} | \tau_2) = \|\tau_2\|_{\min_c}^2 - \|\tau_2\| \|\tau_1\| \cos \theta_{\tau_2 \tau_1} - \delta(y) \frac{1}{2} \|\tau\|_{\min_c}^2 \equiv \frac{1}{2} \|\tau\|_{\min_c}^2,$$

where the equalizer statistic

$$\delta(y) \frac{1}{2} \|\tau\|_{\min_c}^2,$$

equalizes the conditional probabilities $P(\mathbf{x}_{1_{i*}}|\tau_1)$ and $P(\mathbf{x}_{2_{i*}}|\tau_2)$ of observing the $\mathbf{x}_{1_{i*}}$ extreme points $\{\mathbf{x}_{1_{i*}}\}_{i=1}^{l_1}$ and the $\mathbf{x}_{2_{i*}}$ extreme points $\{\mathbf{x}_{2_{i*}}\}_{i=1}^{l_2}$ within the decision space Z .

Thus, the area $P(\mathbf{x}_{1_{i*}}|\tau_1)$ under the class-conditional density function $p(\mathbf{x}_{1_{i*}}|\tau_1)$ in Eq. (72)

$$\begin{aligned} P(\mathbf{x}_{1_{i*}}|\tau_1) &= \int_Z p(\mathbf{x}_{1_{i*}}|\tau_1) d\tau_1, \\ &= \int_Z \tau_1 d\tau_1 = \frac{1}{2} \|\tau\|_{\min_c}^2, \end{aligned}$$

is equal to the area $P(\mathbf{x}_{2_{i*}}|\tau_2)$ under the class-conditional density function $p(\mathbf{x}_{2_{i*}}|\tau_2)$ in Eq. (73)

$$\begin{aligned} P(\mathbf{x}_{2_{i*}}|\tau_2) &= \int_Z p(\mathbf{x}_{2_{i*}}|\tau_2) d\tau_2, \\ &= \int_Z \tau_2 d\tau_2 = \frac{1}{2} \|\tau\|_{\min_c}^2. \end{aligned}$$

Therefore, it is concluded that the class-conditional density functions $p(\mathbf{x}_{1_{i*}}|\tau_1)$ and $p(\mathbf{x}_{2_{i*}}|\tau_2)$ satisfy the integral equation

$$\int_Z p(\mathbf{x}_{1_{i*}}|\tau_1) d\tau_1 = \int_Z p(\mathbf{x}_{2_{i*}}|\tau_2) d\tau_2,$$

over the decision space Z , where $Z = Z_1 + Z_2$, Z_1 and Z_2 are contiguous decision regions, $Z_1 \cong Z_2$, and $Z \subset \mathbb{R}^d$. I will now examine the statistical balancing feat in the decision space Z .

10.3 The Statistical Balancing Feat in Decision Space

I will now show that the conditional risk $\mathfrak{R}(Z_2|\tau_1)$ for class ω_1 is equal to the conditional risk $\mathfrak{R}(Z_1|\tau_2)$ for class ω_2

$$\int_{Z_2} p(\mathbf{x}_{1_{i*}}|\tau_1) d\tau_1 = \int_{Z_1} p(\mathbf{x}_{2_{i*}}|\tau_2) d\tau_2,$$

given the decision regions Z_2 and Z_1 and the conditional densities $p(\mathbf{x}_{1_{i*}}|\tau_1)$ and $p(\mathbf{x}_{2_{i*}}|\tau_2)$.

Recall that each $\psi_{1_{i*}}$ eigen-scale determines a conditional density $p(\mathbf{x}_{1_{i*}}|\text{comp}_{\overrightarrow{\mathbf{x}_{1_{i*}}}(\vec{\tau}))})$ for a correlated extreme point $\mathbf{x}_{1_{i*}}$ and that each $\psi_{2_{i*}}$ eigen-scale determines a conditional density $p(\mathbf{x}_{2_{i*}}|\text{comp}_{\overrightarrow{\mathbf{x}_{2_{i*}}}(\vec{\tau}))})$ for a correlated extreme point $\mathbf{x}_{2_{i*}}$.

Substituting the statistic for τ_0 in Eq. (92) into Eq. (82)

$$\psi_{1_{i*}}(1 - \xi_i) = \psi_{1_{i*}} \mathbf{x}_{1_{i*}}^T \tau + \psi_{1_{i*}} \tau_0, \quad i = 1, \dots, l_1,$$

produces a locus equation that is satisfied by the conditional density $\psi_{1_{i*}} \frac{\mathbf{x}_{1_{i*}}}{\|\mathbf{x}_{1_{i*}}\|}$ of an $\mathbf{x}_{1_{i*}}$ extreme point

$$\begin{aligned} \psi_{1_{i*}} \left[(1 - \xi_i) - \frac{1}{l} \sum_{j=1}^l y_j (1 - \xi_j) \right] &= \psi_{1_{i*}} \mathbf{x}_{1_{i*}}^T [\tau_1 - \tau_2] \\ &+ \psi_{1_{i*}} \sum_{j=1}^l \mathbf{x}_{j*}^T [\tau_2 - \tau_1], \end{aligned}$$

where $\psi_{1_{i*}} \mathbf{x}_{1_{i*}}$ is a principal eigenaxis component on τ_1 and the set of eigen-scaled extreme vectors $\psi_{1_{i*}} \sum_{j=1}^l \mathbf{x}_{j*}$ are symmetrically distributed over $\tau_2 - \tau_1$:

$$\left(\sum_{j=1}^l \psi_{1_{i*}} \mathbf{x}_{j*}^T \right) \tau_2 - \left(\sum_{j=1}^l \psi_{1_{i*}} \mathbf{x}_{j*}^T \right) \tau_1.$$

Substituting the statistic for τ_0 in Eq. (92) into Eq. (84)

$$\psi_{2_{i*}} (1 - \xi_i) = -\psi_{2_{i*}} \mathbf{x}_{2_{i*}}^T \tau - \psi_{2_{i*}} \tau_0, \quad i = 1, \dots, l_2,$$

produces a locus equation that is satisfied by the conditional density $\psi_{2_{i*}} \frac{\mathbf{x}_{2_{i*}}}{\|\mathbf{x}_{2_{i*}}\|}$ of an $\mathbf{x}_{2_{i*}}$ extreme point

$$\begin{aligned} \psi_{2_{i*}} \left[(1 - \xi_i) + \frac{1}{l} \sum_{j=1}^l y_j (1 - \xi_j) \right] &= \psi_{2_{i*}} \mathbf{x}_{2_{i*}}^T [\tau_2 - \tau_1] \\ &+ \psi_{2_{i*}} \sum_{j=1}^l \mathbf{x}_{j*}^T [\tau_1 - \tau_2], \end{aligned}$$

where $\psi_{2_{i*}} \mathbf{x}_{2_{i*}}$ is a principal eigenaxis component on τ_2 and the set of eigen-scaled extreme vectors $\psi_{2_{i*}} \sum_{j=1}^l \mathbf{x}_{j*}$ are symmetrically distributed over $\tau_1 - \tau_2$:

$$\left(\sum_{j=1}^l \psi_{2_{i*}} \mathbf{x}_{j*}^T \right) \tau_1 - \left(\sum_{j=1}^l \psi_{2_{i*}} \mathbf{x}_{j*}^T \right) \tau_2.$$

Using Eq. (83), it follows that the conditional probability $P(\mathbf{x}_{1_{i*}} | \tau_1)$ of observing the $\mathbf{x}_{1_{i*}}$ extreme points $\{\mathbf{x}_{1_{i*}}\}_{i=1}^{l_1}$ within the decision space Z satisfies the locus equation

$$\begin{aligned} P(\mathbf{x}_{1_{i*}} | \tau_1) &= \sum_{i=1}^{l_1} \psi_{1_{i*}} (1 - \xi_i) - \nabla_{eq} \\ &- \sum_{i=1}^{l_1} \psi_{1_{i*}} \sum_{j=1}^l \mathbf{x}_{j*}^T [\tau_2 - \tau_1], \end{aligned} \quad (93)$$

where $\nabla_{eq} = \left(\frac{1}{l} \sum_{j=1}^l y_j (1 - \xi_j) \right) \sum_{i=1}^{l_1} \psi_{1_{i*}}$ and equivalent eigen-scaled sets of extreme vectors are symmetrically distributed over $\tau_2 - \tau_1$:

$$\left(\sum_{i=1}^{l_1} \psi_{1_{i*}} \sum_{j=1}^l \mathbf{x}_{j*}^T \right) \tau_2 - \left(\sum_{i=1}^{l_1} \psi_{1_{i*}} \sum_{j=1}^l \mathbf{x}_{j*}^T \right) \tau_1.$$

Given that symmetrically balanced, joint distributions of principal eigenaxis components on ψ and τ are symmetrically distributed over the axes of all of the Wolf dual principal eigenaxis components $\{\psi_{1i*} \vec{\mathbf{e}}_{1i*}\}_{i=1}^{l_1}$ on ψ_1 and all of the constrained, primal principal eigenaxis components $\{\psi_{1i*} \mathbf{x}_{1i*}\}_{i=1}^{l_1}$ on τ_1 , it follows that

$$\sum_{i=1}^{l_1} \psi_{1i*} \sum_{j=1}^l \mathbf{x}_{j*} = \tau_1. \quad (94)$$

Using Eq. (85), it follows that the conditional probability $P(\mathbf{x}_{2i*}|\tau_2)$ of observing the \mathbf{x}_{2i*} extreme points $\{\mathbf{x}_{2i*}\}_{i=1}^{l_2}$ within the decision space Z satisfies the locus equation

$$\begin{aligned} P(\mathbf{x}_{2i*}|\tau_2) &= \sum_{i=1}^{l_2} \psi_{2i*} (1 - \xi_i) + \nabla_{eq} \\ &\quad - \sum_{i=1}^{l_2} \psi_{2i*} \sum_{j=1}^l \mathbf{x}_{j*}^T [\tau_1 - \tau_2], \end{aligned} \quad (95)$$

where $\nabla_{eq} = \left(\frac{1}{l} \sum_{j=1}^l y_j (1 - \xi_j)\right) \sum_{i=1}^{l_2} \psi_{2i*}$ and equivalent eigen-scaled sets of extreme vectors are symmetrically distributed over $\tau_1 - \tau_2$:

$$\left(\sum_{i=1}^{l_2} \psi_{2i*} \sum_{j=1}^l \mathbf{x}_{j*}^T\right) \tau_1 - \left(\sum_{i=1}^{l_2} \psi_{2i*} \sum_{j=1}^l \mathbf{x}_{j*}^T\right) \tau_2.$$

Given that symmetrically balanced, joint distributions of principal eigenaxis components on ψ and τ are symmetrically distributed over the axes of all of the Wolf dual principal eigenaxis components $\{\psi_{2i*} \vec{\mathbf{e}}_{2i*}\}_{i=1}^{l_2}$ on ψ_2 and all of the constrained, primal principal eigenaxis components $\{\psi_{2i*} \mathbf{x}_{2i*}\}_{i=1}^{l_2}$ on τ_2 , it follows that

$$\sum_{i=1}^{l_2} \psi_{2i*} \sum_{j=1}^l \mathbf{x}_{j*} = \tau_2. \quad (96)$$

10.4 Balancing the Bayes' Risk

Consider again the expressions for the conditional probabilities $P(\mathbf{x}_{1i*}|\tau_1)$ and $P(\mathbf{x}_{2i*}|\tau_2)$ in Eqs (93) and (95). Given that the conditional probabilities of observing the \mathbf{x}_{1i*} and \mathbf{x}_{2i*} extreme points within the decision space Z are equal

$$P(\mathbf{x}_{1i*}|\tau_1) = P(\mathbf{x}_{2i*}|\tau_2),$$

and the conditional probability densities of the \mathbf{x}_{1i*} and \mathbf{x}_{2i*} extreme points satisfy the state of statistical equilibrium

$$\sum_{i=1}^{l_1} \psi_{1i*} \frac{\mathbf{x}_{1i*}}{\|\mathbf{x}_{1i*}\|} (1 - \xi_i) = \sum_{i=1}^{l_2} \psi_{2i*} \frac{\mathbf{x}_{2i*}}{\|\mathbf{x}_{2i*}\|} (1 - \xi_i),$$

it follows that eigen-scaled sets of extreme vectors are distributed over a linear eigenlocus $\tau = \tau_1 - \tau_2$ in the symmetrically balanced manner

$$\begin{aligned} & \sum_{i=1}^{l_1} \psi_{1_{i*}} \left[\sum_{j=1}^l \mathbf{x}_{j*}^T [\tau_2 - \tau_1] \right] + \nabla_{eq} \\ &= \sum_{i=1}^{l_2} \psi_{2_{i*}} \left[\sum_{j=1}^l \mathbf{x}_{j*}^T [\tau_1 - \tau_2] \right] - \nabla_{eq}. \end{aligned} \quad (97)$$

Given that $\psi_{1_{i*}}$ describes a distribution (a spread) for an $\mathbf{x}_{1_{i*}}$ extreme point relative to a given collection of extreme points $\{\mathbf{x}_{j*}\}_{j=1}^l$, the statistic $\sum_{j=1}^l \psi_{1_{i*}} \mathbf{x}_{j*}$ describes the expected value $E[\mathbf{x}_{1_{i*}}]$ of $\mathbf{x}_{1_{i*}}$:

$$\sum_{j=1}^l \psi_{1_{i*}} \mathbf{x}_{j*} = E[\mathbf{x}_{1_{i*}}]. \quad (98)$$

Likewise, given that $\psi_{2_{i*}}$ describes a distribution (a spread) for an $\mathbf{x}_{2_{i*}}$ extreme point relative to a given collection of extreme points $\{\mathbf{x}_{j*}\}_{j=1}^l$, the statistic $\sum_{j=1}^l \psi_{2_{i*}} \mathbf{x}_{j*}$ describes the expected value $E[\mathbf{x}_{2_{i*}}]$ of $\mathbf{x}_{2_{i*}}$:

$$\sum_{j=1}^l \psi_{2_{i*}} \mathbf{x}_{j*} = E[\mathbf{x}_{2_{i*}}]. \quad (99)$$

Using Eqs (94), (96), (98), and (99), Eq. (97) can be rewritten as

$$\sum_{i=1}^{l_1} E[\mathbf{x}_{1_{i*}}^T] \tau_2 - \|\tau_1\|_{\min_c}^2 + \nabla_{eq} = \sum_{i=1}^{l_2} E[\mathbf{x}_{2_{i*}}^T] \tau_1 - \|\tau_2\|_{\min_c}^2 - \nabla_{eq}. \quad (100)$$

Using Eqs (90) and (91), where the total allowed eigenenergies $\|\tau_1\|_{\min_c}^2$ and $\|\tau_2\|_{\min_c}^2$ are equalized by the equalizer statistic ∇_{eq} ,

$$\|\tau_1\|_{\min_c}^2 + \nabla_{eq} \equiv \|\tau_2\|_{\min_c}^2 - \nabla_{eq},$$

it follows that Eq. (100) reduces to the expression

$$\sum_{i=1}^{l_1} E[\mathbf{x}_{1_{i*}}^T] \tau_2 = \sum_{i=1}^{l_2} E[\mathbf{x}_{2_{i*}}^T] \tau_1,$$

which indicates that the conditional probability of observing the $\mathbf{x}_{1_{i*}}$ extreme points $\{\mathbf{x}_{1_{i*}}\}_{i=1}^{l_1}$ within the Z_2 decision region is *equal* to the conditional probability of observing the $\mathbf{x}_{2_{i*}}$ extreme points $\{\mathbf{x}_{2_{i*}}\}_{i=1}^{l_2}$ within the Z_1 decision region.

Thus, it is concluded that the conditional probability $P(\mathbf{x}_{1_{i*}}|\tau_1)$ of observing the $\mathbf{x}_{1_{i*}}$ extreme points $\{\mathbf{x}_{1_{i*}}\}_{i=1}^{l_1}$ within the Z_2 decision region is equal to the conditional probability $P(\mathbf{x}_{2_{i*}}|\tau_2)$ of observing the $\mathbf{x}_{2_{i*}}$ extreme points $\{\mathbf{x}_{2_{i*}}\}_{i=1}^{l_2}$ within the Z_1 decision region:

$$\int_{Z_2} p(\mathbf{x}_{1_{i*}}|\tau_1) d\tau_1 = \int_{Z_1} p(\mathbf{x}_{2_{i*}}|\tau_2) d\tau_2.$$

It follows that the probability of making a decision error $P(D_1|\omega_2)$ in the Z_2 decision region is equal to the probability of making a decision error $P(D_2|\omega_1)$ in the Z_1 decision region.

Therefore, it follows that the conditional risk $\mathfrak{R}(Z_2|\tau_1)$ for class ω_1

$$\mathfrak{R}(Z_2|\tau_1) = \int_{Z_2} p(\mathbf{x}_{1i*}|\tau_1) d\tau_1,$$

and the conditional risk $\mathfrak{R}(Z_1|\tau_2)$ for class ω_2

$$\mathfrak{R}(Z_1|\tau_2) = \int_{Z_1} p(\mathbf{x}_{2i*}|\tau_2) d\tau_2,$$

satisfy Bayes' minimax risk $\mathfrak{R}_{mm}(Z|\tau)$

$$\begin{aligned} \mathfrak{R}_{mm}(Z|\tau) &= \int_{Z_2} p(\mathbf{x}_{1i*}|\tau_1) d\tau_1 \\ &= \int_{Z_1} p(\mathbf{x}_{2i*}|\tau_2) d\tau_2, \end{aligned}$$

where the conditional risk $\mathfrak{R}(Z_2|\tau_1)$ for class ω_1 , given the decision region Z_2 and the conditional density $p(\mathbf{x}_{1i*}|\tau_1)$, is equal to the conditional risk $\mathfrak{R}(Z_1|\tau_2)$ for class ω_2 , given the decision region Z_1 and the conditional density $p(\mathbf{x}_{2i*}|\tau_2)$.

Figure 22 illustrates the manner in which linear eigenlocus discriminant functions $D(\mathbf{x}) = \tau^T \mathbf{x} + \tau_0$ minimize Bayes' minimax risk $\mathfrak{R}_{mm}(Z|\tau)$, where Bayes' classification error $\mathfrak{R}(Z_2|\tau_1)$ for class ω_1 is symmetrically balanced with Bayes' classification error $\mathfrak{R}(Z_1|\tau_2)$ for class ω_2 , such that $\mathfrak{R}(Z_1|\tau_2) \equiv \mathfrak{R}(Z_2|\tau_1)$ for *any* two classes of feature or pattern vectors.

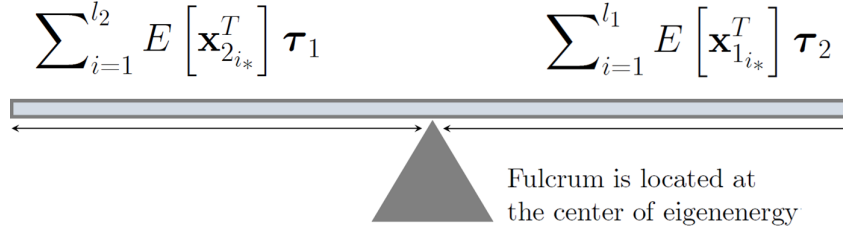
It is concluded that $\tau = \tau_1 - \tau_2$ is a parameter vector of likelihoods

$$\begin{aligned} \hat{\Lambda}(\mathbf{x}) &= \sum_{i=1}^{l_1} p(\mathbf{x}_{1i*} | \text{comp}_{\overrightarrow{\mathbf{x}_{1i*}}}(\overrightarrow{\tau})) \mathbf{x}_{1i*} \\ &\quad - \sum_{i=1}^{l_2} p(\mathbf{x}_{2i*} | \text{comp}_{\overrightarrow{\mathbf{x}_{2i*}}}(\overrightarrow{\tau})) \mathbf{x}_{2i*}, \end{aligned}$$

which satisfies a linear decision boundary in terms of a minimum total probability of error $\mathcal{P}_e(Z)$, where $\mathfrak{R}(Z_1|\tau_2) = \mathfrak{R}(Z_2|\tau_1)$.

By way of illustration, Fig. 23 shows that linear eigenlocus transforms generate decision regions Z_1 and Z_2 that minimize Bayes' minimax risk $\mathfrak{R}_{mm}(Z|\tau)$, where $\mathfrak{R}(Z_1|\tau_2) = \mathfrak{R}(Z_2|\tau_1)$, for highly overlapping data distributions, completely overlapping data distributions, and non-overlapping data distributions. Accordingly, linear eigenlocus discriminant functions $D(\mathbf{x}) = \tau^T \mathbf{x} + \tau_0$ determine Bayes' linear decision boundaries for highly overlapping data distributions (see Fig. 23a and

Equal Bayes' Classification Errors on Equal Sides of τ



Axis of τ is symmetrically balanced with respect to
conditional risks $\Re(Z_2|\tau_1)$ and $\Re(Z_1|\tau_2)$

Figure 22: Linear eigenlocus transforms determine linear discriminant functions $D(\mathbf{x}) = \tau^T \mathbf{x} + \tau_0$ that are Bayes' equalizer rules, where Bayes' classification error $\Re(Z_2|\tau_1)$ for class ω_1 is symmetrically balanced with Bayes' classification error $\Re(Z_1|\tau_2)$ for class ω_2 .

Fig. 23b), completely overlapping data distributions (see Fig. 23c and Fig. 23d), and non-overlapping data distributions (see Fig. 23e and Fig. 23f), where unconstrained, primal, principal eigenaxis components (extreme points) are enclosed in blue circles.

I will now develop an expression for a linear eigenlocus that is a locus of discrete conditional probabilities.

10.5 Linear Eigenlocus of Discrete Probabilities

Write a linear eigenlocus τ in terms of

$$\begin{aligned} \tau = & \lambda_{\max_\psi}^{-1} \sum_{i=1}^{l_1} \frac{\mathbf{x}_{1_{i*}}}{\|\mathbf{x}_{1_{i*}}\|} \|\mathbf{x}_{1_{i*}}\|^2 \widehat{\text{cov}}_{sm_\uparrow}(\mathbf{x}_{1_{i*}}) \\ & - \lambda_{\max_\psi}^{-1} \sum_{i=1}^{l_2} \frac{\mathbf{x}_{2_{i*}}}{\|\mathbf{x}_{2_{i*}}\|} \|\mathbf{x}_{2_{i*}}\|^2 \widehat{\text{cov}}_{sm_\uparrow}(\mathbf{x}_{2_{i*}}), \end{aligned}$$

where $\widehat{\text{cov}}_{sm_\uparrow}(\mathbf{x}_{1_{i*}})$ and $\widehat{\text{cov}}_{sm_\uparrow}(\mathbf{x}_{2_{i*}})$ denote the symmetrically balanced, signed magnitudes in Eqs (67) and (71), and the terms $\frac{\|\mathbf{x}_{1_{i*}}\|}{\|\mathbf{x}_{1_{i*}}\|}$ and $\frac{\|\mathbf{x}_{2_{i*}}\|}{\|\mathbf{x}_{2_{i*}}\|}$ have been introduced and rearranged.

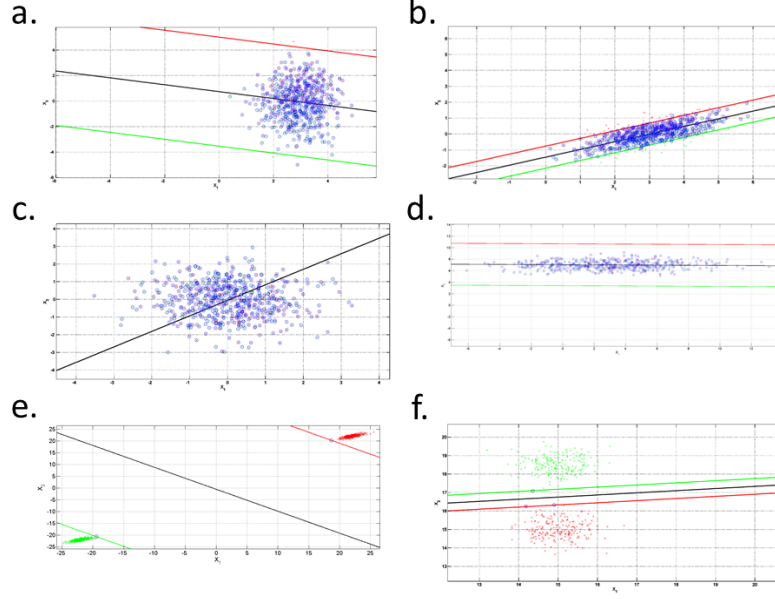


Figure 23: Linear eigenlocus discriminant functions determine Bayes' linear decision boundaries for (1) highly overlapping data distributions: see (a) and (b), (2) completely overlapping data distributions: see (c) and (d), and (3) non-overlapping data distributions: see (e) and (f).

Rewrite τ in terms of total allowed eigenenergies

$$\begin{aligned} \tau = & \sum_{i=1}^{l_1} \left\| \lambda_{\max_\psi}^{-1} \left(\widehat{\text{cov}}_{sm\uparrow}(\mathbf{x}_{1_{i*}}) \right)^{\frac{1}{2}} \mathbf{x}_{1_{i*}} \right\|_{\min_c}^2 \frac{\mathbf{x}_{1_{i*}}}{\|\mathbf{x}_{1_{i*}}\|} \\ & - \sum_{i=1}^{l_2} \left\| \lambda_{\max_\psi}^{-1} \left(\widehat{\text{cov}}_{sm\uparrow}(\mathbf{x}_{2_{i*}}) \right)^{\frac{1}{2}} \mathbf{x}_{2_{i*}} \right\|_{\min_c}^2 \frac{\mathbf{x}_{2_{i*}}}{\|\mathbf{x}_{2_{i*}}\|}, \end{aligned} \quad (101)$$

where $\left\| \lambda_{\max_\psi}^{-1} \left(\widehat{\text{cov}}_{sm\uparrow}(\mathbf{x}_{1_{i*}}) \right)^{\frac{1}{2}} \mathbf{x}_{1_{i*}} \right\|_{\min_c}^2$ and $\left\| \lambda_{\max_\psi}^{-1} \left(\widehat{\text{cov}}_{sm\uparrow}(\mathbf{x}_{2_{i*}}) \right)^{\frac{1}{2}} \mathbf{x}_{2_{i*}} \right\|_{\min_c}^2$ are conditional probabilities $\mathcal{P} \left(\widehat{Z}(\mathbf{x}_{1_{i*}}) \right)$ and $\mathcal{P} \left(\widehat{Z}(\mathbf{x}_{2_{i*}}) \right)$ of observing $\mathbf{x}_{1_{i*}}$ and $\mathbf{x}_{2_{i*}}$ extreme points in a decision space \widehat{Z} .

Now rewrite Eq. (101) as a locus of discrete conditional probabilities:

$$\begin{aligned} \tau_1 - \tau_2 = & \sum_{i=1}^{l_1} \mathcal{P} \left(\widehat{Z}(\mathbf{x}_{1_{i*}}) \right) \frac{\mathbf{x}_{1_{i*}}}{\|\mathbf{x}_{1_{i*}}\|} \\ & - \sum_{i=1}^{l_2} \mathcal{P} \left(\widehat{Z}(\mathbf{x}_{2_{i*}}) \right) \frac{\mathbf{x}_{2_{i*}}}{\|\mathbf{x}_{2_{i*}}\|}, \end{aligned} \quad (102)$$

which provides discrete measures for conditional probabilities of classification errors $\mathcal{P}_e \left(\widehat{Z}_2(\mathbf{x}_{1_{i*}}) \right)$ and $\mathcal{P}_e \left(\widehat{Z}_1(\mathbf{x}_{2_{i*}}) \right)$ for $\mathbf{x}_{1_{i*}}$ extreme points

that lie in the Z_2 decision region and $\mathbf{x}_{2_{i*}}$ extreme points that lie in the Z_1 decision region.

10.6 The Probabilistic Eigenlocus Test

Returning to Eq. (49), consider the estimate $\hat{\Lambda}(\mathbf{x})$ that an unknown pattern vector \mathbf{x} is located within some particular region of \mathbb{R}^d

$$\hat{\Lambda}(\mathbf{x}) = (\mathbf{x} - \bar{\mathbf{x}}_{i*})^T \tau / \|\tau\|, \\ + \frac{1}{l \|\tau\|} \sum_{i=1}^l y_i (1 - \xi_i),$$

based on the value of the decision locus $\text{comp}_{\hat{\tau}} \left(\overrightarrow{(\mathbf{x} - \bar{\mathbf{x}}_{i*})} \right)$, and class membership statistic $\frac{1}{l \|\tau\|} \sum_{i=1}^l y_i (1 - \xi_i)$, where $\text{comp}_{\hat{\tau}} \left(\overrightarrow{(\mathbf{x} - \bar{\mathbf{x}}_{i*})} \right)$ denotes a signed magnitude $\|\mathbf{x} - \bar{\mathbf{x}}_{i*}\| \cos \theta$ along the axis of $\hat{\tau}$, θ is the angle between the vector $\mathbf{x} - \bar{\mathbf{x}}_{i*}$ and $\hat{\tau}$, and $\hat{\tau}$ denotes the unit linear eigenlocus $\tau / \|\tau\|$. I will now demonstrate that the signed magnitude expression $(\mathbf{x} - \bar{\mathbf{x}}_{i*})^T \tau / \|\tau\|$ is a locus of discrete conditional probabilities.

Substitute the expression for $\tau_1 - \tau_2$ in Eq. (102) into the expression for the linear eigenlocus test in Eq. (48). Denote the unit primal principal eigenaxis components $\frac{\mathbf{x}_{1_{i*}}}{\|\mathbf{x}_{1_{i*}}\|}$ and $\frac{\mathbf{x}_{2_{i*}}}{\|\mathbf{x}_{2_{i*}}\|}$ by $\hat{\mathbf{x}}_{1_{i*}}$ and $\hat{\mathbf{x}}_{2_{i*}}$. It follows that the probability that the unknown pattern vector \mathbf{x} is located within a specific region of \mathbb{R}^d is provided by the expression

$$\hat{\Lambda}(\mathbf{x}) = \sum_{i=1}^{l_1} \left[(\mathbf{x} - \bar{\mathbf{x}}_{i*})^T \hat{\mathbf{x}}_{1_{i*}} \right] \mathcal{P} \left(\hat{Z}(\mathbf{x}_{1_{i*}}) \right) \\ - \sum_{i=1}^{l_2} \left[(\mathbf{x} - \bar{\mathbf{x}}_{i*})^T \hat{\mathbf{x}}_{2_{i*}} \right] \mathcal{P} \left(\hat{Z}(\mathbf{x}_{2_{i*}}) \right) \\ + \frac{1}{l \|\tau\|} \sum_{i=1}^l y_i (1 - \xi_i),$$

where $\mathcal{P} \left(\hat{Z}(\mathbf{x}_{1_{i*}}) \right)$ and $\mathcal{P} \left(\hat{Z}(\mathbf{x}_{2_{i*}}) \right)$ provides discrete measures for conditional probabilities of classification errors $\mathcal{P}_e \left(\hat{Z}_2(\mathbf{x}_{1_{i*}}) \right)$ and $\mathcal{P}_e \left(\hat{Z}_1(\mathbf{x}_{2_{i*}}) \right)$ for $\mathbf{x}_{1_{i*}}$ extreme points that lie in the Z_2 decision region and $\mathbf{x}_{2_{i*}}$ extreme points that lie in the Z_1 decision region.

The above expression reduces to a locus of discrete conditional prob-

abilities

$$\begin{aligned}\Lambda_\tau(\mathbf{x}) = & \sum_{i=1}^{l_1} \text{comp}_{\widehat{\mathbf{x}}_{1i*}}^{\rightarrow} \left(\overrightarrow{(\mathbf{x} - \overline{\mathbf{x}}_{i*})} \right) \mathcal{P} \left(\widehat{Z}(\mathbf{x}_{1i*}) \right) \\ & - \sum_{i=1}^{l_2} \text{comp}_{\widehat{\mathbf{x}}_{2i*}}^{\rightarrow} \left(\overrightarrow{(\mathbf{x} - \overline{\mathbf{x}}_{i*})} \right) \mathcal{P} \left(\widehat{Z}(\mathbf{x}_{2i*}) \right) \\ & + \frac{1}{l \|\tau\|} \sum_{i=1}^l y_i (1 - \xi_i),\end{aligned}\quad (103)$$

where the likelihood statistics

$$\text{comp}_{\widehat{\mathbf{x}}_{1i*}}^{\rightarrow} \left(\overrightarrow{(\mathbf{x} - \overline{\mathbf{x}}_{i*})} \right) \mathcal{P} \left(\widehat{Z}(\mathbf{x}_{1i*}) \right), \quad (104)$$

and

$$\text{comp}_{\widehat{\mathbf{x}}_{2i*}}^{\rightarrow} \left(\overrightarrow{(\mathbf{x} - \overline{\mathbf{x}}_{i*})} \right) \mathcal{P} \left(\widehat{Z}(\mathbf{x}_{2i*}) \right), \quad (105)$$

determine probabilities $\mathcal{P} \left(\widehat{Z}(\mathbf{x}_{1i*}) \right)$ and $\mathcal{P} \left(\widehat{Z}(\mathbf{x}_{2i*}) \right)$ of finding the unknown pattern vector \mathbf{x} within localized regions $\widehat{Z}(\mathbf{x}_{1i*})$ and $\widehat{Z}(\mathbf{x}_{2i*})$ of the decision space Z . The likelihood statistic in Eq. (104) is proportional, according to the signed magnitude $\text{comp}_{\widehat{\mathbf{x}}_{1i*}}^{\rightarrow} \left(\overrightarrow{(\mathbf{x} - \overline{\mathbf{x}}_{i*})} \right)$ along the axis of $\widehat{\mathbf{x}}_{1i*}$, to the probability $\mathcal{P} \left(\widehat{Z}(\mathbf{x}_{1i*}) \right)$ of finding the extreme point \mathbf{x}_{1i*} within a localized region $\widehat{Z}(\mathbf{x}_{1i*})$ of the decision space Z . Similarly, the likelihood statistic in Eq. (105) is proportional, according to the signed magnitude $\text{comp}_{\widehat{\mathbf{x}}_{2i*}}^{\rightarrow} \left(\overrightarrow{(\mathbf{x} - \overline{\mathbf{x}}_{i*})} \right)$ along the axis of $\widehat{\mathbf{x}}_{2i*}$, to the probability $P \left(\mathbf{x}_{2i*} | \widehat{Z}_{Pe}(\mathbf{x}_{2i*}) \right)$ of finding the extreme point \mathbf{x}_{2i*} within a localized region $\widehat{Z}(\mathbf{x}_{2i*})$ of the decision space Z .

It is concluded that the signed magnitude expression $(\mathbf{x} - \overline{\mathbf{x}}_{i*})^T \tau / \|\tau\|$ in Eq. (49) is a locus of discrete conditional probabilities that satisfies the minimax risk \mathfrak{R}_{mm} in Eq. (8).

I will now consider the design and development of Bayes' minimax pattern recognition systems using linear eigenlocus discriminant and decision functions.

11 Design and Development of Bayes' Minimax Pattern Recognition Systems

It has been shown that the linear discriminant function $D(\mathbf{x}) = \tau^T \mathbf{x} + \tau_0$ is an equalizer rule that performs well over a range of prior probabilities. Accordingly, a constrained, primal linear eigenlocus $\tau^T \mathbf{x} + \tau_0$ satisfies

Bayes' minimax risk $\mathfrak{R}_{mm}(Z|\tau)$:

$$\begin{aligned}\mathfrak{R}_{mm}(Z|\tau) &= \int_{Z_2} p(\mathbf{x}_{1i*}|\tau_1) d\tau_1 \\ &= \int_{Z_1} p(\mathbf{x}_{2i*}|\tau_2) d\tau_2,\end{aligned}$$

where the conditional risk $\mathfrak{R}(Z_2|\tau_1)$ for class ω_1 , given the decision region Z_2 and conditional density $p(\mathbf{x}_{1i*}|\tau_1)$, is equal to the conditional risk $\mathfrak{R}(Z_1|\tau_2)$ for class ω_2 , given the decision region Z_1 and conditional density $p(\mathbf{x}_{2i*}|\tau_2)$.

Moreover, linear combinations of linear eigenlocus discriminant functions can be used to build Bayes' minimax pattern recognition systems, where the overall system complexity is scale-invariant for the feature space dimension and the number of pattern classes.

It follows that a linear discriminant function $D(\mathbf{x}) = \tau^T \mathbf{x} + \tau_0$ is a scalable module for Bayes' minimax pattern recognition systems. The decision function $\text{sign}(\hat{\Lambda}(\mathbf{x}))$

$$\text{sign}(\hat{\Lambda}(\mathbf{x})) = \text{sign}(\tau^T \mathbf{x} + \tau_0)$$

where $\text{sign}(x) \equiv \frac{x}{|x|}$ for $x \neq 0$, provides a natural means for discriminating between multiple classes of data, where decisions can be made that are based on the largest probabilistic output of decision banks of $\text{sign}(\hat{\Lambda}(\mathbf{x}))$. Decision banks are formed by the system of scalable modules outlined below.

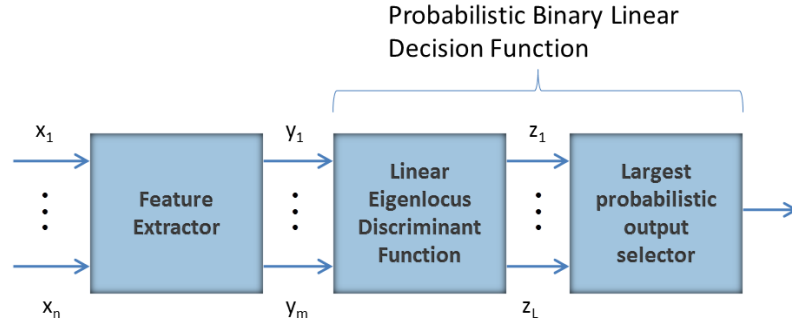
11.1 Systems of Scalable Modules

Figure 24 illustrates a system of scalable modules that can be used to build a Bayes' minimax pattern recognition system which distinguishes between the objects in M different pattern classes $\{\mathbf{X}_i\}_{i=1}^M$.

Objects in pattern classes can involve any type of distinguishing features that have been extracted from collections of:

1. Networks formed by interconnected systems of people and/or things.
2. Documents.
3. Images.
4. Waveforms, signals, or sequences, including stationary random processes.

Bayes' Minimax Binary Linear Classification System



System of scalable modules used to build
Bayes' minimax pattern recognition systems

Figure 24: Bayes' minimax pattern recognition systems are based on a system of scalable modules which includes a feature extractor, a linear eigenlocus discriminant function $D(\mathbf{x}) = \tau^T \mathbf{x} + \tau_0$ and a decision function $\text{sign}(\tau^T \mathbf{x} + \tau_0)$.

The design of Bayes' minimax pattern recognition systems $P_{\mathfrak{B}\epsilon}(\mathbf{x})$ involves designing M decision banks, where each decision bank contains $M - 1$ decision functions $\text{sign}(\hat{\Lambda}(\mathbf{x}))$, and each decision function is determined by a feature extractor and a linear eigenlocus discriminant function. A feature extractor generates d -dimensional feature vectors from collections of networks, documents, images, or signals for *all* of the M pattern classes. Alternatively, feature vectors from collections of networks, documents, images, or signals can be fused with each other.

Fusion of Feature Vectors Inductive matrix completion methods enable the fusion of feature vectors from collections of networks, documents, images, and signals, where the dimension of the feature vectors for different collections may differ (see Jain and Dhillon, 2013).

Suppose that M sets of d -dimensional feature vectors have been extracted from collections of networks, documents, images, or signals for M pattern classes. A Bayes' minimax pattern recognition system $P_{\mathfrak{B}\epsilon}(\mathbf{x})$ is created in the following manner.

11.2 Decision Banks

A decision bank $DB_{\mathbf{X}_i}$ $\left[\left\{ \text{sign} \left(\hat{\Lambda}_j(\mathbf{x}) \right) \right\}_{j=1}^{M-1} \right]$ is created for each pattern class \mathbf{X}_i that consists of a bank of $M - 1$ decision functions $\text{sign} \left(\hat{\Lambda}(\mathbf{x}) \right)$. Build $M - 1$ linear eigenlocus discriminant functions, where the pattern vectors in the given class \mathbf{X}_i have the training label $+1$ and the pattern vectors in all of the other pattern classes have the training label -1 . Accordingly, the decision bank $DB_{\mathbf{X}_i}$ for the pattern class \mathbf{X}_i is a linear combination of decision functions

$$DB_{\mathbf{X}_i}(\mathbf{x}) = \sum_{j=1}^{M-1} \text{sign} \left(\hat{\Lambda}_j(\mathbf{x}) \right).$$

The pattern recognition system $P_{\mathfrak{B}\mathfrak{E}}(\mathbf{x})$

$$P_{\mathfrak{B}\mathfrak{E}}(\mathbf{x}) \left[\left\{ DB_{\mathbf{X}_i} \left[\left\{ \text{sign} \left(\hat{\Lambda}_j(\mathbf{x}) \right) \right\}_{j=1}^{M-1} \right] \right\}_{i=1}^M \right],$$

provides a set of $M \times (M - 1)$ decision statistics $\text{sign} \left(\hat{\Lambda}(\mathbf{x}) \right)$, where the maximum value selector of the pattern recognition system $P_{\mathfrak{B}\mathfrak{E}}(\mathbf{x})$ chooses the pattern class \mathbf{X}_i for which a decision bank $DB_{\mathbf{X}_i}(\mathbf{x})$ has the maximum probabilistic output. Because the pattern recognition system $P_{\mathfrak{B}\mathfrak{E}}(\mathbf{x})$ is a linear combination of linear eigenlocus discriminant functions, the overall network complexity is scale-invariant for the feature space dimension and the number of pattern classes.

Superior Generalization Performance

All classes of feature vectors drawn from non-overlapping probability distributions exhibit optimal discrimination capacity, where Bayes' error is zero. Therefore, given M pattern classes, if a feature extractor can be developed for which negligible or no overlap exists between all M data distributions, then the scale-invariance of the pattern recognition system $P_{\mathfrak{B}\mathfrak{E}}(\mathbf{x})$ described above ensures low estimation variance and superior generalization performance.

The probability of error is the key parameter of all statistical pattern recognition systems. The amount of overlap between data distributions determines the Bayes' classification error rate which is the lowest error rate that can be achieved by any classifier. In general, Bayes' error rate is difficult to evaluate (Fukunaga, 1990).

11.3 Design of Feature Vectors

Geman et al. (1992) suggested that some important biases or generalizations can be achieved through proper data representations. For the

problem of learning decision boundaries, an important form of proper data representations involves the identification and exploitation of distinguishing features that are simple to extract, invariant to irrelevant transformations, insensitive to noise, and useful for discriminating between objects in different categories (Duda et al., 2001).

Sufficient Class Separability Useful sets of distinguishing features for discrimination tasks must exhibit sufficient class separability, i.e., a negligible overlap exists between all data distributions. In general, the design of distinguishing feature vectors which exhibit sufficient class separability is the most fundamental and difficult problem in the overall design of a statistical pattern recognition system (Fukunaga, 1990; Jain et al., 2000; Duda et al., 2001).

11.3.1 Measures of Feature Vector Effectiveness

The criteria to evaluate the effectiveness of feature vectors must be a measure of the overlap or class separability among data distributions, and not a measure of fit such as the mean-square error of a statistical model (Fukunaga, 1990). For example, the Bhattacharyya distance provides a convenient measure of class separability for two pattern classes. The measure provides an upper bound of the Bayes' error if training data are drawn from Gaussian distributions. However, the upper bound may be significantly higher than the Bayes' error. Also, the Bhattacharyya distance is difficult to evaluate because the trace and the determinant of matrices are combined in the criterion (Fukunaga, 1990).

Alternatively, linear eigenlocus discriminant functions provide a robust measure of class separability and Bayes' error rate for two given sets of feature vectors whose mean and covariance functions remain constant over time.

11.4 A Practical Statistical Multimeter

Linear eigenlocus decision functions $\text{sign}(\tau^T \mathbf{x} + \tau_0)$ provide a practical statistical gauge for measuring data distribution overlap and Bayes' error rate for two given sets of feature or pattern vectors.

Linear eigenlocus discriminant functions $D(\mathbf{x}) = \tau^T \mathbf{x} + \tau_0$ are Bayes' equalizer rules $\Lambda_{\mathfrak{B}\mathfrak{E}}(\mathbf{x})$ that perform well over a range of prior probabilities, where any given equalizer rule $\Lambda_{\mathfrak{B}\mathfrak{E}}(\mathbf{x})$ is a decision rule with equal Bayes' error $\mathfrak{R}(Z_1) = \mathfrak{R}(Z_2)$ for two given pattern classes. Accordingly, linear eigenlocus decision functions $\text{sign}(\Lambda_{\mathfrak{B}\mathfrak{E}}(\mathbf{x}))$ can be used to measure data distribution overlap and Bayes' error rate for any two given sets of feature vectors whose mean and covariance functions are constant over time.

To measure Bayes' error rate and data distribution overlap, build

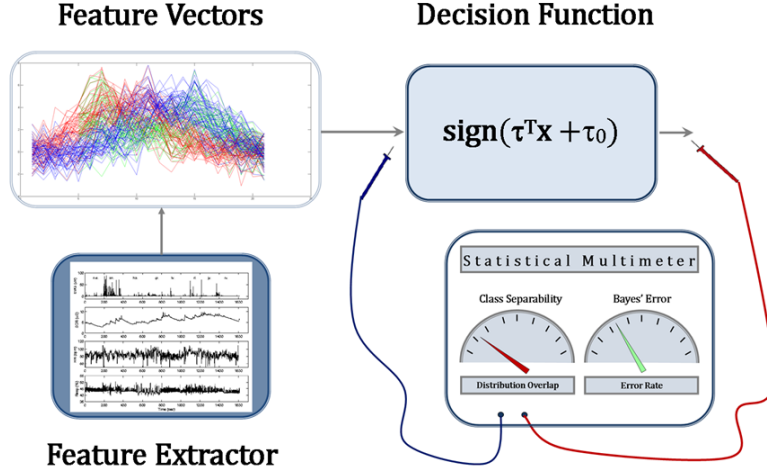


Figure 25: Linear eigenlocus decision functions $\text{sign}(\tau^T \mathbf{x} + \tau_0)$ provide a practical statistical multimeter for measuring data distribution overlap and Bayes' error rate for two given sets of feature vectors.

a linear eigenlocus discriminant function $\Lambda_{\mathfrak{B}\mathfrak{E}}(\mathbf{x})$ using feature vectors which have been extracted from any given collections of networks, documents, images, or signals for two pattern classes. While equal numbers of training examples are not absolutely necessary, the number of training examples from each of the pattern classes should be reasonably balanced with each other.

Apply the decision function $\text{sign}(\Lambda_{\mathfrak{B}\mathfrak{E}}(\mathbf{x}))$ to a collection of feature vectors which have not been used to build the discriminant function. In general, if τ is based on a small number of principal eigenaxis components, i.e., 2 – 10, the data distributions are not overlapping with each other and Bayes' error is negligible or zero.

If data collection is cost prohibitive, use k -fold cross validation, where a collection of feature vectors is split randomly into k partitions. Build a linear eigenlocus discriminant function $\Lambda_{BE}(\mathbf{x})$ with a data set consisting of $k - 1$ of the original k parts, and use the remaining portion for testing. Repeat this process k times. Bayes' error rate and data distribution overlap is the average over the k test runs. Figure 25 illustrates how linear eigenlocus decision functions $\text{sign}(\tau^T \mathbf{x} + \tau_0)$ provide a practical statistical multimeter for measuring data distribution overlap and Bayes' error rate.

11.5 A Practical Statistical Gauge

Linear eigenlocus decision functions $\text{sign}(\Lambda_{\mathfrak{B}\mathfrak{E}}(\mathbf{x}))$ can also be used to identify homogeneous data distributions. Build a linear eigenlocus discriminant function $\Lambda_{\mathfrak{B}\mathfrak{E}}(\mathbf{x})$ using samples drawn from two distributions. Apply the decision function $\text{sign}(\Lambda_{\mathfrak{B}\mathfrak{E}}(\mathbf{x}))$ to samples which have not been used to build the discriminant function.

Given homogeneous data distributions, essentially all of the training data are transformed into constrained, primal principal eigenaxis components, and the error rate of the discriminant function $\tau^T \mathbf{x} + \tau_0$ is 50%.

If data collection is cost prohibitive, use k -fold cross validation, where a collection of feature vectors is split randomly into k partitions. Build a linear eigenlocus discriminant function $\Lambda_{BE}(\mathbf{x})$ with a data set consisting of $k - 1$ of the original k parts, and use the remaining portion for testing. Repeat this process k times. Bayes' error rate and data distribution overlap is the average over the k test runs.

The Two Sample Problem Alternatively, linear eigenlocus decision functions $\text{sign}(\Lambda_{\mathfrak{B}\mathfrak{E}}(\mathbf{x}))$ can be used to determine if two samples are from different distributions. Build a linear eigenlocus discriminant function $\Lambda_{\mathfrak{B}\mathfrak{E}}(\mathbf{x})$ using samples drawn from two distributions. Apply the decision function $\text{sign}(\Lambda_{\mathfrak{B}\mathfrak{E}}(\mathbf{x}))$ to samples which have not been used to build the discriminant function. Given different data distributions, the error rate of the discriminant function $\tau^T \mathbf{x} + \tau_0$ is less than 50%.

12 Concluding Remarks

In this paper, I have formulated the problem of learning unknown linear discriminant functions from data as a locus problem, thereby formulating geometric locus methods within a statistical framework. Solving locus problems involves finding the equation of a curve or surface defined by a given property, and finding the graph or locus of a given equation.

I have devised a system of locus equations which determines linear discriminant functions that are Bayes' equalizer rules. The system of locus equations is based on a variant of the inequality constrained optimization problem for linear kernel support vector machines. Bayes' equalizer rules, which are also known as Bayes' minimax tests, determine linear decision boundaries that satisfy Bayes' minimax risk \mathfrak{R}_{mm} , where two-class feature spaces are divided into decision regions that have equal classification errors.

I have demonstrated that an equalizer rule or minimax test describes the locus of a linear decision boundary for any two classes of feature vectors, including completely overlapping data distributions. For data distributions that have similar covariance matrices, the minimax test is

identical to the minimum probability of error test.

I have demonstrated that the system of locus equations forms a locus of weighted extreme points, where extreme points are data points located in overlapping regions or tails regions between two data distributions, which is a dual locus of likelihoods and principal eigenaxis components, where each weight encodes a class membership statistic and conditional density for an extreme point, and each weight determines the magnitude and eigenenergy of an extreme vector. I have shown that each weight is chosen in a manner which ensures that:

1. Each conditional density of an extreme point describes the central location (expected value) and the spread (covariance) of the extreme point.
2. Distributions of the extreme points are distributed over the locus of likelihoods in a symmetrically balanced and well-proportioned manner.
3. The total allowed eigenenergy possessed by each weighted extreme vector describes the probability of observing the extreme point within a localized region.
4. The total allowed eigenenergies of weighted extreme vectors are symmetrically balanced with each other about a center of total allowed eigenenergy.
5. The locus of principal eigenaxis components formed by weighted extreme vectors partitions any given feature space into congruent decision regions which are symmetrically partitioned by a linear decision boundary.
6. The locus of principal eigenaxis components formed by weighted extreme vectors satisfies the linear decision boundary in terms of a critical minimum eigenenergy.
7. The locus of likelihoods formed by weighted extreme points satisfies the linear decision boundary in terms of a minimum total probability of error.
8. The Bayes' error, i.e., the conditional risk, in the congruent decision regions is equal.

I have named an equalizer rule which is formed by a locus of weighted extreme points a linear eigenlocus. I have named the process that generates a linear eigenlocus a linear eigenlocus transform.

Linear eigenlocus transforms generate linear discriminant functions that are fundamental building blocks for Bayes' minimax, binary and multiclass, linear classification systems. Because any given Bayes' minimax pattern recognition system is a linear combination of linear eigenlocus discriminant functions, the overall network complexity is scale-invariant for the feature space dimension and the number of pattern classes.

Finally, I have defined innovative ways to use linear eigenlocus decision functions as statistical multimeters or statistical gauges. Linear eigenlocus decision functions provide a robust measure of class separability and Bayes' error rate for two given sets of pattern or feature vectors whose mean and covariance functions remain constant over time. Linear eigenlocus decision functions can also be used to identify homogeneous data distributions. Alternatively, linear eigenlocus decision functions can be used to determine if two samples are from different distributions.

References

- C. Ash. *The Probability Tutoring Book*. IEEE Press, 1993.
- I. Asimov. *Understanding Physics: Motion, Sound, and Heat*. Mentor, 1966.
- A. Barron, J. Rissanen, and B. Yu. The minimum description length principle in modeling and coding. *Information Theory, IEEE Transactions on*, 44(6):4–37, Oct. 1998.
- K. P. Bennett and C. Campbell. Support vector machines: Hype or hallelujah? *SIGKDD Explorations*, 2(2):1–13, 2000.
- B. Boser, I. Guyon, and V. Vapnik. A training algorithm for optimal margin classifiers. In *Proceedings of the 5th Annual ACM Workshop on Computational Learning Theory*, pages 144–152. ACM Press, 1992.
- L. Breiman. Statistical modeling: The two cultures. *Statistical Science*, 16(3):199–231, 1991.
- C. Burges. A tutorial on support vector machines for pattern recognition. *Data Mining and Knowledge Discovery*, 2:121–167, 1998.
- H. Byun and S. Lee. Applications of support vector machines for pattern recognition: A survey. *LNCS*, 2388:213–236, 2002.
- C. Cortes and V. Vapnik. Support-vector networks. *Machine Learning*, 20(3):273–297, 1995.

- T. Cover. Geometrical and statistical properties of systems of linear inequalities with applications in pattern recognition. *IEEE Transactions on Electronic Computers*, pages 326–334, 1965.
- N. Cristianini and J. Shawe-Taylor. *An Introduction to Support Vector Machines and Other Kernel-based Learning Methods*. Cambridge University Press, 2000.
- C. Daniel and F. Wood. *Fitting Equations to Data*. John Wiley and Sons, 1979.
- P. J. Davis. *The Mathematics of Matrices*. John Wiley and Sons, 1973.
- R. Duda, P. Hart, and D. Stork. *Pattern Classification*. John Wiley and Sons, 2001.
- L. Eisenhart. *Coordinate Geometry*. Dover Publications, 1939.
- W. H. Engl, M. Hanke, and A. Neubauer. *Regularization of Inverse Problems*. Kluwer Academic Publishers, 2000.
- R. Fletcher. *Practical Methods of Optimization*. Wiley, 2000.
- B. Flury. *A First Course in Multivariate Statistics*. Springer-Verlag, 1997.
- K. Fukunaga. *Introduction to Statistical Pattern Recognition*. Academic Press, 1990.
- S. Geman, E. Bienenstock, and R. Doursat. Neural networks and the bias/variance dilemma. *Neural Computation*, 4:1–58, 1992.
- N. Gershenfeld. *The Nature of Mathematical Modeling*. Cambridge University Press, 1999.
- C. Groetsch. *The Theory of Tikhonov Regularization for Fredholm Equations of the First Kind*. Pitman Advanced Publishing Group, 1984.
- C. Groetsch. *Inverse Problems in the Mathematical Sciences*. Vieweg, 1993.
- I. Guyon, V. Vapnik, B. Boser, L. Bottou, and S. Solla. Capacity control in linear classifiers for pattern recognition. In *Pattern Recognition, 1992. Vol. II. Conference B: Pattern Recognition Methodology and Systems, Proceedings., 11th IAPR International Conference on*, pages 385–388. IEEE, 1992.

- P. C. Hansen. *Rank-Deficient and Discrete Ill-Posed Problems*. SIAM, 1998.
- T. Hastie, R. Tibshirani, and J. Friedman. *The Elements of Statistical Learning*. Springer, 2001.
- S. Haykin. *Neural Networks and Learning Machines*. Prentice Hall, 2009.
- S. Hewson. *A Mathematical Bridge*. World Scientific Publishing, 2009.
- O. Ivanciuc. Applications of support vector machines in chemistry. *Reviews in computational chemistry*, 23:291, 2007.
- A. K. Jain, R. P. Duin, and J. Mao. Statistical pattern recognition: A review. *Pattern Analysis and Machine Intelligence, IEEE Transactions on*, 22(1):4–37, 2000.
- P. Jain and I. S. Dhillon. Provable inductive matrix completion. *arXiv preprint arXiv:1306.0626*, 2013.
- C. Jirousek. *Art, Design, and Visual Thinking*. Cornell University, 1995.
- I. Jolliffe. *Principal Component Analysis*. Springer, 2002.
- B. P. Lathi. *Signal Processing and Linear Systems*. Berkley-Cambridge, 1998.
- D. C. Lay. *Linear Algebra and Its Applications*. Addison Wesley, 2006.
- Y. Liang, Q. Xu, H. Li, and D. Cao. *Support Vector Machines and Their Application in Chemistry and Biotechnology*. CRC Press, 2011.
- P. Linz. *Theoretical Numerical Analysis*. Dover Publications, 1979.
- P. Linz and R. Wang. *Exploring Numerical Methods*. Jones and Bartlett Publishers, 2003.
- D. Luenberger. *Optimization by Vector Space Methods*. John Wiley and Sons, 1969.
- D. Luenberger. *Linear and Nonlinear Programming*. Kluwer Academic Publishers, 2003.
- C. Meyer. *Matrix Analysis and Applied Linear Algebra*. SIAM, 2000.
- S. Nash and A. Sofer. *Linear and Nonlinear Programming*. McGraw-Hill Company, 1996.

- A. Naylor and G. Sell. *Linear Operator Theory in Engineering and Science*. Holt Rinehart and Winston, 1971.
- E. Nichols. *Analytic Geometry*. D. C. Heath and Company, 1893.
- H. Poor. *An Introduction to Signal Detection and Estimation*. Springer, 1994.
- D. M. Reeves. *Properly Specified Functional Mappings and Support Vector Learning Machines*. PhD thesis, George Mason University, 2009.
- D. M. Reeves. Resolving the geometric locus dilemma for support vector learning machines. *arXiv preprint arXiv:1511.05102*, 2015.
- D. M. Reeves and G. M. Jacyna. Support vector machine regularization. *WIREs Computational Statistics*, 3:204–215, 2011.
- B. Scholkopf and A. Smola. *Learning with Kernels*. MIT Press, 2002.
- M. Srinath, P. Rajasekaran, and R. Viswanathan. *Statistical Signal Processing with Applications*. Prentice Hall, 1996.
- J. Stewart. *Multivariable Calculus: Concepts and Contexts*. Cengage Learning, 2009.
- G. Strang. *Introduction to Applied Mathematics*. Wellesley-Cambridge Press, 1986.
- R. Sundaram. *A First Course in Optimization Theory*. Cambridge University Press, 1996.
- Tanner and Allen. *Analytic Geometry*. American Book Company, 1898.
- L. N. Trefethen and D. Bau. *Numerical Linear Algebra*. SIAM, 1998.
- H. VanTrees. *Detection, Estimation, and Modulation Theory: Part I*. John Wiley and Sons, 1968.
- G. Wahba. *Inverse and Ill-Posed Problems*. Academic Press, 1987.
- A. Whitehead. *An Introduction to Mathematics*. Henry Holt and Company, 1911.
- M. Zhdanov. *Geophysical Inverse Theory and Regularization Problems*. Elsevier Science, 2002.